Alma Mater Studiorum · University of Bologna

School of Science
Department of Physics and Astronomy
Master Degree in Physics

Fuel safety criteria for space nuclear reactor: the case of TRISO and UZrH fuels

Supervisor:
Prof. Paolo Finelli

Co-supervisor:
Dr. Francesco Lodi

Submitted by:
Simone Friggieri

Academic Year 2023/2024

A mamma e papà

Abstract

Space agencies showed a renewed interest in human settlements on the Moon or Mars, mainly to support further space exploration and test new technologies. In this context, nuclear power can be a strategic choice for providing the necessary energy.

After a brief review of space reactor history, their requirements and key components, a review of possible fuels and safety concept is made. Among the safety aspects of a space nuclear reactor, a particular emphasis is given to fuel safety criteria: indeed, this thesis aims to define safety limits under normal operation that will ensure the fuel's integrity and the proper implementation of the radioactive material confinement safety function.

The focus is on two candidate fuels, TRISO (TRi-structural ISOtropic) particle fuel and Uranium Zirconium Hydride (UZrH) fuels, that have been considered suitable due to their maturity and safety characteristics.

To draw up these fuel safety criteria, firstly the behaviour of these fuels under irradiation is presented; then, from the identification of the main causes of fuel failures, the development of potential safety criteria is done, with an explicit reference to the concept of margin, that must always be present in a safety criterion to ensure conservative choices.

The analysis of identified fuel failures in TRISO and UZrH fuels has led to the identification of twelve and nine fuel safety criteria, respectively, that depend mainly on operational conditions and some manufacturing characteristics.

The fuel safety criteria presented are intended as a guide for fuel designers in developing appropriate fuels for space reactors, emphasising the most critical dependencies and guiding to specifications for fabrication purposes.

While not exhaustive, these criteria can offer a basis for ensuring fuel integrity and safety in space reactor applications.

Contents

Acronyms

Anular Core Pulsing Reactor (ACPR) Research reactor using Uranium Zirconium Hydride fuel, whose function is to study the transient behaviour of materials to intense radiation for short time durations. 92

Fuel cladding mechanical interaction (FCMI) Mechanical interaction between nuclear fuel and its cladding, which can impact the integrity and performance of the fuel during reactor operation. 83

Fundamental Safety Functions (FSFs) A specific purpose that must be accomplished for safety for a facility or activity to prevent or to mitigate radiological consequences, due to normal operation and accident conditions. 23

High Assay Low Enriched Uranium (HALEU) Uranium enriched between 5% and 20%. 12

Highly Enriched Uranium (HEU) Uranium enriched above 20%. 10

Lithium Hydride (LiH) An inorganic compound made of Lithium and Hydrogen. In the context of space nuclear reactors, it is used as a neutron absorber and shielding material due to its high neutron cross-section and low mass. 9, 11

Radar Ocean Reconnaissance Satellites (RORSATs) Soviet reconnaissance satellites equipped with nuclear reactors to power their radar systems. 10

Sodium-Potassium alloy (NaK) An alloy of sodium and potassium, liquid at room temperature, known for its excellent thermal conductivity. Among other uses, it is a coolant in nuclear reactors. 9, 11

Space Nuclear Reactor (SNR) A device that uses nuclear fission to generate power for spacecraft, providing electricity and heat for missions in space. 10

TRi-structural ISOtropic particle fuel (TRISO) A nuclear particle-type fuel. It consists of uranium-based kernels encapsulated in multiple layers of carbon and ceramic materials, making it highly resistant to temperatures and radiation. 17

Uranium Zirconium Hydride (UZrH) A type of metallic nuclear fuel made of Uranium and Zirconium hydride. It is used mainly in TRIGA reactors and is known for its inherent safety characteristic of negative temperature coefficient of reactivity. 9, 17

Chapter 1

Space nuclear reactors and safety concepts

1.1 Space nuclear reactor and its history

Space agencies are interested in human settlements on Moon or Mars because it can be a base for further space exploration, allowing to test new technologies which can have broader applications, to make important research on the history of planets and solar system and to make scientific insight in the understanding of life. Furthermore, human presence into space can enhance in various way the chances of humanity survival [ESA].

To achieve human settlement on the lunar surface or on Mars in the future, a power system that produces electrical energy is needed: but since the crew presence in the settlement would like to be prolonged, it is important that this system produces the necessary amount of energy for life support, communications, operating rovers, etc. [PL23]. Nuclear systems could be a strategic choice because of their high power density, reliability, their lifetime, and their ability to operate even in the absence of sunlight. In particular, nuclear power is justified when the solar option is inadequate or impractical.

The use of radioactivity in space for energy production also includes the use of radioisotope thermoelectric generators, that convert the heat produced by radioactive decay (and not induced fission) into electrical energy via thermocouples. In this work they are not considered because of their low power output, despite they have been used extensively in space applications like rover motion (Curiosity, Perseverance) or for spacecraft probes that traveled far from the Sun (Pioneer 10, Voyager 1 etc.).

Nuclear reactors could also be used for space propulsion. Apart from some exotic concepts, these technologies can be divided into nuclear thermal and nuclear electric propulsion. In the first case, the propellant is heated directly with the heat of the nuclear reactor. The second technology exploits electricity from the nuclear reactor system to propel a thrusting fluid, which can be a gas, an ionized medium, or a plasma.

However, this type of application is not of interest to this thesis and will therefore not be investigated further.

Whilst nuclear power systems have been deployed in space missions, most of the applications have been for relatively low power applications (<10 kWe) and with only three nuclear fission power system designs being successfully launched into space. Let us focus on their history.

1.1.1 History

1.1.1.1 Reactors with actual launch and operation in space

US and Soviet Union (and Russia) have been designing and testing space reactor systems and components for more than five decades, even if only few had been actually deployed into space.

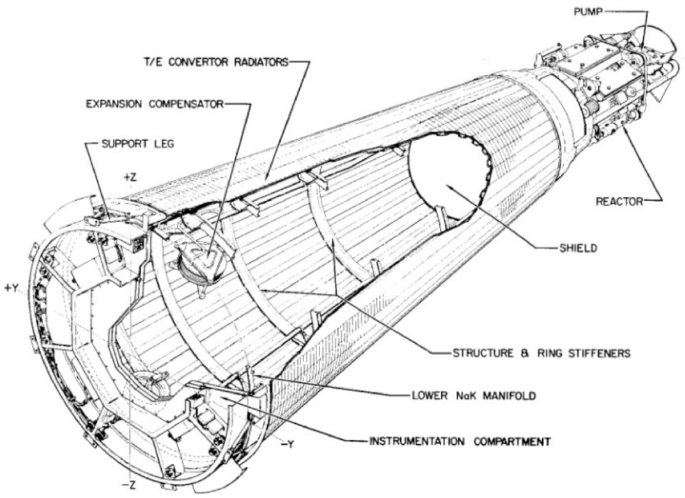

Figure 1.1: A diagram of the SNAP-10A reactor system

In April 1965, the first nuclear reactor for space applications was sent into orbit. It was the SNAP-10A, which was developed by US Atomic Energy Commission. SNAP-10A was designed to power satellites and was intended to supply 500 W of electricity for a year. It was a thermal spectrum reactor fueled with Uranium Zirconium Hydride (UZrH), where ZrH was the moderator, and eutectic Sodium-Potassium alloy (NaK) as liquid coolant, having electromagnetic pump to make coolant circulating, also after shutdown. The radiation shadow shield was made of Lithium Hydride (LiH). The energy conversion was thermoeletric (using thermocouples) and the reactor was surrounded by

beryllium reflector. In fact, reactivity was controlled using four outer elements of half-cylindrical Be parts: their rotation changed reflector worth and the neutron leakage from the reactor core. The cold reactor was significantly subcritical, for safety during handling, transportation, integration into the launch vehicle, and accidental submersion. However, the reactor stopped working after just 43 days due to an electronic fault. It continues to be the only US Space Nuclear Reactor (SNR) that operated in space missions [El-09]. A diagram of the reactor system is shown in Figure 1.1.

On the other hand, former Soviet Union routinely used space reactor power systems in a relatively low Earth orbit between 1970 and 1988 to power 31 Radar Ocean Reconnaissance Satellites (RORSATs). Those spacecraft were powered with nuclear reactor, called "Buk". The first one was launched in October 1970.

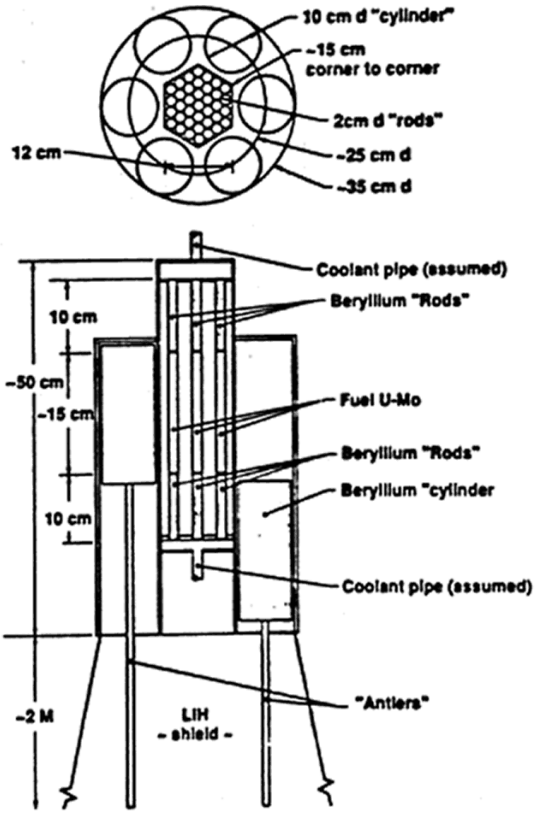

Figure 1.2: A diagram of the Buk reactor system. Source Wikipedia

It was a fast reactor with U-Mo alloy fuel rods, with Highly Enriched Uranium (HEU) and stainless steel clad, and it was surrounded by a circular radial beryllium reflector. The electric power generated using thermoelectric converters was about 3 kWe. The Buk reactor was controlled using six sliding beryllium cylinders: they were moved axially to adjust the neutron leakage from the reactor core. The shadow radiation shield was made

with LiH. A diagram of the reactor system is shown in Figure 1.2. At the end of their life, the reactor systems were boosted into a storage orbit where the radioactivity of the fission products would decay to that of actinides after several hundred years. Only two of them, due to a malfunction in the boost system in the storage orbit, returned to earth, one falling into the Atlantic Ocean and the other over Queen Charlotte Island in Northern Canada [El-09].

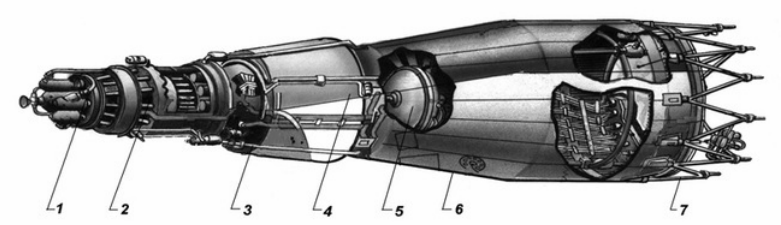

Figure 1.3: A diagram of the Topaz 1 reactor system. cesium vapour supply system and control drum drive unit, (2) thermionic reactor converter, (3) liquid metal circuit pipeline, (4) reactor shielding, (5) liquid metal circuit expansion tank, (6) radiator, (7) frame structure. Source: Kurchatov Institute

These reactors were followed by Topaz-1 reactors, with thermionic conversion systems using cesium vapour, generating about 5 kWe. Topaz-1 was launched in 1987 to test ion engines. The epithermal reactor was cooled with liquid NaK, made circulating by electromagnetic pumps. It was loaded with 96 wt% enriched UO_2 fuel pellets and beryllium oxide pellets served as neutron reflectors, while ZrH was the moderator. Reactivity was controlled by 12 beryllium rotating drums with boron carbide as a neutron absorber. The control drums maintained the reactor subcritical during launch and were used to start the reactor in orbit, regulate its operation and shut it down. The radiation shadow shield was made of LiH and depleted uranium for shielding neutrons and gamma photons from the reactor. It is shown in Figure 1.3. One reactor ran for six months, the other for a year, and then the Topaz-1 program was stopped. [Ass+21] [El-09]

1.1.1.2 Reactor concepts that have been tested

In addition to the three reactor models launched into space, some prototypes have only been designed, and others have also been partly tested. Among the latter, one should mention:

- DUFF reactor, designed to demonstrate key technologies and integration of various components such us core, heat pipe and Stirling engine. It was not prototypic of the configuration that would be employed in an actual reactor design for launch, but it marked a milestone in space nuclear technology, being the first system to produce electricity by the use of Stirling converters with the heat conducted with

heat pipes: if one considers the goal of demonstrating key technologies, the DUFF experiment can be considered successful [AG18];

- KRUSTY was a small (5 kWth), solid U-Mo block with HEU (93% 235U) fission power source: it uses sodium heat pipes to transfer energy from the reactor to Stirling energy converters. It was operated and tested, including some failure scenarios, in March 2018 to demonstrate the feasibility of this device: the operation was a success but the reactor has not been launched into space, being a demonstrator reactor;

- SP-100 was a fast spectrum, lithium-cooled reactor fuelled with UN HEU fuel, with a thermoelectric conversion system. It underwent extensive testing of components, but the project was dismissed in 1995 and was not flown into space;

- The Topaz-2 was a 5-6 kWe nuclear power system, fuelled with HEU Uranium dioxide, and with heat conversion based on thermionic conversion. Topaz-2 was produced in several units that underwent extensive ground testing but none were flown;

Other experiments and prototypes seem to have been tested to some extent, like Romashka systems, as reported in [PL23].

1.1.2 Overview of requirement of a space reactor

As it was seen in precedent paragraphs, reactors launched into space have been used for relatively low power applications, below 10 kWe, and they have relied on highly enriched uranium.

The use of highly enriched uranium on the one hand makes it possible to have a lighter reactor, carrying more fissile material but, on the other hand, it raises concerns about nuclear proliferation. This is why the most modern designs of space reactors focus on High Assay Low Enriched Uranium (HALEU), i.e. systems with enrichment between 5 and 20 wt.%.

As far as it regards the power output, the requirement is different from precedent space reactors used for satellites. For a first reactor, to create an outpost for further settlement in the future, the power output should be around 40 kWe, which is a likely requirement for an initial settlement phase on the Moon or on Mars, as foreseen in [Ole+22]. For a following and more stable mission, an higher power output may be needed.

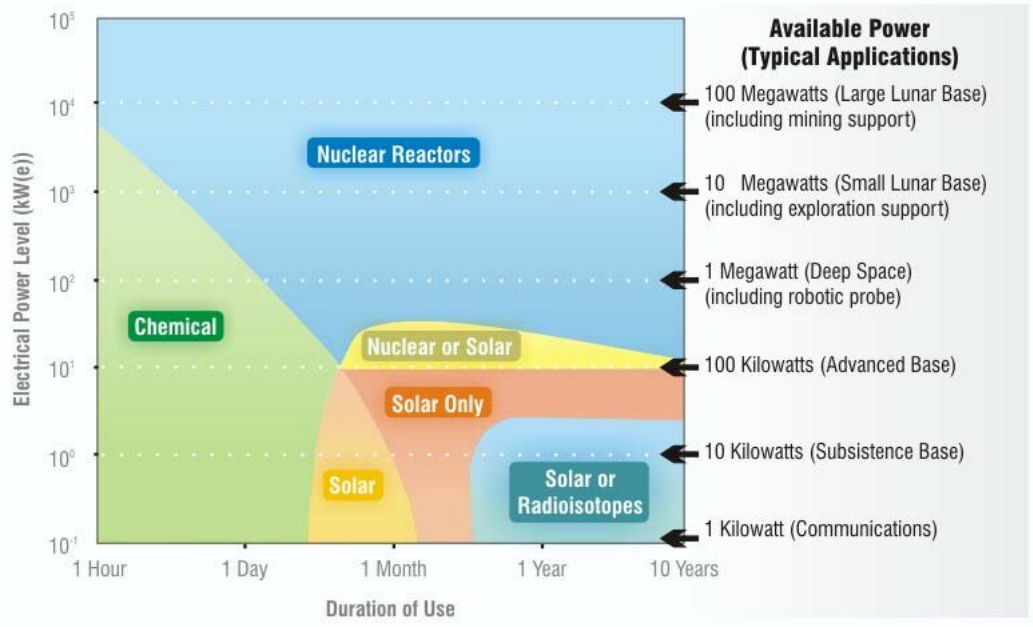

Figure 1.4: Regimes of possible space power applicability, as a function of power level needed and duration of use. On the right, typical application of power levels. From [Cam+09].

The use of nuclear reactors in human space settlement is coherent with precedent evaluation. Indeed, a space mission involving human settlement needs power for more uses than an orbiting satellite: for warming and cooling, lighting and vital systems (i.e., oxygen and water management), instrumentation and communication and much more. Being the position of the settlement static, the mission may be in the dark sometimes and the solar panels would be inadequate without a storage system.

In the Figure 1.4, one can see a diagram of possible applicability regimes for different power systems, according [Sta05]: it is shown, for example, that nuclear reactors can provide almost limitless power for any duration; however, they may not be convenient and the best choice under 10 kW. According to this diagram, a nuclear reactor becomes reasonable for a requirement of 40 kWe if the mission duration is longer than a dozen days. Among the other power supplies, chemical fuels can provide large amounts of energy but for a limited amount of time, while solar panels could provide power levels of some dozen kW for as long as it is needed; however, they are not practicable to provide rapid surges of large amounts of energy or in places without sun. Production of energy from radioactive decay is suitable for the continuous supply of low levels of power, below 5 kWe.

Requirements on space reactors regard also their lifetime, mass and volume. For an initial human settlement, the reactor should guarantee around 10 years of lifetime [Ole+22]. Past space reactor or reactor concepts foreseen lifetimes were in general above 5 years.

The reactor should also respect the mass and volume limits imposed by its transportation method [Ole+22]. As an example, the actual requirements for the Fission Power System of NASA are: mass lower than 6000 Kg and that the reactor should fit within a 4 m diameter cylinder with a height of 6 m.

In a space context, there is also the need for high reliability and low maintenance of the system. For this reason, minimizing moving parts can create motivation for the choice of one technology over another, both of the reactor and of the conversion system.

Other requirements regard modularity, user load, fault tolerance and transportability but analyzing them is out of the scope of this thesis: the interested reader can learn more in [Ole+22]. This list of requirements has been given to give an idea of the many requirements that a reactor must fulfil, but it is not exhaustive. These requirements may also change over time, depending on the objectives of the space mission.

1.1.3 Technologies of interest for space reactors

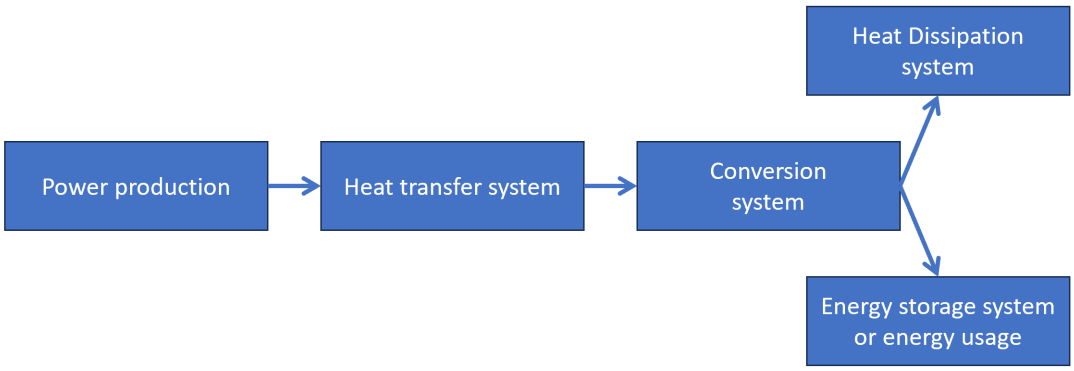

Figure 1.5: Schematic showing of a generic design concept for a space nuclear power system

The key subsystems for energy production are shown in the figure 1.5. There is the power production system, that in this case is the nuclear reactor. Then, there is the heat transfer system that will allow the exchange of energy from the reactor to the conversion system. The conversion system transform the thermal energy in the type of energy needed. The excess of heat must be dissipated through a dissipation system.

As we have seen in the preceding paragraph 1.1.1 on history, the reactors launched into space and the prototype reactors have relied on technologies that often differ from one another, both in terms of the type of fuel, the type of coolant and how it flows through the reactor, and the neutron energy spectrum, as well as how the thermal energy

produced is converted into electrical energy. For this reason, the following paragraphs will present briefly some of the key components, just for knowledge, of the subsystems presented above: in particular, the fuel type, the coolant, structural materials such as cladding, the conversion and the dissipation system.

As far as it regards to fuel type, different fuel compositions and fuel forms exist: being the main interest of this thesis, fuel composition will be presented in a separate paragraph (1.1.4).

The choice of the coolant is a critical factor in a reactor system as it influences a lot of design aspects, such as the heat transfer throughout the system. Coolant can flow due to natural phenomena, like in heat pipes, or with the help of pumps. In the case of a space reactor, heat pipes are often considered in many designs because they use capillary forces instead of moving parts, making them reliable and efficient. When the coolant is driven by pumps, they can be mechanically driven or they can be electromagnetic pumps with no moving parts, if the coolant has a high electrical conductivity. According to [PHM18], the ideal coolant should possess some key characteristics: it should have a high volumetric heat capacity to have a high power output with lower temperature increase; no phase changes, to enable also high temperatures operation; low neutron absorption, in particular if the enrichement is below 20%; good thermal conductivity to limit peak temperature and good chemical compatibility. These characteristics should ensure the coolant can efficiently support the reactor's operation while maintaining safety and efficiency. In space reactors, coolants considered as promising candidates are heat pipe systems (containing alkali metals); gaseous coolants; liquid metals and molten salts.

The choice of fuel cladding if present, or structural material in general, is mostly determined by the coolant, with material/coolant and temperature compatibility being the most crucial factors. When choosing these materials and establishing their geometry, it is important to minimize undesired neutron absorption, maintaining structural integrity and the capacity to extract heat from the fuel.

As far as it regards power conversion systems, they can be divided into static and dynamic conversion systems. The former have no moving parts, improving system reliability, and they include thermophotovoltaic cells, thermoelectric conversion or thermionic conversion. The drawback of these systems is usually the lower efficiency. Dynamic conversion systems have higher efficiencies and are generally considered for higher power applications. They usually are engines working with different cycles, like the Stirling one, and with various working fluids.

Thermal management in space power systems is crucial due to the vacuum environment, which necessitates radiative heat transfer using radiators because it cannot rely on convection. The effectiveness of radiators depends on their surface area and operating temperature, being this process governed the Stefan–Boltzmann law:

$$q = \varepsilon \sigma T^4$$

where q is the total energy radiated per unit surface area per unit time, ε is the emissivity

of the surface, σ is the Stefan–Boltzmann constant and T is the absolute temperature of the surface. So, higher temperatures reduce the needed area of the radiator and consequently the mass. However, increasing the temperature of the radiator, everything else being fixed, decreases power conversion efficiency. So a trade-off between mass and temperature must be made. Heat pipes may also be useful for radiators, but more exotic radiator prototypes have been proposed.

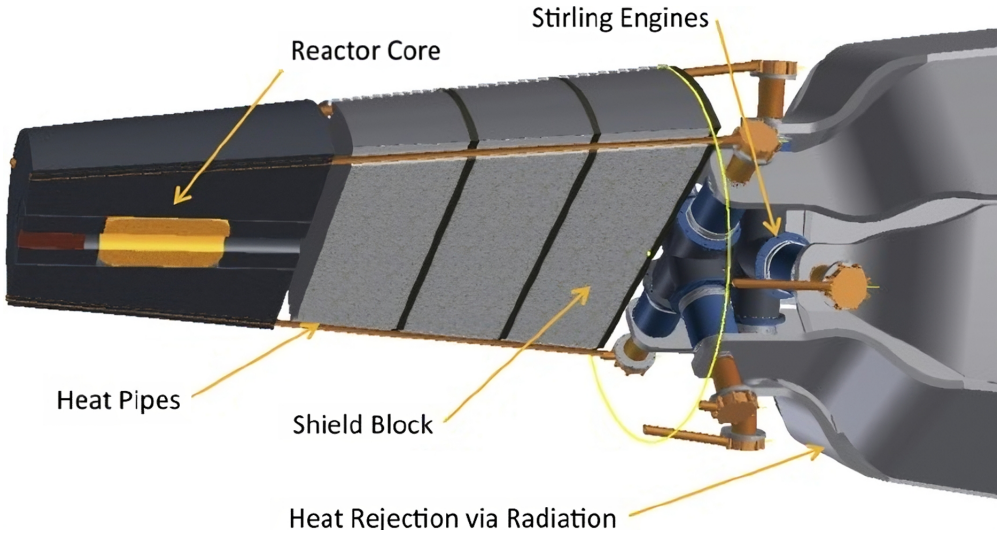

Figure 1.6: Artist conception of a small space reactor with heat pipe–Stirling engine. From [Pos+14]

An artist's depiction of how a space reactor with heat pipes and Stirling engines should look is shown in Figure 1.6. The list of technologies presented may not be complete or exhaustive, considering that many ideas and prototypes have been conceived or developed, but it was presented to give an idea of the most promising technologies for space reactors.

1.1.4 Fuel options

Let us deepen our knowledge of the type of fuel available, as this thesis will concentrate on fuel safety criteria.

Nuclear fuel is a material used in nuclear reactors to sustain the fission chain reaction and consequently, the primary function of the fuel is to produce heat, which is used to generate electricity. Another important function of the fuel is also related to safety. In fact, the first barrier to prevent the radioactive release of fission products to the environment is the fuel itself, by containing the fission product in the fuel matrix. The importance of barriers in the context of nuclear safety will be further presented in the Section 1.2.1.2. However, it is not always possible to fully retain fission products, in

particular as far as it regards gaseous species at high burnup and high temperatures [And+23].

The most common nuclear [PL23] fuels used in terrestrial reactors are oxide of uranium-235 and plutonium-239 or a mixture of them.

Another kind of fuel is metallic fuels, which are usually an alloy of uranium with some other element like zirconium or molybdenum. Among metallic fuels, the most common is the Uranium Zirconium Hydride (UZrH) alloy, which is still used in the TRIGA reactor series [PL23]. Metal fuels have a high fissile density and thermal conductivity, but they swell significantly and they can exhibit chemical evolution during irradiation. They have a lower melting point, to some extent counteracted by their high thermal conductivity.

There are also non-oxide ceramic fuels, made of uranium nitride or uranium carbide, that were studied in the past but are not common for commercial use: however, some of their characteristics may be interesting for space reactors. Non-oxide ceramic fuels generally have higher swelling than UO_2, in particular at high burnups and temperatures. These effects can be managed with appropriate limits. Uranium nitride and carbides are of interest for space reactors because of their fissile density and better thermal conductivity.

For the peculiar characteristics of being in a particulate form and having different barriers inside the particle, the TRi-structural ISOtropic particle fuel (TRISO) might deserve a separate category, although it contains already cited fuel materials. TRISO fuel consists of a uranium-based kernel, typically uranium dioxide, carbide or a mixture of them, surrounded by layers of carbon-based materials that enhance thermal stability, conductivity and effectively retain fission products.

All these types of fuels will be further presented below.

Finally, there are forms of nuclear fuel in a liquid phase: this is a benefit because there is less worry about structural irradiation effects like swelling of the fuel, degradation of thermal conductivity or amorphization. For example, molten salt fuels are mixtures of actinide salts, like uranium fluoride, used above their melting points. The main challenge related to molten salt fuel is the corrosion of structural materials in contact with salts. However, molten salt fuel will not be further analyzed because this thesis want to focus on those fuel that have been considered for space reactor systems.

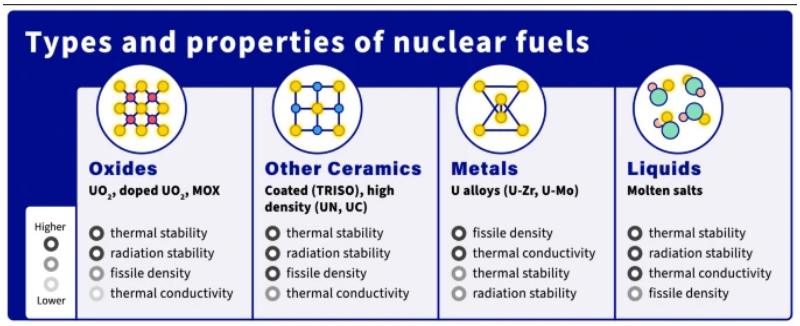

Figure 1.7: A summarizing image of different fuel types with its own relative strengths. From [And+23]

A summarizing image of the different fuel types is presented below in figure 1.7, showing the relative strength of each type of fuel. However let's concentrate on fuels that have been used or hypothesized for space reactors, focusing on pros and cons.

1.1.4.1 Oxide fuel

Uranium dioxide fuels are the predominant fuel for nuclear reactors due to its balance of advantages and limitations. They offer good fissile density, good stability, effective retention of fission products, and high resistance to radiation damage (retaining its crystalline structure). They also exhibit lower fuel swelling than nitride and carbide fuel, which reduces the probability of cladding failure. However, oxides have relatively poor thermal conductivity, making energy extraction less efficient, a drawback which is generally counteracted by their high melting point. Its fissile density, while sufficient for current commercial reactors, limits the power output, necessitating larger reactors or increased enrichment for smaller designs. Because Uranium oxide fuels are the most widely used, their behaviour is known, both in thermal and fast reactor conditions.

1.1.4.2 U-Mo alloys

Concerning metallic fuels, they have a higher thermal conductivity and two, in particular, have been used or considered for space reactors: an alloy of uranium and molybdenum and an alloy of uranium zirconium hydride. The first one has a weight percentage of molybdenum that can be from 6 to 10%, but most of the experience is with 10 wt.% of Mo. This fuel was considered for the KRUSTY space reactor prototype, but most of the experience comes from two legacy reactors working in the Sixties: the data on the performance of this fuel is very limited, regarding low burnup, and for this reason, the understanding of the fuel behaviour is weaker: it is known that swelling increases with burnup and that U-Mo alloys seem to have better performance at temperatures above 600 °C [PL23].

1.1.4.3 Uranium Zirconium Hydride

The other metallic fuel of interest, Uranium zirconium hydride, has been already used in the context of space reactor i.e., SNAP reactors, and it is currently of interest for the MARVEL reactor program. Furthermore, the knowledge of this fuel behaviour has been qualified by the use in TRIGA research reactors, that use this fuel enveloped in a stainless steel cladding. Initially, UZrH used HEU fuel, but more recent versions use HALEU, with an increased uranium content to compensate for the lower reactivity. In fact, the typical composition now is U0.3ZrH1.6, compared to U0.085ZrH1.6 in earlier fuels. As a metallic fuel, it has a higher thermal conductivity, and among the advantages of this fuel, there is a very negative prompt temperature coefficient of reactivity, which ensures increased safety. On the other hand, the swelling behaviour of the fuel may require temperature limitation or modifications of the gap between pellets and cladding to avoid pellet-cladding mechanical interaction. Diffusion of Hydrogen is an issue at higher temperatures. Modern TRIGA fuel can achieve burnups of around 120 GWd/tHM and is anticipated to perform well at higher operating temperatures, as required for space reactors [PL23].

1.1.4.4 Uranium carbide

Although several uranium and carbon compounds have been considered as nuclear fuels, most of the experience comes from uranium carbide (UC) fuel from the Indian nuclear program. Uranium dicarbide has been used in some space and nuclear programs, including the Russian Romashka concept and the 1960s KIWI and PHOEBUS propulsion reactor program [PL23]. These experiences revealed performance issues with UC fuels, in particular its tendency to swell significantly during irradiation, more than oxide fuels. Despite extensive experience, especially from the Indian UC fuel program, UC is considered to have medium technical maturity, while other uranium-carbon compounds have low technical maturity due to less experience [PL23].

1.1.4.5 Uranium nitride

Uranium nitride (UN) fuel has several favourable properties to be a candidate for space reactors. It supports high power density operation due to the high thermal conductivity and high melting point, while the theoretical high density of uranium is useful to minimize the core size, given a fixed enrichment. However, uranium nitride fuel presents peculiar challenges: the major one is that nitrogen-14, which is the most common nitrogen isotope, parasitically absorbs neutrons, producing also large amount of the radioactive isotope carbon-14. This would require an expensive process of nitrogen enrichment, in particular, if the reactor works at conditions that make this absorption more probable, like working in the thermal spectrum or using HALEU fuel. Furthermore, nitride fuel swelling is a concern and seems to be highly sensitive to fuel temperature. UN fuel has a lower creep

behaviour, which is unfavourable as creep usually helps to reduce the stresses between fuel and cladding, and this behaviour depends on density, with lower densities (higher porosities) resulting in higher creep behaviour. Despite these challenges, there has been some successful irradiation of UN fuel, all with natural nitrogen, making UN a reasonable choice for a space fuel, if density and porosity are managed and fuel temperatures are kept sufficiently low. For example, the SP-100 reactor prototype successfully used UN fuel, which employed fuel with a relatively low theoretical density and porosity and operating at a fuel temperature of 1500 K. While there have been some irradiation campaigns with UN fuel, the level of experience is much lower compared to uranium oxide fuel [PL23].

1.1.4.6 TRISO

As already said, TRISO fuel consists of a uranium-based kernel surrounded by layers of carbon-based materials (made of carbon or silicon carbide) that enhance thermal stability, structural integrity and effectively retain fission products. TRISO Fuel was developed in the 1960s and was studied and used in some reactors, some of them still working. Now TRISO has gained renewed interest for the Generation IV reactors. As far as it regards space reactors, different concepts using TRISO fuel have been conceived, in particular in the past for space propulsion, while now there are some concepts, like the IGCR-200 reactor [Li+20], and NASA has awarded contracts to develop concepts for 40 kWe systems to different companies, with at least one of these concepts uses TRISO fuel [PL23].

1.1.5 Fuel chosen for this thesis work

Of all the fuels presented in the previous sections, our analysis focused on two fuels in particular: TRISO particles and uranium-zirconium hydride fuels. The reasons for this choice are presented below.

In their analysis, the authors of [PL23] assigned each fuel type a maturity level, based on considerations of current experience with that fuel and knowledge of its behaviour. According to this analysis, the fuels that have the highest maturity are uranium oxide fuels, mainly due to the huge experience built up, and uranium-zirconium hydride fuels, because of their extensive use on terrestrial (mainly TRIGA) reactors. If we consider particle fuel and similar criteria for establishing maturity, the TRISO fuel could also be assigned a high maturity because more than five terrestrial reactors now use or have used this type of fuel in the past and knowledge of its behaviour is good. In addition, some space reactor concepts plan to use this fuel. Finally, TRISO fuel contains uranium oxide, the behaviour of which is widely known.

The decision to investigate the two fuels mentioned earlier is due to certain characteristics that make them suitable for space reactors.

TRISO fuel is innovative and has the already cited passive safety features of enchanted thermal resistance and confinement performance [Got22]. TRISO fuel has also features that are interesting in a space exploration context: for example, if there is a containment breach of the reactor, the fuel is already self-contained, and due to the high-temperature resistance, fuel melting is improbable [RKJ21]. In fact, fuel particles are usually enveloped in materials with large thermal capability and transfer properties, and the coolant (gas or heat pipe system) enables passive removal of decay heat in the case of an accident [Got22]. Furthermore, TRISO fuel has reached higher burnup than LWR fuels, which is an important characteristic because a space reactor has limited or no opportunities to refuel. TRISO-based fuel could be used in a solid-core reactor which would have an additional safety benefit during launch [RKJ21]. In fact, a solid block core is less susceptible to damage from the mechanical stresses experienced during launch, for example because it eliminates potential fuel pin or grid plate movements [Pos+20].

Among the drawbacks of TRISO fuel, one can cite that uranium density is lower than other types of fuel, which may increase the sizes and masses of space nuclear reactors [Li+20], and that it is difficult to recycle, although this fact is not strictly important in the space context and that there is progress in TRISO recycling process.

On the other hand, uranium-zirconium hydride fuels, besides having a known behaviour and having already been used in space reactors and Triga reactors, possess a prompt negative temperature coefficient of reactivity, meaning that as the temperature increases, the reactor's reactivity decreases. This inherent safety characteristic and the possibility to reach high burnup is interesting in the space context.

For all the above reasons, those two fuels have been chosen to be further analysed.

1.2 Safety concepts

Space reactor power systems should be designed with safety and operational reliability as intrinsic elements. It is important to prevent unwanted radioactive exposure to astronauts and contamination of the environment or exposure of current or future space assets to structural debris and radiation [El-09]. For this reason, some concepts concerning safety will be presented and then it will be explained how they are relevant for this thesis work. In particular, the concept of Defence in depth will be firstly analyzed, then focusing on the concepts of barrier and safety functions. Thus, the concept of fuel safety criteria and margin will be presented.

1.2.1 The concept of defence in depth

There is a safety concept that permeates the entire life cycle of a reactor, from design to maintenance and decommissioning, which is that of defence in depth: it has been

extensively described and explained by the IAEA in the publication [INS97] and it could be seen as a strategy to meet safety objectives with large confidence (margin).

IAEA nuclear safety and security glossary [IAE22] defines defence in depth as

Defence in depth

A hierarchical deployment of different levels of diverse equipment and procedures to prevent the escalation of anticipated operational occurrences and to maintain the effectiveness of physical barriers placed between a radiation source or radioactive material and workers, members of the public or the environment, in operational states and, for some barriers, in accident conditions.

Anticipated operational occurrences (AAO) is a term that represents a design considered state of a nuclear plant, that is a deviation of an operational process from normal operation, and it is expected to occur at least once during the operating lifetime of a facility (usually they are event whose probability of occurrence varied from 1 to 10^{-2} / year [Bec+12]). An AAO, given appropriate design provisions, does not cause any significant damage to items which are important to safety or it does not lead to accident conditions. For example, an anticipated operational occurrence is the loss of normal electrical power. Accidents, instead, are deviations from normal operations that are less frequent and more severe than anticipated operational occurrences [IAE22].

1.2.1.1 Defence in depth main objectives

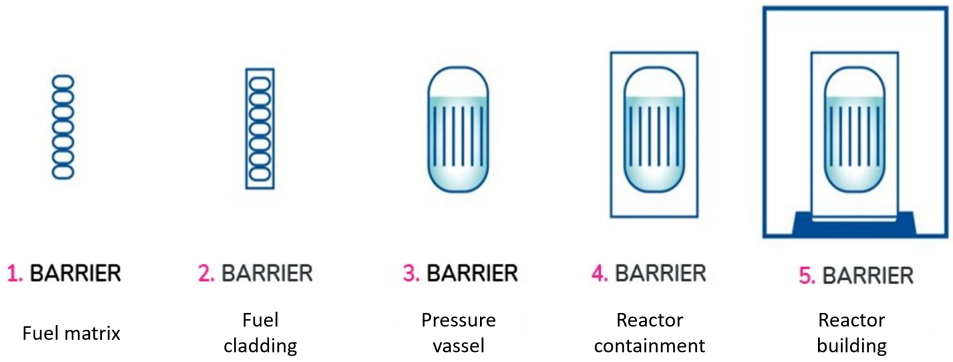

Figure 1.8: Typical barriers of a terrestrial reactor. Barriers may vary in number and design. Image modified from [TVO]

There are three basic objectives of defence in depth, which are

- to compensate for human and component failure

- to maintain the effectiveness of the barrier
- to protect humans and the environment

We will focus on the second objective: maintaining the effectiveness of the barriers. A barrier is a physical obstruction that prevents or inhibits the movement of people, radionuclides or some other phenomenon (e.g. fire), or provides shielding against radiation [IAE22]. The Figure 1.8, for example, shows the main barriers for a terrestrial reactor. Barriers may vary in number and design (for example, the fuel matrix, the fuel cladding, the boundary of the reactor coolant system, and the containment system are barriers), but one of these barriers that must be maintained effective is indeed the fuel, both the matrix and the fuel cladding.

Furthermore, to achieve the three general objectives of defence-in-depth, the strategy is twofold: one should prevent accident conditions and, if prevention fails, limit their consequences. The priority of prevention actions over mitigation ones is because they are more effective and predictable than the second ones. After all, performances generally deteriorate when the status of the system departs from normal conditions. For these reasons, this thesis will focus on preventive provisions (i.e. inherent plant safety characteristics, safety margins, system design features and operational measures), called fuel safety criteria, intended to help maintain an intact fuel [IAE05].

1.2.1.2 Fundamental Safety Functions

To ensure safety in general and to avoid the failure of the barrier, three Fundamental Safety Functions (FSFs) have to be always performed, in operational states and in design basis accident and beyond:

- Control of the reactivity
- Removal of heat from the fuel
- Confinement of radioactive material

These functions are needed because they are a measure of the appropriate implementation of the defence in depth concept through the safety provisions used at each level: if a provision helps to maintain one of these functions, it helps to reach safety objectives and to maintain intact barriers [IAE05].

The concept of defence in depth relies on a high degree of independence between the levels of defence, in order to allow the independence in the performance of the three fundamental safety functions. For these reasons, also the barriers should be more than one, to assure different level of defence, and independent to the extent practicable [IAE05]. Considerations on multiple and independent levels are of particular importance for barriers, as they are, indeed, the main element in a reactor system that performs the safety function of radioactive material confinement.

1.2.1.3 Defence in depth levels for a nuclear reactor

Level of defence	Objectives	Essential means
1	Prevention of abnormal operation and failures	Conservative design and high quality in construction and operation
2	Control of abnormal operation and detection of failures	Control, limiting and protection systems and other surveillance features
3	Control of accidents within the design basis	Engineered safety features and accident procedures
4	Control of severe plant conditions including prevention of accident progression and mitigation of the consequences of severe accidents	Complementary measures and accident management
5	Mitigation of radiological consequences of significant releases of radioactive materials	Off-site emergency response
Always present prerequisites: Conservatism, Quality assurance and Safety Culture		

Table 1.1: Level, objectives and means of defence in depth [INS97]

The implementation of the concept of defence in depth of a nuclear reactor includes five levels of defence, intended as a set of procedures, inherent features, design characteristics and equipment aimed to prevent accidents and limit their consequences. [INS97] cite also the means to achieve them, tools and basic prerequisite for defence in depth: these prerequisites are conservatorism, quality assurance and safety culture and they should be present in all these levels. In the nuclear industry, conservatism is a practice of making cautious and safety-oriented assumptions during the life of a nuclear installation, from the design to decommissioning.

These levels, which are summarized in the Table 1.1, are: prevent abnormal operation and failure, control them, control accident conditions within design basis, control severe conditions with the prevention of accident progression and if all the other levels fail, mitigation of radiological consequences. The levels are intended to be independent of each other, and this independence is crucial to avoid that failure can jeopardize more levels of defence [IAE05].

In the flow chart presented in Figure 1.9, the logic of defence in depth is shown. The success of provisions of each level ensures that fundamental safety functions presented above are successfully performed. However, according to the philosophy of defence in depth, if provisions from a given level fail to control the evolution of a sequence, the subsequent level comes into play, as explained here below. The objective of the first level of defence is the prevention of abnormal operations and system failures. If there is a

failure at this level, an initiating event takes place. Then, the second level will detect these failures, to ensure his objective of avoiding or controlling the abnormal operation. If this level fails, the third level provisions should ensure that the consequences of the accidents foreseen in the design basis (design basis accidents) will be limited. Should the third level fail, the fourth level limits accident progression by accident management, to prevent or mitigate severe accident conditions with radioactive material release. If all the levels have failed, provisions of the fifth level should ensure the mitigation of radiological release consequences [IAE05].

Defense-in-depth can be implemented in different ways and with different provisions, because of differences in designs, national safety regulations, technological solutions, management and cultural strategy to safety. However, the approach of defence in depth offers the most comprehensive basis for achieving safety. If the defence-in-depth concept is correctly implemented, it ensures that a failure at one level or even combinations of them, will not propagate to jeopardize defence-in-depth at subsequent levels.

1.2.2 Fuel safety criteria and the concept of margin

As explained above, the success of provisions of one level of defence ensures that the three fundamental safety functions are successfully performed.To achieve the goal of reactor safety (i.e. the operation of a nuclear reactor does not contribute significantly to health risk), fuel operational and design limits should be introduced to avoid failures during normal operation, maintain the integrity of the barrier, and mitigate consequences of accidents, as dictated by the concept defence in depth: those limits are part of fuel safety criteria.

The definition of a fuel safety criteria is not unique and different fuel criteria can be recognized. For example, in the NEA report "Fuel Safety Criteria in NEA Member Counties" [03], fuel criteria are divided into three categories:

- Safety criteria which are imposed by the regulator and ensure that the impact on the environment of a design-based accident is acceptable
- Operational criteria which are imposed by the fuel vendor as a part of the license and ensure that safety criteria are not violated
- Design criteria, that are employed by fuel vendors and utilities for fuel design and should be preserved in normal operation and anticipated transients

However, sometimes is difficult to identify criteria according to the originating authorities. Furthermore, it is also debated the relative order of these categories. For example, in Nuclear Fuel Safety Criteria Technical Review by NEA [Bec+12], other definitions of criteria are reported: like the one from the Institute for Nuclear Power Operation which identifies operating, design and analytical limits, from the most restrictive to the least

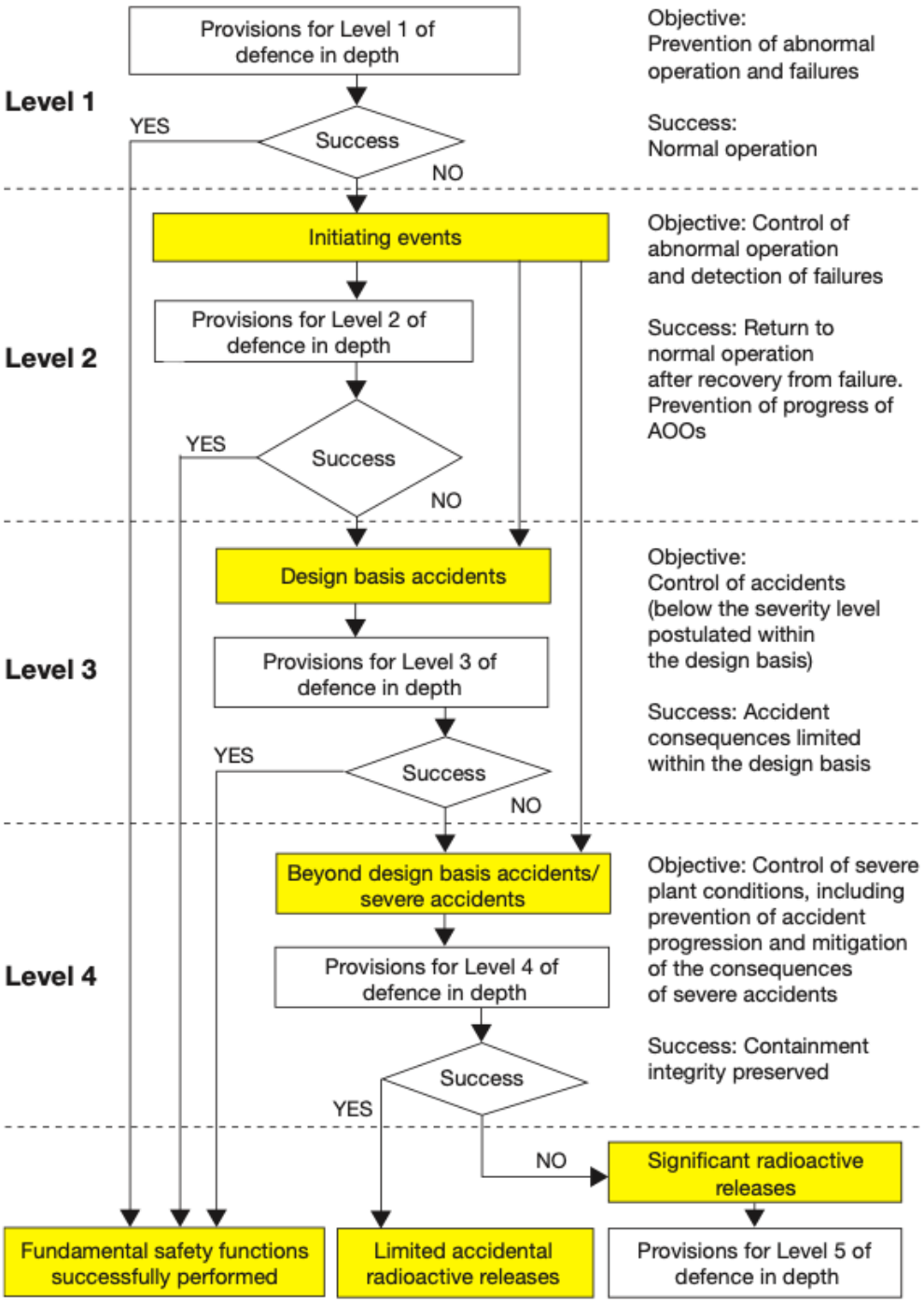

Figure 1.9: The flow chart of defence in depth, from [IAE05]

one (so, name and order of this criteria are different). The authors of the review agree in general with the concept of safety, operational and design criteria presented above, but they prefer to place all of them under the category of fuel safety criteria.

However, a concept common to all definitions is that of margin: which is the difference between the actual state (load) and the damaged state (strength), as defined in [Hre+07] and shown in Figure 1.10.

The concept of margin is introduced because uncertainty exists in the safety variable value at which damage occurs, and on the actual load: both load and strength, in fact, are not fixed values but follow a probability density function around a mean value. In this case, the figure shows the probability densities for the load and the strength where the load is smaller than the strength. The difference is the total margin. Then, one can set a safety limit, so that the total margin is divided into two parts. The first one, that can be called the design margin, is a margin where the load state can operate safely by design, while the other part of the total margin is to ensure that one of the prerequisites of defence in depth, conservatism, is present in the definition of the limit. For that reason, violating a safety limit does not necessarily mean that the barrier fails, thanks to conservatism, but remaining inside the limit helps to ensure that the safety functions are maintained. However, quantifying the total margin is difficult, also under experimental conditions, and so is establishing safety limits. For this reason, the safety limit concept may be simple, but it is difficult to apply in practice [Bec+12].

The safety limit itself and the safety variables on which a limit should be set are selected based on preventing that a barrier fails. Thus, there can be different safety criteria, regarding different barriers or systems (fuel safety criteria, primary circuit criteria, containment criteria etc.). In particular, limits that prevent failure of the fuel are the Fuel safety Criteria.

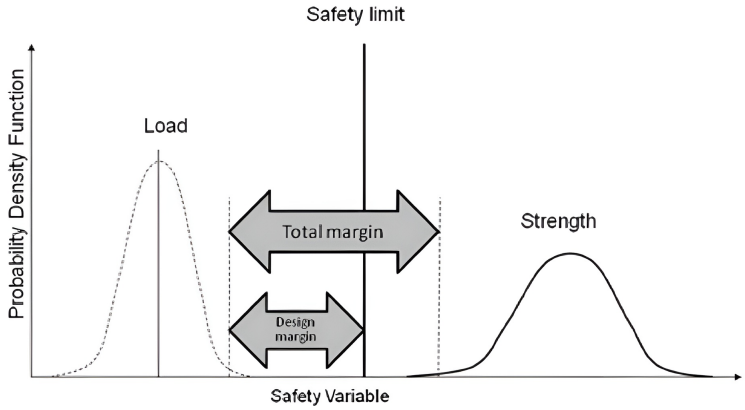

Figure 1.10: The relationship between load and strength in terms of margin. From [Bec+12]

Fuel safety criteria are specific to both the type of fuel considered and the reactor

in which this fuel is placed. For example, the same fuel might behave differently in a fast reactor than in a thermal reactor, or different reactor concepts with the same fuel may reach different temperatures or have different thermal gradients. They may also vary according to national laws in different countries. Fuel safety Criteria may regard different parts of the fuel (the fuel pellet, the cladding if present, the assembly etc..), and interaction between them (e.g.: the interaction between the pellet and the fuel cladding) and they are all set to maintain the integrity of the fuel. Just as an example, some fuel safety criteria for light water reactors are presented, to give an idea:

- On rod internal gas pressure: fission gas release and resulting fuel rod internal pressure is an important aspect of fuel behaviour. The fission gas release depends on a lot of parameters, from the fuel microstructure to the fuel temperature, which is strongly influenced by the power rating and the burn-up. Increases in fission gas release can lead to high fuel rod internal pressures and could also lead to a deterioration of the thermal conductivity. For this reason, a criterion is usually set so that the rod internal pressure is held below the nominal pressure in the reactor coolant system during normal operation.

- On Assembly hold-down force: LWR fuel assemblies are equipped with hold-down springs in the top piece, to provide sufficient forces to prevent fuel assembly lift-off due to hydraulic loads, thus preventing some assemblies from interacting with others, by moving and not being in the correct position. The safety criteria in different countries are usually defined so that vertical lift-off forces must not unseat the lower fuel assembly tieplate from the fuel support structure.

In practice, one considers one way in which the fuel barrier can fail, then looks at what variables this failure depends on, and finally sets a limit or a requirement on it, with a margin of conservatism, so that one can be sure that the fuel maintains its safety functions.

1.2.3 Fuel performance model

The search for fuel safety criteria is closely linked to the tool of fuel performance models. These tools are software that simulate the behaviour of the fuel according to fuel irradiation history and properties of fuel materials, focusing, in particular, on mechanical and thermochemical calculations. The design, fabrication, research, optimization, experiment design, and comprehension of fuel behaviour under both normal and accident conditions are all aided by fuel performance modelling.

The quality of modelling depends both on the validity of the code and on the knowledge of the material properties of the fuel modelled: if the knowledge is incomplete, the results may be less precise. For this reason, is useful to make more experimental work on material properties to reduce uncertainties in the input data [Ske24]. Fuel performance

code also aids in fuel design optimization, planning test irradiations, and interpreting irradiation results. Furthermore, modelling allows quick and cost-effective calculations, complementing experimental studies. Agreement between modelling predictions and irradiation results validates assumptions, while discrepancies encourage scientific progress. Continuous collaboration between modellers and experimenters is essential to align observations and predictions, and modelling may also uncover new failure mechanisms for experimental investigations [Age10].

Helping the nuclear industry find and model failure of the fuel, Fuel performance model codes are important tools in safety considerations because they help both establish and verify limits, and thus fuel safety criteria. In fact, fuel performance modelling depends also upon identifying the possible failure modes for the fuel and finding which modes are limiting, thus helping to assess the fuel behaviour relative to these criteria [PW10]. In fact, knowing the fuel safety criteria helps the fuel performance code programmer pay special attention to the variables that influence failures.

1.2.4 Safety concept in this work

As already said, one of the objectives of defence in depth is to maintain the effectiveness of the barriers. Defence in depth and the integrity of barriers are even more important concepts in the space context, where the possibilities for intervention are reduced.

In this work, we will focus on the barriers regarding the fuel, searching for limits during normal operation that would ensure that these barriers will remain intact, and so the safety function of radioactive material confinement is correctly performed. The focus on the fuel barriers and on normal conditions is due to the fact the reactor has not yet been defined. Obviously, fuel contributes to some degree all three fundamental safety functions presented in previous paragraphs, but of particular interest to this work will be the function of radioactive material confinement.

The following chapters will analyze the literature on that fuel, presenting the history and the main characteristics of the fuels under consideration (TRISO and uranium-zirconium hydride). Then, the behaviour under irradiation and the main causes of failure will be presented. Thus, focusing on the variables that cause individual failures, possible safety criteria will be presented. If the literature also reports values for these variables as limits, these will be reported. If, on the other hand, explicit values are not found, the safety criterion will be formulated as a requirement, whose limit value will have to be found by further experimentation or simulation with fuel performance code. In any case, explicit reference will always be made to the concept of margin, which must always be present in a safety criterion to ensure conservative choices.

Chapter 2

TRISO fuel

2.1 Fuel History

Tristructural isotropic fuel particle, or TRISO, is a nuclear fuel in the form of multilayer particles and it is the most chosen fuel technology for high-temperature gas reactors (HTGR). This technology, however, has been evaluated as a possible fuel for space reactors, due to some interesting characteristics outlined in the precedent chapter.

The idea of a particle fuel dates back to the 1950s, when different countries wanted to investigate particles of uranium disseminated in a conducting graphite matrix, to have better thermal exchanges between fuel and gas coolant. Early advances in this field have been made in England, Germany and the United States [DLH19]. The first nuclear fuel in the form of a coated particle was developed in the late 1950s for the Dragon reactor in the UK.

At the origin, the fuel particle was covered with a single pyrocarbon layer to protect the kernel during fabrication, but over the following years, this kind of fuel quickly developed into increasingly sophisticated and effective particle designs. In fact, it was discovered that the pyrocarbon layer of these particles could fracture under irradiation. One of the first design modifications was the introduction of a sacrificial buffer layer made of lower-density carbon, between the dense outer pyrocarbon layer and the kernel, to accommodate irradiation modification of the kernel and fission gases. Some examples of this design have been referred to as BISO particles (for Buffer-isotropic or Bistructural isotropic).

To further improve performances, trying to resolve the problem of cracking propagation in coating layers, various experiments and modifications were made, both in terms of design, manufacturing methods and their related parameters. However, the main improvement was the addition of a ceramic layer made of silicon carbide between two pyrocarbon layers, to provide significantly improved particle strength and retention of fission products: this design advancement, along with the addition of a buffer layer, was

the groundwork for the current TRISO particle. Due to their improved structural integrity and retention of fission products, TRISO coatings gained popularity during the 1970s, becoming the actual state-of-the-art fuel for HTGR [DLH19] [Bea+09].

Up to now, coated particle fuel has been used in several experimental and demonstrator reactors: Dragon in the UK, Peach Bottom 1 and Fort St. Vrain in the US, AVR and THTR in Germany. The HTTR reactor in Japan, built in the 90s is still active, as are two other rectors in China (HTR-10 and HTR-PM). Even today, particle fuel remains a field of research under development, mainly intending to find kernels with better performance under irradiation and coating layers that better retain fission products.

2.2 Fuel particle structure

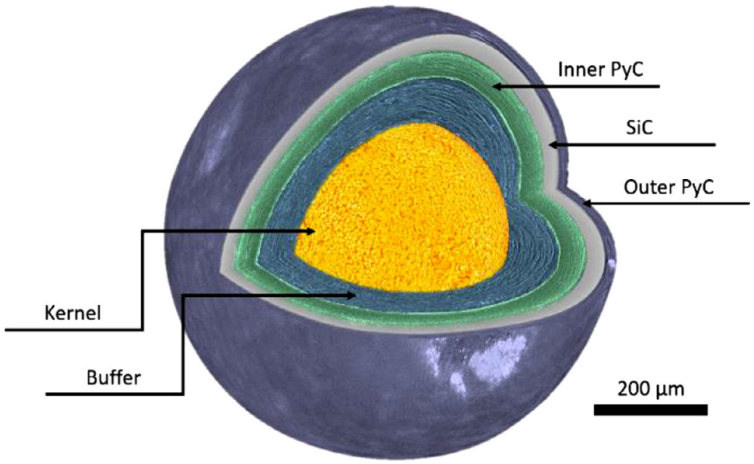

Figure 2.1: Illustration of a TRISO particle from [Kan+22]

TRSIO particles are composed by a kernel of fuel and four coating layers: a buffer layer, an inner pyrolytic carbon layer, a ceramic SiC layer and externally an outer pyrolytic carbon layer, as depicted in Figure 2.1. TRISO particles are typically 750-830 μm in diameter and each layer has its own characteristics [WPG21] [Wan04] [Mor+04] [MS19]:

- the kernel is a sphere of fissionable fuel, usually an oxide, carbide or oxicarbide of uranium, thorium or plutonium; during the fission process, the kernel produces the power and an ensemble of fission products: the kernel is, indeed, the first retention to radionuclide release; according to different design, its diameter varies from 350 to 600 μm;

- the porous carbon buffer layer surrounds the kernel; its main functions are to dampen fission product recoil, to provide empty space to accommodate kernel

swelling and the buildup of gases (mainly fission gases and carbon monoxide, which is produced by chemical reactions between the components of this layer and oxygen liberated from UO_2); its dimension is generally around 100 μm;

- then a first inner pyrolitic carbon dense layer, called IPyC, is the first load-bearing barrier in the particle; it has the purpose of providing structural support for the successive layer, also giving a smooth surface for its deposition and protecting it from fission products; it protects the kernel from corrosive gases during manufacturing process and it resists the migration of some fission products (it is a barrier mainly for Krypton, Xenon and Iodine, while it is to a lesser extent for Strontium and Cesium, and hardly at all for Silver). Its thickness is around 40 μm
- the successive layer is a high density and high strength ceramic layer made of silicon carbide (SiC), whose functions are to give the structural strength to the particle and to be its pressure vessel for fission gases; it is the main barrier that provides impermeability to metallic fission products (except silver) and gas retainment; this layer typically measures 35 μm;
- the last layer is a second layer of high-density pyrolitic carbon, referred to as OPyC; it is another barrier to the release of fission product and it gives structural support to the SiC layer, maintaining it in compression; it is also the bounding surface between the particle and the fuel compact, protecting inner layers during particle life; OPyC layer has a thickness around 40 μm.

Then, thousands of TRISO particles are embedded in a structure called fuel compact. This structure is usually composed of a carbonaceous matrix that improves heat transfer, temperature uniformity and fission product retention. It gives a rigid structure and it allows the handling of the fuel without damage to the particles. The fuel matrix is generally composed of graphite and other binder components, but there are also other concepts with a SiC matrix [Woo+23].

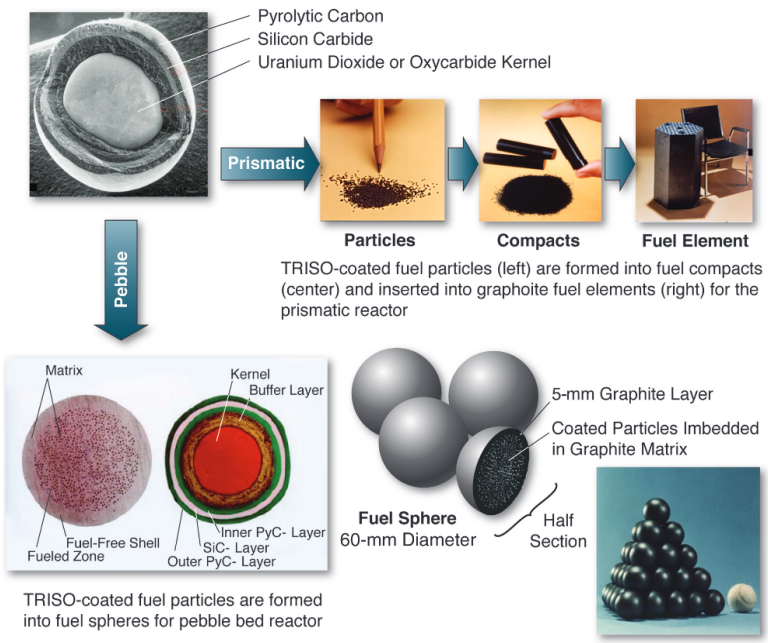

Figure 2.2: TRISO particle and the two kinds of compacts, with their dimensions and compared with ordinary objects. From [PCC09].

There are two main fuel compact designs, as shown in figure 2.2. It can be a sphere, where fuel particles are suspended in a sphere-shaped matrix surrounded by an outer unfueled layer of matrix material. This fuel compact is called "pebble" and it has typically a diameter of 6 cm (more or less a billiard ball) containing about 15000 TRISO particles. It is used in pebble-bed type reactor designs.

The second one is the cylindrical fuel compact, in a solid or annular configuration, that usually contains about 10,000 particles, surrounded by an unfueled matrix. Typical dimensions of this design are 5 cm in length and a diameter of about 1 cm. Those presented are the fuel compacts that have been used in the past, however there is nothing to prevent the development of fuel compacts of different shapes and sizes depending on reactor requirements: in fact, TRISO fuel offers flexibility in manufacturing.

There are two main reasons why it is necessary to bind TRISO particles in a fuel compact: heat transfer and mismatches in thermal expansion of particles. In fact, the flow impedance of small and closely packed TRISO particles would be high, limiting heat removal, and particles would have a low contact area and a large amount of void space in this configuration, giving rise to a lower heat transfer than TRISO particle surrounded by a matrix.

The second reason for combining particles in a fixed matrix material, which is the more limiting, is the differences in the thermal expansion of the particles and holder: particles settle under vibration and temperature cycling, and this cycling after particles

settlement would result in compression forces that could lead to particle damage or holder rupture [Mor+04].

2.3 Fuel behaviour

To understand how a TRISO particle behaves under irradiation the main interactions occurring within the particle are presented below, highlighting the most important failure mechanisms. Then, it will be presented how the fuel performance code PARFUME models the thermal and mechanical behaviour of the particle fuel.

2.3.1 Kernel

The kernel, which contains nuclear fuel, produces power and its composition is crucial for controlling the particle environment's chemistry.

One concern about the kernel is the oxygen potential inside the particle, which is determined by the amount of oxygen in the system and the affinity of particular elements for it, and determines which elements can compete for the oxygen and which cannot. It must be managed either by limiting burnup or adjusting the kernel composition for two main reasons. One is to prevent that the oxygen released during the fission of uranium dioxide reacts with the carbon buffer layer to form carbon monoxide: CO, in fact, can increase particle pressure and the likelihood of failure, and can cause the kernel to migrate from its centred position due to thermal gradients. The second reason is to ensure that rare earth elements are oxidized and so immobilized, preventing them from migrating to and reacting with the silicon carbide (SiC) layer. Kernel composition can be adjusted in different ways, for example adding a "getter" element in the kernel to absorb free oxygen, or using a two-phase fuel, called UCO: this fuel is composed of a phase of uranium dioxide and a phase of uranium dicarbide, and works well in reducing CO production because as oxygen is liberated, it first oxidizes the UC_2 and rare earth elements.

As other uranium oxide fuels, both UO_2 and UCO kernels swell due to fission product and irradiation effects. However, swelling of the kernel in TRISO particle is not a concern beacuse the buffer is foreseen to manage it.

Another concern for the kernel is the retention of fission gases and volatile fission products. In general, they are contained by the coatings, but kernel offers a helpful and important retention of fission gases up to moderate burnup levels. This retention helps in controlling particle pressure. However, as burnup increases, the uniformity of kernel structure deteriorates and outer coatings must be able to contain fission products.

As far as it regards kernel composition, UO_2 fuel has been proposed as the fuel of choice in reactors with low-temperature gradients and burnups near 10%. In the case of

reactors with higher temperature gradients and burnup, other kernel compositions may be considered [Mor+04].

Analysing the kernel behaviour, kernel migration has been identified as a failure and will be further analyzed in a dedicated chapter.

2.3.2 Buffer later

As explained above, the three main functions of the buffer layer are to attenuate fission product recoil, to provide a void volume with its porosity for gas generation and to accommodate the swelling of the kernel.

The thickness of the buffer layer is important because it should be thick enough to shield the IPyC layer from the recoil of fission products, but it also affects the particle pressure: a missing or thin buffer can induce increased internal pressure, causing the particle to fail sooner than expected. On the other hand, a too-thick buffer can cause higher temperatures due to its lower thermal conductivity than other layers.

The buffer layer is not required to hold much of the particle strength and some amount of shrinkage and cracking due to irradiation is acceptable [Mor+04]. So, as far as it regards the buffer layer, no particular failures are highlighted.

2.3.3 Inner pyrocarbon layer IPyC

Two of the functions of the inner pyrocarbon layer are to give a smooth surface for the deposition of the SiC layer and to protect the kernel during this process. In fact, SiC is deposited using chlorine compounds and chlorine can migrate to the kernel, react with uranium and produce volatile compounds that can complicate the fabrication and operation of the particles. Then, it delays the transport of fission products, except for some metals, and it isolates the SiC layer from carbon monoxide, which can attack the SiC at higher temperatures.

One mechanically important function of the IPyC layer is to maintain the SiC layer in compression, due to its irradiation-induced shrinkage. However, good irradiation behaviour is achieved if the pyrocarbon layer shows similar dimensional changes in the radial and tangential directions for the fluence of interest. Those properties can be ensured with a carbon deposition that has a random macroscopic crystal orientation, having a Bacon Anisotropy Factor near 1.

The Bacon Anisotropy Factor is a parameter that has been used in the context of carbon deposited using fluid beds, and it can assume values from 1 to ∞. For a perfectly isotropic material BAF is 1, and for a perfectly oriented medium BAF results ∞. It is usually calculated based on an x-ray measurement technique [MS19].

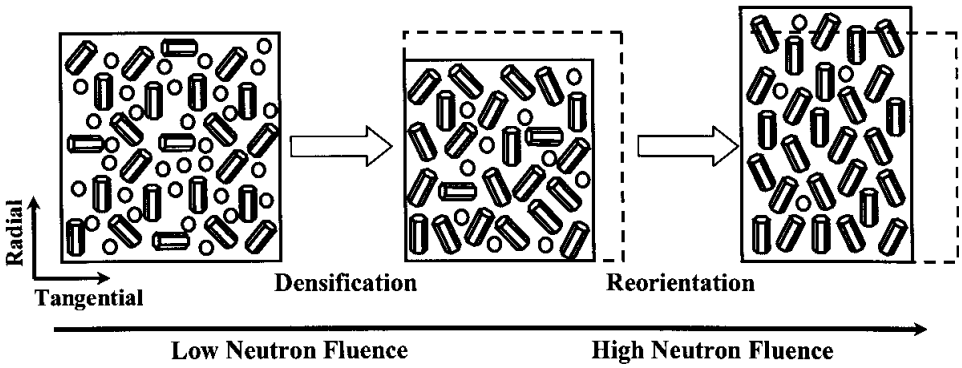

Figure 2.3: Irradiation induced mechanism in PyC layers. Bars represent graphite crystal while circles represent defects and vacancies. From [Wan04]

The dimensional change in pyrocarbon layers is a very complex phenomenon, as shown in figure 2.3, mainly because of its structure. As deposited, this material is basically composed of anisotropic crystals of graphite, almost arranged in all directions, with other micro-structures between them like cross-links, vacancies, voids and defects, indeed having a macroscopic isotropic behaviour. Then, fast neutron irradiation causes collisions that re-displace carbon atoms and annihilate vacancies, resulting in densification and shrinking in both tangential and radial directions; another result of fast neutron irradiation is the reorientation of graphite crystal structure in their preferred direction, causing swelling in the radial direction. These two processes take place simultaneously but, as irradiation continues, there is no other space for densification and reorientation becomes the leading mechanism. This explains why in the tangential direction the pyrocarbon layers shrink, while in the radial direction, there is a turnaround point after which begin to swell [Wan04].

It is important to note that the shrinkage and creep behaviour under irradiation of this layer is significant for good particle performance. In fact, if the shrinkage causes stress to rise in this layer and creep is not able to loosen them, the IPyC layer can crack. Those cracks can induce high tensile stress on the SiC layer, causing a higher probability of failure, or they can allow the CO gas to attack the SiC layer. The IPyC behaviour under irradiation can also induce the debonding of this layer, and the tip of the debonded region can cause higher stress on the SiC layer and again an increased failure probability. The IPyC behaviour under irradiation will be further analyzed in the following paragraphs.

Another property of the pyrocarbon layer that should be considered during the design of the particle is the thickness, because of its mechanical importance, as far as an increased thickness induces higher stresses in this layer and consequently an higher failure probability of the particle [Mor+04].

Considering the IPyC layer behaviour, IPyC layer cracking and debonding have been identified as important failures and will be further analyzed in a dedicated chapter.

2.3.4 SiC Layer

The SiC layer is the most important, as it is the main barrier to fission products and radioactive material release and it provides the main structural support to hold the internal pressure increase. In fact, as will be explained in detail in the following sections, gas pressure builds up during irradiation due to the production of fission gases and due to the production of carbon monoxide, especially for uranium oxide kernels.

Although pyrocarbon layers also offer structural resistance to the pressure, the latter acts mainly on the SiC layer, exerting tensile stress. The stress is counteracted by inner and outer PyC layers irradiation shrinkage, which provides a helpful compressive stress. If the total tensile stress on the SiC layer overcomes the strength of this layer, it can crack, losing its ability to retain radioactive material. This tensile stress increase can be the result of pressure increase, but also of cracked or debonded IPyC layer. In fact, SiC layer failure is significantly influenced by the strain interactions with the pyrocarbon layers and, in practice, to obtain the best SiC behaviour, pyrocarbon layers should keep the SiC layer compressed as far as possible and they should remain intact over the designed lifetime.

Another concern for the SiC layer, especially if the temperature increases, is that fission products can attack the layer. Among them, the main attention should be given to palladium and lanthanides. A good kernel design, however, can retain lanthanides as oxides, while palladium is not tied up. Other metals of concern are Cesium, which has shown some capacity to attack the SiC layer in laboratory experiments, and Silver, which cannot be retained by coating layers and should be considered in radiological evaluations.

If the temperature further increases, particularly above 1600 ^{o}C, the fission product release increases, meaning that the SiC layer cannot exploit its main function in the best way. This release increase can be the result of different processes, both corrosion from fission products and thermal decomposition. The latter is the dominant failure mechanism above 2000^{o}C.

Finally, if the IPyC layer is failed and cracked, in UO_2 fuel the attack of carbon monoxide is a concern, as far as it is no longer retained by pyrocarbon and it can oxidize the SiC layer with a consequent increase of failure probability [Mor+04].

Summing up, the failure mechanisms identified as linked to the SiC layer are: pressure vessel failure, fission product attack (palladium, caesium), thermal decomposition and CO attack.

2.3.5 OPyC layer

The outer pyrocarbon layer is the last layer and it serves as a connection between the particle and the material composing the fuel compact. It protects SiC during particle handling and from successive external reactions. Mechanically, it compresses the SiC layer as the IPyC layer does, and for this reason, good irradiation stability is still needed.

Furthermore, it acts as an ulterior barrier to fission product release.

As far as the performance of the OPyC layer, they are similar to those of the IPyC layer and its integrity guarantees a lower failure probability. However, if this layer is too porous, the interface strength between this layer and the outer matrix may become too strong and the layer could crack due to the different shrinkage behaviour of the layer and the matrix.

For these reasons, as far as it regards to OPyC layer, only the interaction between the layer and the matrix will be further analyzed in a dedicated chapter.

2.3.6 Thermal modelization and temperature profile

The modelization of TRISO fuel is very complex, due to the different types of fuel compacts that can be used, the high number of particles, and because of the different layers in the particles. However, let's analyse how fuel temperature and stresses are analysed in PARFUME, one of the most complete and used fuel performance model for TRISO particle available today.

After the specification of involved geometry (planar, prismatic or spherical), as shown in Figure 2.4, the program makes a "macro" thermal analysis, related to the fuel compact, which is based on boundary condition (like coolant temperature) and power generation. Then it starts the simulation for the specified number of particles. For each particle, it calculates a "micro" temperature profile, according to the specified position of the particle in the fuel element. Using the temperatures inside the particle and after the calculation of gas pressure, the program makes a stress analysis. With the calculated stresses, it makes the failure probability analysis and a fission element transport analysis.

Let's concentrate on the temperature modelization, to understand the temperature profile in a particle. After the identification of temperature boundaries condition, the distribution of temperatures inside the fuel compact is calculated using the general heat conduction equation [SD18]:

$$\rho c_p \frac{\partial T}{\partial t} = k \cdot \nabla^2 T + \dot{q} \tag{2.1}$$

where ρ is the density (kg/m^3), T is the temperature (K), t is the time (s), k is the thermal conductivity (W/m-K) and $\dot{q}$ is the volumetric heat generation rate (W/m^3).

Then, known the OPyC exterior surface temperature according to its position in the "macro" temperature profile, the temperature profile of a single particle is calculated assuming: a spherical symmetry (no defects) and isotropic material, thermal properties dependent only on temperature, internal (volumetric) heat generation exists only in the kernel layer, the contact resistance between particle layers is negligible and the gap between the buffer and the IPyC layer, if any, can be treated as a conducting medium. Furthermore, it is assumed a quasi-steady state approach, which means that the time rate of temperature change within the particle is approximated as zero [SD18].

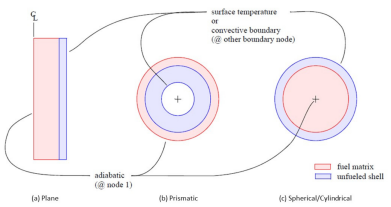

(a) A "macro" mesh of the fuel element

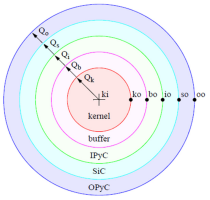

(b) A "micro" mesh of the particle

Figure 2.4: In the first picture different macro meshes are shown, developed for different fuel compact (planar, prismatic and spherical geometry): in red there is the fueled matrix, while the blue part represents the unfuelled matrix. In the other picture, the particle "micro" mesh with different layers. From [SD18]

The general conduction equation in spherical coordinates, with an internal heat source (as in the case of the particle), under the assumptions of spherical symmetry and quasi-steady-state, reduces to:

$$0 = \frac{1}{r^2}\frac{d}{dr}\left(r^2\frac{dT}{dr}\right) + \frac{\dot{q}}{k} \tag{2.2}$$

where r is the radius in meters. The solution of the last equation is given in this form:

$$T = \frac{\dot{q}}{6k}(R^2 - r^2) + T_R \tag{2.3}$$

where R is the outer radius of the sphere and T_R is the temperature at the radius R. This formula allows to calculate the temperature at any radius in the kernel.

However, we still don't know the temperature at R (so at the kernel surface) and neither the temperature profile. To know them, we need to set the boundaries of the outer temperature of the OPyC layer given from the "macro" temperature profile. Furthermore, we assume the quasi-steady-state that implies that each heat flow Q_{layer} through a layer is equal to the heat flow from the kernel, which is equal to internal volumetric heat generation in the kernel layer multiplied by the kernel volume $Q_{layer} = \dot{q}_k V_k$.

So given this last formula, and considering the heat transport law for spherical coordinates, one can get the temperature of an inner i-1 layer:

$$T_{i-1} = T_i + \frac{\dot{q}_k V_k (r_i - r_{i-1})}{4\pi r_i r_{i-1} k_{i-layer}} \tag{2.4}$$

where $k_{i-layer}$ is the conductivity of the layer between r_i and r_{i-1}.

So, for example, given the boundary of the outer OPyC layer T_{oo} as a first T_i temperature, one can get the temperature T_{os} at the outer surface of the SiC layer, as

$$T_{os} = T_{oo} + \frac{\dot{q}_k V_k (r_{oo} - r_{so})}{4\pi r_{oo} r_{so} k_{OPyC}} \tag{2.5}$$

Equations similar to those given allow the sequential calculation of temperatures between the layers, up to the kernel surface.

Calculated the outer kernel surface T_{ko}, one can calculate the temperature at the kernel centerline using 2.3. In the way presented above one can calculate temperature at any radius inside the particle.

2.3.7 Mechanical modelization

Another important part of the particle modelization is the mechanical analysis, with the calculation of stresses and strains in the layers, stresses that are then needed to evaluate the failure probability. The mechanical analysis of a solid element is governed by three basic mechanical principles: the condition for equilibrium, strain compatibility, and stress-strain equations.

For a differential element in a solid, the equilibrium equations can be written in terms of stresses. In fact, a form of the second law of dynamics, using stresses and matrix notation is

$$\nabla \cdot \overline{\overline{\sigma}} + \rho f = \rho a \tag{2.6}$$

where $\nabla \cdot \sigma$ is the divergence of the stress tensor, ρ the density, f is a force per unit mass vector related to the forces acting on the solid element (body forces), and a an acceleration vector. If no net forces f are acting on the element, the equilibrium condition reduces to: $\nabla \cdot \sigma = 0$. In spherical coordinates and considering the radial symmetry, this condition reduces to:

$$\frac{d\sigma_r}{dr} + \frac{2}{r}(\sigma_r - \sigma_t) = 0 \tag{2.7}$$

where σ_r is the radial stress and σ_t is the tangential hoop stress.

The principle of strain compatibility ensures that the deformation of a solid element is continuous and compatible throughout the material, and is given by the equation:

$$\frac{d\varepsilon_t}{dr} + \frac{(\varepsilon_t - \varepsilon_r)}{r} = 0 \tag{2.8}$$

Finally, the stress and strain equation describes the relationship between stresses and strains in a material. It can be expressed in a general way with tensors, under a small strain assumption [Lai+19]:

$$\dot{\overline{\overline{\sigma}}} = \overline{\overline{\overline{\overline{H}}}} : \left[\dot{\overline{\overline{\varepsilon}}}_{tot} - \left(\dot{\overline{\overline{\varepsilon}}}_{th} + \dot{\overline{\overline{\varepsilon}}}_{swell} + \dot{\overline{\overline{\varepsilon}}}_{p} + \dot{\overline{\overline{\varepsilon}}}_{creep}\right)\right] \tag{2.9}$$

where overlines represent the order of the tensor and $\dot{\overline{\overline{\sigma}}}$ is the stress rate tensor, $\overline{\overline{\overline{\overline{H}}}}$ is the Hooke tensor, $\dot{\overline{\overline{\varepsilon}}}_{tot}$ is the total strain rate tensor, $\dot{\overline{\overline{\varepsilon}}}_{th}$ is the strain rate tensor due to thermal dilatation, $\dot{\overline{\overline{\varepsilon}}}_{swell}$ is the strain rate tensor due to irradiation induced swelling, $\dot{\overline{\overline{\varepsilon}}}_{p}$ is the strain rate tensor due to plasticity and $\dot{\overline{\overline{\varepsilon}}}_{creep}$ is the strain rate tensor due to creep.

In other words, the stress rate tensor is determined by the contracted product of the Hooke tensor applied to the elastic strain rate tensor. The latter is the term in square brackets and it is calculated as the difference between the total strain rate tensor and the sum of terms corresponding to stress free strain mechanisms (swelling and thermal dilatation) and inelastic strain mechanisms (plasticity and creep) [Lai+19].

This formula, developed for TRISO particle behaviour in spherical coordinates and considering radial symmetry, becomes these two equations for radial $\frac{\partial \varepsilon_r}{\partial t}$ and tangential total strain rate $\frac{\partial \varepsilon_t}{\partial t}$ [SD18]:

$$\frac{\partial \varepsilon_r}{\partial t} = \frac{1}{E}\left(\frac{\partial \sigma_r}{\partial t} - 2\mu\frac{\partial \sigma_t}{\partial t}\right) + c(\sigma_r - 2\nu\sigma_t) + S_r + \alpha_r \dot{T} \tag{2.10}$$

and

$$\frac{\partial \varepsilon_t}{\partial t} = \frac{1}{E}\left[(1-\mu)\frac{\partial \sigma_t}{\partial t} - \mu\frac{\partial \sigma_r}{\partial t}\right] + c\left[(1-\nu)\sigma_t - \nu\sigma_r\right] + S_t + \alpha_t \dot{T} \tag{2.11}$$

where, for a coating layer, E is its modulus of elasticity, σ_r and σ_t are radial and tangential stresses, μ its Poisson's ratio, ν Poisson's ratio due to creep, c the irradiation-induced creep coefficient , α_r and α_r are the radial and tangential thermal expansion coefficient, $\dot{T}$ is rate of change in temperature [SD18].

In practice, the four terms on the right-hand side represent, respectively, the elastic strain caused by radial and tangential stress components, the irradiation-induced creep strain due to the stress components (considered as secondary creep, i.e. creep strain rate is proportional to the stress), the irradiation-induced swelling strain and the fourth term represents strain caused by thermal expansion.

This is how the fuel performance model PARFUME models strains for the pyrocarbon layers: for describing the SiC layer, the same equations are used, but omitting creep and swelling terms.

The three principles presented in the equations 2.7, 2.8 and 2.9 are the governing equation of the problem, and then each fuel performance program solves these equations to get stresses and strains. The approach used by PARFUME is to resolve the solution into time increments, using stresses calculated at the precedent step as the initial condition for the following one. Solving the problem in this way, allows the material properties and irradiation temperature to change with time.

However, fuel performance codes solve those equations in different manners and with different approximations: the interested readers can deepen their knowledge of the solution methods in dedicated papers.

2.4 Known failure behaviour

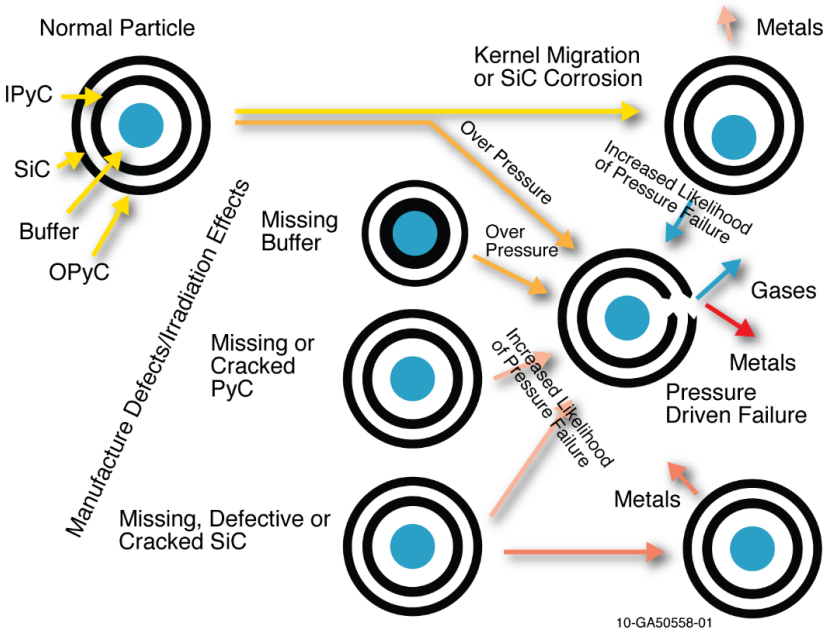

Figure 2.5: Main TRISO failure summarized, from [Mor+04]

Now that an overview of the fuel behaviour has been made and failure mechanisms have been identified, let us discuss the failures and how they happen.

As it was shown, TRISO particles have different ways to fail, but the basic concept is that if radioactive material or fission products find a way out of the particle, then it can be considered to have failed in its confinement function. These radioactive materials can mainly come out in two ways: either through a break in the main containing layer, the silicon carbide layer, or through some kind of thermochemical interaction that makes the layers more or less permeable for certain chemical elements, as summarized in 2.5. Fuel failures during operation can be attributed to a variety of factors, including design or manufacturing defects, and operating conditions: however, fuel failure due to the manufacturing process can be reduced with a good quality control system [Mor+04].

A possible classification of failures can be made according to the nature of the mechanism: in fact, some of them are mainly structural/mechanical failures, due to stress in or between the layers (e.g. pressure vessel failure or debonding between IPyC-SiC layers), while others originate from thermochemical causes, for example kernel migration or SiC thermal decomposition [MS19]. Then, some of these failures can be classified according to how they are addressed within fuel performance models: for example, pressure vessel failure is usually modelled as a 1D effect, while the majority of fuel failures are multidimensional failures (and they are usually addressed with finite elements analysis).

TRISO failure that has been identified before or found in the literature are:

- Pressure vessel failure
- IPyC crack-induced failure
- IPyC debonding induced failure
- SiC thermal decomposition
- Kernel migration
- Fission product interaction or attack and CO attack
- Matrix-OPyC interaction
- Creep failure of PyC
- Kernel coating mechanical interaction

Let's further analyze them in detail.

2.4.1 Pressure vessel failure

One of the earliest failures discovered was the increase of pressure, that stresses TRISO coatings. Under irradiation, fission gases are produced from the kernel. In addition to these gases, the excess of oxygen released during fission reacts with carbon from the buffer layer producing CO and CO_2: this last kind of gas production is particularly relevant for UO_2 particle kernels.

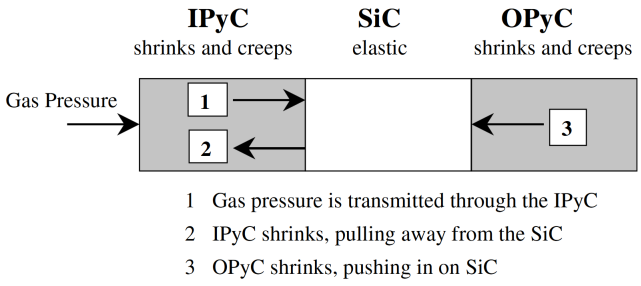

Figure 2.6: Main behaviour of coatings layers in a fuel particle. From [Mil+01]

In a TRISO particle, gas pressure builds up during irradiation and the pyrocarbon and SiC layers offer a structural resistance to this pressure. The pressure grows continuously during irradiation, exerting a tensile hoop (i.e., tangential) stress on the SiC layer.

This stress is counteracted by inner and outer PyC layers. In fact, pyrocarbon layers shrink under irradiation in both radial and tangential directions: if the PyC is tightly bonded with the SiC layer, this behaviour provides helpful compressive stress that reduces the tensile stress generated by gas buildup, as shown in figure 2.6. Then, creep in pyrocarbon layers reduces the stresses in those layers, also reducing the helpful effect of shrinkage on SiC. During irradiation, the SiC layer is considered to exhibit an elastic response because it has a much higher elastic modulus than PyC layers, bearing most of the pressure [MS19].

For all these reasons, and considering the fact that pressure buildup continues, the tangential stress on the SiC layer reaches a compressive minimum value during the early stages of irradiation, and then steadily increases up to the end of the irradiation, as shown qualitatively by the purple line in Figure 2.7.

As already said, this pressure acts on the three principal structural layers, but mainly on the SiC layer: pressure vessel failure takes place when the stress becomes tensile in the SiC layer and exceeds its fracture strength. For the reasons explained above, this failure is not expected at the earlier stages of irradiation.

As far as it regards dependencies, the production of CO_2, CO and fission gases is mainly a function of burnup and temperature [Age10].

Nevertheless, nominal TRISO particles are generally designed with a void volume in the porous buffer layer, which is enough to avoid overpressure particle failure: in fact, the literature suggests that failure due to overpressure is dominated by failure of particles that do not meet design specification (for example, insufficient buffer layer or improper porosity) [Age10] [WPG21].

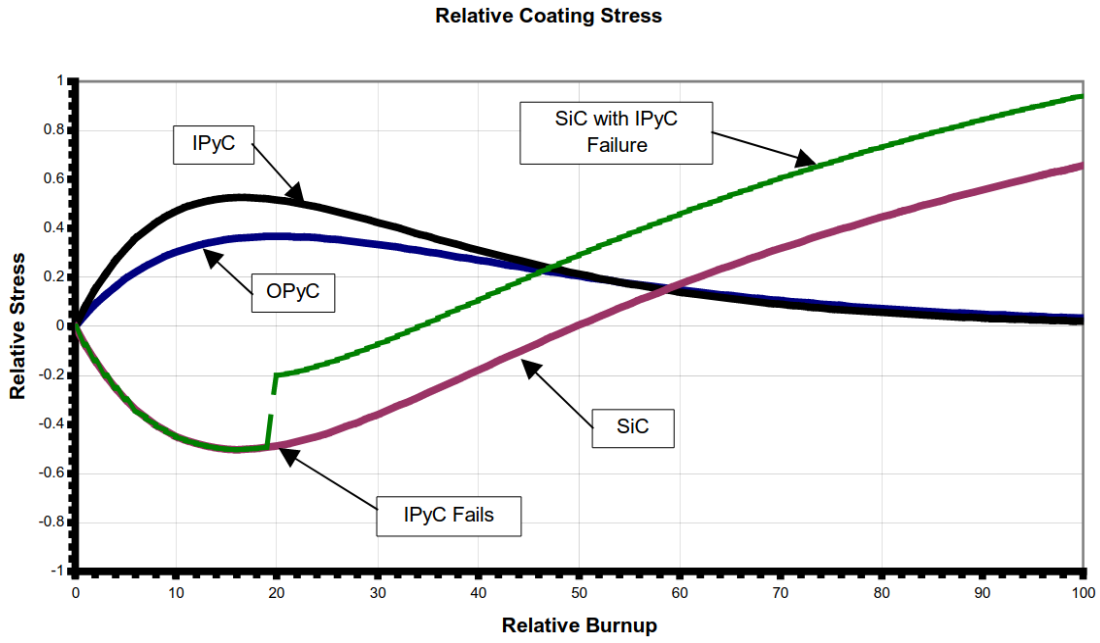

Figure 2.7: A qualitative representation of relative maximum stress for TRISO coating layers. From [Mor+04]

2.4.2 IPyC Crack induced failure

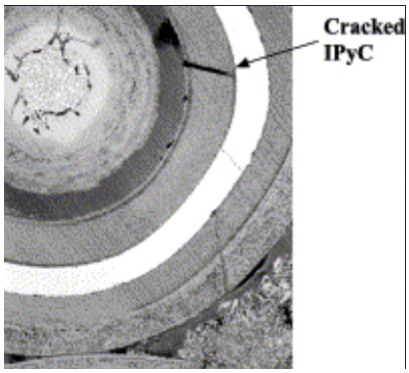

Figure 2.8: A TRISO particle with a cracked IPyC layer [Mil+01].

As explained in the paragraph 2.4.1, gas pressure builds up during irradiation. The pressure creates tensile hoop stress on the SiC layer, which is counteracted by the shrinkage of the inner and outer PyC layers. However, creep in the PyC layers lessens this beneficial effect, allowing stress on the SiC to become tensile and increase over time. Eventually, if the stress exceeds SiC fracture strength, "pressure vessel" failure occurs.

However, fuel experiments in the US have shown higher failure percentages than what is predicted from pressure vessel failure alone, indicating that other mechanisms can contribute to the failure of particles. Post irradiation experiments showed, among others, radial cracks in IPyC and OPyC layers, or particles with debonded IPyC-SiC layers. Those two mechanisms have been investigated, and are thought to cause a higher number of failures, as explained in this Section and in Section 2.4.3. [Mil+01].

How the IPyC cracking failure happens is well explained in [Mil+01]: in this article, the authors performed a simulation to evaluate if stresses in the IPyC layer due to shrinkage could cause a crack in that layer; after demonstrating the possibility of cracking, they simulated cracked particles to verify the stresses on the SiC layer.

Their simulation showed that the shrinkage of the IPyC layer induces tensile stress in that layer, later counteracted by creep: for this reason, the tensile stress in the IPyC layer reaches a maximum early during irradiation and then decreases over time, as shown qualitatively in Figure 2.7.

After verifying that the probability of cracks of this layer due to this tensile stress is not negligible, they performed a stress analysis of the SiC layer for a particle with a cracked IPyC layer: the research revealed a concentration of stress in the SiC layer close to the fracture tip, reaching a peak long before the internal pressure reaches its maximum value. Then they evaluated the probability of the SiC layer failure due to these stresses, concluding that that the cracking of the IPyC layer can be a significant contributor to the failure of particles.

As far as it regards dependences, in this study it is shown that cracking of IPyC is significant for particles with well-bonded SiC and IPyC layers, and that stresses in both IPyC and SiC layer are sensible to variation of the BAF anisotropy factor of the IPyC layer. Also, irradiation temperature plays a role, because lower temperature causes a lower creep relaxation and consequently higher stresses.

2.4.3 Debonding between IPyC and SiC Layers Failure

IPyC and SiC layers can debond from each other, as has been observed in many US irradiation tests; this failure mechanism is due to IPyC shrinkage and it occurs when the radial stress between the two layers exceeds their bond strength: this process is a gradual unzipping that starts from a weak interface point. This debonding can induce higher tensile stress in the SiC layer, in particular at the tip of the debonded region, causing eventually a SiC failure. Stresses due to the debonded layer are although smaller than in the case of cracked IPyC, and they can be relieved by irradiation-induced creep at longer times. Failure rates due to debonding are low, but not negligible [Mor+04] [MPM04].

From calculations made and reported in [MPM04], the number of failures due to debonding seems to be strongly dependent on the bond strength between IPyC and SiC layers, and on irradiation temperature. In fact, if the bond strength is low, the IPyC layer debonds readily, producing lower stress in SiC and resulting in a lower number of

failures; on the other hand, a high bond strength prevents radial stress from overcoming this bond, still resulting in a low failure rate. For these reasons, at intermediate bond strength, the number of failures due to this mechanism is expected to be greater. The dependence on irradiation temperature is due to the fact that creep in the pyrocarbon layer is higher at higher temperatures and it tends to alleviate stresses due to shrinkage, reducing the number of failures. Also, some material properties of the pyrocarbon affect the failure mechanism. For example, anisotropy (measured with Bacon anisotropy factor) plays a measurable role: in fact lower anisotropy results in a lower failure rate due to debonding [MPM04]. On the other hand, a different porosity of the pyrocarbon layer due to the manufacturing process can produce different bond tightness at the interface, and consequently different failure rates: to support this thesis, [Age10] displays two photomicrographs of German and US particles interface, showing that German fuel layers are more tightly bound; furthermore, it reports that German experiments, with this higher porosity of the pyrocarbon layer, never showed debonding during irradiation, with respect to US experiments.

2.4.4 SiC thermal decomposition

The SiC layer tends to undergo thermal decomposition into its constituent elements at very high temperatures (above 2000 °C). After the silicon evaporates, a porous carbon structure is left behind [MS19].

From the literature, this failure mechanism seems to be mainly temperature dependent [Mor+04]. In the article [ZT11], which summarizes fuel tests made by others up to 2600 °C, is concluded that the failure rate starts to increase significantly around 2200 °C, and almost all particles are failed at 2600 °C. It is also noted that fuel temperature above 1600 °C, if kept for a long period, can lead to failure. In fact, in [Mor+04] it is also reported that fuel release in general increases above 1600 °C, albeit releases in the range 1600°C - 1800 °C may be due to a combination of corrosion and decomposition. For these reasons, thermal decomposition is not considered an important mechanism of failure under normal conditions.

2.4.5 Kernel migration (Amoeba effect)

Kernel migration is the movement of the kernel toward particle coatings, away from the center of the particle. This movement is mainly caused by carbon transport due to the presence of a temperature gradient in the particle. If the kernel migrates too much and penetrates TRISO coating, it can lead to particle failure: when the SiC layer is eroded, the confinement function is lost.

But why does this mechanism happen? Oxygen is released from fuel material fission and firstly oxidizes elements with greater oxygen affinity. If free oxygen is still present, it reacts with carbon in coating layers, producing CO and CO_2. Normally there is

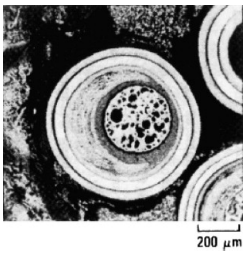

(a) A TRISO particle with kernel migration

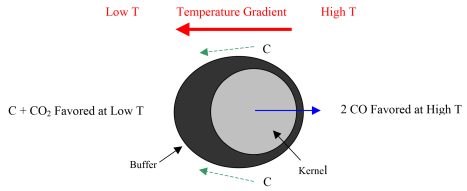

(b) An image that explains the process

Figure 2.9: A TRISO particle with kernel migration and an explanatory image of this process. respectively from [PW10] and [Mor+04]

chemical equilibrium between C, UO_2 and CO and CO_2, but with the presence of a thermal gradient the equilibrium is different at the different sides of the particle: for this reason, gases migrate down the temperature gradient to the colder side of the particle, where another reaction takes place and carbon return to the solid state. Over time, carbon builds up in the colder side and pushes the kernel towards the other side, up to the temperature gradient.

The literature reports that this mechanism is strongly dependent on temperature and macroscopic temperature gradient. Burn-up seems to be a secondary dependence or a non-dependence at all [Mak+07][Mor+04]. For these reasons, the potential for this mechanism to occur is lower in pebble reactor core design, due to the lower power densities and thereby lower gradients. To avoid this phenomenon oxycarbide kernel can be used, where no CO is produced and carbon transportation is not expected to occur.

2.4.6 Fission product interaction or attack and CO attack

Some fission products can migrate from the kernel to the other layer and interact with them. Special attention should be given to the SiC layer and elements that interact with this layer, because it is the main barrier for fission product confinement. In particular, noble metals are produced with relatively high yields under irradiation and thermochemical conditions make the formation of more stable oxides unfavourable, allowing them to diffuse out of the kernel.

As already said, experimental observation shows that Palladium (Pd) can interact with the SiC layer and cause its local thinning, and consequently a higher risk of failure.

Another metal of concern is Silver (Ag), both for UO_2 and UCO kernel. In fact, it has been observed that Silver can migrate through apparently intact particles and diffuse out of the particle. [Pet+03]

Fission product transport and consequently the attack seems to depend on temperature, temperature gradient and burnup [WPG21] [Pet+03], although the phenomenon is not fully understood. In particular, the degree of fission product attack seems to be

generally correlated with the temperature gradient in the fuel and so this failure mechanism should play a more important role in reactors with higher power densities [Pet+03]. Fission product attack is more significant for UO_2 fuel with respect to UCO ones because the UCO kernel can retain fission products better, as carbide or oxide with lower mobility. However, Pd transport has still been observed in UCO particles. Also, the enrichment of the fuel plays a role in the importance of the Pd and Ag problem: in fact, the yield of Pd and Ag is between 25 and 50 times higher for Pu than for U. At the end of the life of LEU fuel, a large part of the material that undergoes fission is Plutonium, and so the concentration of these two fission product can be higher in LEU fuel than in HEU with the same burnup. [Pet+03]

Furthermore, some fuel elements which were exposed at high burnup (over 14 % FIMA) and high fluence have shown in heating tests a greater release of fission products, like Cesium and Krypton, than other particles exposed to less severe conditions. The reason for this difference in release is not well understood, but some hypotheses on the underlying mechanism have been made.

In fact, some experiments made in the 70s have shown that Cesium vapor can produce a pitting attack of SiC at temperatures above 1500°C, depending also on silicon carbide microstructure, instead of a simple diffusion process. However, this process lacks of further experimentation. [Mak+07]

Another hypothesis is that the SiC layer can also be degraded or corroded by carbon monoxide CO, which is produced during irradiation of UO_2 kernels. In fact, as reported in the literature in [Min+91] and in [Age10], CO can attack the SiC layer if the IPyC layer becomes permeable or cracked, losing its protection function from CO (for example, after a crack due to shrinkage). When CO comes into contact with the SiC layer, the latter is oxidized. Due to its high rate of vapour transport from the corroded area to the cold part of the particle and the kernel, SiO gas is moved and in this region, it reacts to form SiO_2 or more stable oxides, and silicides with some fission products in the kernel. For these reasons, SiO_2 is not found in the corroded area, enabling CO to still react with the SiC layer [Min+91]. The kinetics of this these reactions are not fully understood, but they are thermodynamically possible. This mechanism may be significant at high burnup in UO_2 TRISO particle fuels where CO production is predicted to be considerable, in particular in the case of LEU kernel (at lower enrichment and higher burnup, a bigger amount of fission comes Plutonium and it has a greater oxygen release per fission with respect to Uranium) [Age10].

2.4.7 Matrix-OPyC interactions and OPyC irradiation-induced cracking

In the earlier irradiations of US fuels, a high number of failure cracks and debonding of the OPyC layer were observed. This kind of failure has been attributed to the fabrication

mechanism: the low-viscosity carbonaceous matrix material's infiltration into the OPyC during compact manufacturing and subsequent shrinking induced by irradiation can lead to failure.

To limit this failure mechanism, specification on matrix material and its injection were introduced, while German fuel did not exhibit any comparable behaviour due to the higher isotropy of the OPyC layer and the use of a high viscosity matrix/binder mix that does not penetrate the OPyC [Age10] [Mor+04].

This failure has been cited for the seek of knowledge and will not be discussed beyond, since it is not analysed further in the literature and because it concerns production processes that in some cases have already been outdated.

2.4.8 Creep failure of PyC

[Age10] reports that in some post-irradiation heating test photomicrographs, thinning and failure of the PyC were observed. It was primarily for tests where thermal creep can occur due to extended periods at high temperatures, above 2000 °C. However, it has not led to SiC failure.

This mechanism will not be further analyzed, considering that it is not studied in the literature and that it seems not able to induce a SiC failure and, in practice, that it refers to temperatures far above the expected operational temperature of the reactor.

2.4.9 Kernel-coating mechanical interaction (KCMI)

Kenrel coating mechanical interaction consists of the contact and mechanical interaction between the kernel and coatings: in fact, at a high enough burnup level, all the gaps between the kernel and coatings will unavoidably close because of kernel irradiation swelling. According to modelling studies, the SiC layer will fail soon, once KCMI starts.

This failure mechanism has not been observed in post-irradiation examinations, maybe due to cooling of the kernel, but it is evident that when efforts are made to get higher burn-up values, this failure mechanism may become more significant [Age10] [WPG21]. At present, no fuel performance code models this failure mechanism.

Considering the fact that the literature on this topic is poor and it doesn't seem a concern as far as really high burnups are reached (which is not the case for SNRs), this failure mechanism will not be further analysed: to find fuel safety criteria related to it, more experiments are needed.

2.5 Fuel safety criteria for TRISO

Retaining fission products within particles is crucial for the safety design of TRISO fuels in order to limit their release to the primary system. According to this perspective,

minimizing the failure fraction of the fuel coating layers as they are manufactured and preventing additional failures during operation are fundamental safety concepts. In particular, this work will focus on the latter concept, dwelling on what causes failures during operations.

Starting from the failure mechanisms previously identified, the literature will be reviewed and the major dependencies of these phenomena will be highlighted. Finally, starting from these dependencies, fuel safety criteria will be presented. These can be used in the design phase to focus on the evaluation of the most important phenomena.

2.5.1 Due to SiC thermal decomposition

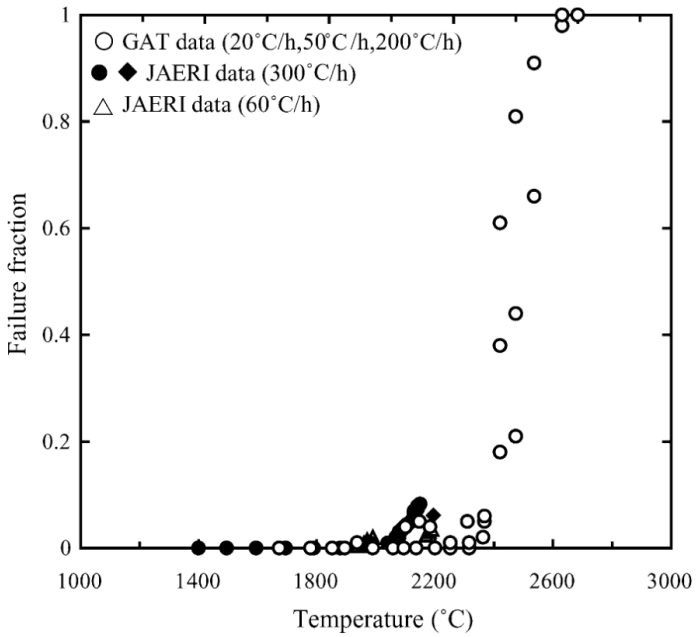

Figure 2.10: Failure fraction versus temperature of different experiment, from [SU04]

As reported in paragraph 2.4.4, the failure due to SiC decomposition is mainly temperature dependent and it is the primary failure mechanism in the temperature range between 1900 °C and 2500 °C [Nab+89].

Figure 2.10 reports the failure fraction of particles versus the temperature in different experiments. As shown, particle failure increases around 2200 °C, with almost all particles failing above 2400 °C [SU04]. The experiments shown were ramp tests of the order of tens of hours, but some authors ([ZT11] and [Mor+04]) report that temperature above 1600°C, if kept for extended period, can still induce a high failure rate: this

change in behaviour of SiC could be caused by different factors, including change in microstructure of SiC, decomposition or other mechanism like corrosion.

To be conservative, one could consider 1600°C as a temperature that should not be overcome during normal operation and anticipated transient, to ensure the safe continuation of reactor operation. This ensures also a safety margin that allows the temperature to be overcome in design basis accidents for a short period of time.

For all those reasons, the following fuel safety criterion can be set:

Fuel safety criterion 1: Limit SiC thermal decomposition - Temperature

The temperature of the SiC layer in the particles of the fuel shall not exceed 1600 °C during normal operation and at any anticipated operational occurrence, to avoid failures due to the thermal decomposition of the SiC layer.

If this criterion is met, the TRISO particles are unlikely to fail due to the decomposition of the silicon carbide layer. This criterion is also consistent with safety design requirements for the Japan HTTR reactor [STS94].

2.5.2 Due to pression vessel

As explained earlier, in TRISO particles gas pressure from fission gases and carbon monoxide builds up during irradiation, causing tensile stress on the SiC layer, which is initially counteracted by compressive stress from shrinking PyC layers, but as irradiation continues, the stress on the SiC layer increases and can lead to failure when it exceeds the SiC's fracture strength.

In general, the pressure vessel failure is influenced by parameters that modify the mechanical strength of the layers, like the layer thicknesses and the strength of the layer material, but it is also affected by parameters that condition the production of gases, like the kernel composition, and those that condition their accommodation, like the buffer density (a less dense layer has more void volume to accommodate gases).

However, the following analysis will focus on the factors influencing the increase in particle pressure, which are fission gas production and carbon monoxide production. As reported in the literature, both fission gas release from the kernel and CO production depend on burnup and temperature.

This dependence is complex, because of all the thermochemical interactions happening in the particle kernel and surroundings. For example, burnup determines the quantity of fission product in the kernel, and also its ability to retain fission gases decreases as burnup increases. CO production depends on temperature and burnup, and it involves, for example, the calculation of oxygen potential (the oxygen potential is determined by

	Temperature (°C)				
Burnup (%)	1100	1150	1200	1250	1300
8	1.00	1.28	1.62	2.04	2.52
10	1.33	1.69	2.14	2.68	3.28
15	2.26	2.86	3.60	4.47	5.42
20	3.32	4.21	5.28	6.53	7.89

(a) Fission gas pressure

	Temperature (°C)				
Burnup (%)	1100	1150	1200	1250	1300
8	1.00	1.15	1.28	1.38	1.44
10	1.35	1.55	1.71	1.84	1.92
15	2.16	2.46	2.72	2.92	3.06
20	2.84	3.24	3.60	3.91	4.16

(b) CO pressure

Figure 2.11: Comparison of fission gas and CO pressure in a German particle as temperature and burnup increase (normalized to 1.0 at 8% FIMA burnup and 1100 °C). From [Mak+07]

the amount of oxygen in the system and the affinity of particular elements for it), which depends on burnup.

The two tables in Figure 2.11, present thermodynamical calculations that make comparisons of fission gas pressure and CO pressure in a German particle as temperature and burnup increase, with values normalized to 1.0 at 8% FIMA burnup and 1100 °C. As can be seen, both fission gas pressure and CO pressure increase as burnup and temperature increase. For example, as shown in Figure 2.11a, the fission gas pressure increases by a factor of almost eight as temperature increases from 1100 °C to 1300 °C and burn-up from 8 to 20% FIMA. The CO production has a similar trend, with an increase of a factor of four with the same increase in temperature and burnup.

For these reasons, seems reasonable to establish two fuel safety criteria regarding temperature and burnup:

Fuel safety criterion 2: Limit overpressure failure - Temperature

The irradiation temperature of the particle during normal operation shall be limited, with a margin, in order to avoid tensile stress on the SiC layer, due to the total amount of pressure inside the particle, is above the ultimate tensile strength of the SiC layer during the lifetime of the reactor.

Fuel safety criterion 3: Limit overpressure failure - Burnup

The burnup of the particle kernel shall be limited, with a margin, in order to avoid that tensile stress on the SiC layer, due to the total amount of pressure inside the particle, is above the ultimate tensile strength of the SiC layer during the lifetime of the reactor.

The respect of these fuel safety criteria should be established with calculations from fuel performance models that take into account both fission gases and CO production.

Nevertheless, nominal TRISO particles are generally designed with a sufficient void

volume in the porous buffer layer, which is enough to avoid overpressure particle failure: in fact, the literature suggests that failure due to overpressure is dominated by failure of particles that do not meet design specification (for example, insufficient buffer layer or improper porosity) [Age10] [WPG21].

An interesting consideration in the evaluation of the best fuel for a space reactor is that CO pressure dominates internal gas pressure [ZT11], and so the two-phase UCO kernel should be considered as a good alternative to reduce this failure probability, as in UCO fuel the CO production is suppressed.

2.5.3 Due to Fission product interaction and CO attack

2.5.3.1 Palladium and Silver

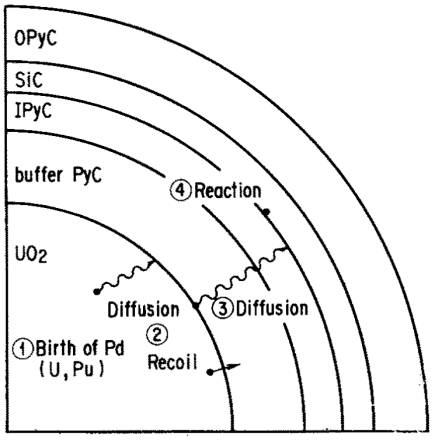

Figure 2.12: Steps of the corrosion mechanism of the SiC layers by Palladium, from [Min+90]. Step 1 is the birth in the kernel, step 2 is the release out of the kernel, step 3 is the transport to the Sic layer through the PyC layers and step 4 is the reaction with the Sic layer

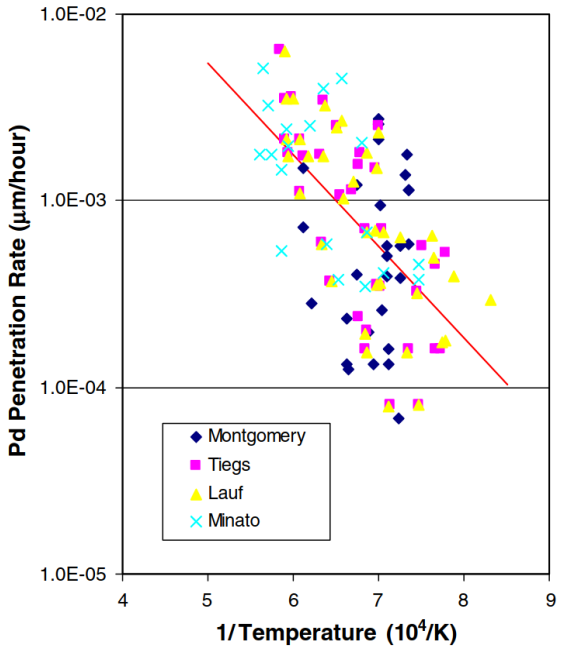

Figure 2.13: Pd penetration rate as a function of the inverse of temperature, from [Mak+07]. The graph reports results from different experiments, and the red line is the combined data fit, used in the PARFUME fuel performance model for Pd attack.

The literature agrees that Palladium attacks SiC in a localized manner. Furthermore, since a fully penetrating Pd–SiC interaction is expected to result in a loss of fission product retention in the SiC coating layer, the penetration depth of the Pd–SiC interaction should not be greater than the thickness of the SiC layer.

The process, by which the Palladium causes the SiC layer to deteriorate, can be divided into sequential steps, as shown in Figure 2.12: the birth of Palladium in the fuel kernel, its release from the fuel kernel (both because of diffusion and recoil as a fission product), its movement through the PyC layers and its reaction with the Sic layer.

Assuming that the slowest step limits the interaction between SiC and Pd, the authors of [Min+90] conclude that the release of Palladium from the kernel controls the reaction: in fact, the diffusion in the buffer and pyrocarbon layers is much faster than in the kernel, and the reaction of Palladium with the SiC layer is fast enough, as out-of reactor-tests suggest. Considering the release of Palladium from the kernel as the controlling reaction, the authors conclude that the factors influencing this reaction are: the composition of the fuel kernel, Palladium birth rate, irradiation temperature and time.

The dependence on kernel composition is not so strong [Mak+07], but generally UCO fuel can retain better fission products as carbides. Furthermore, low-enriched uranium fuel has a higher production of Palladium as burnup increases, due to the production of Palladium by Plutonium with a higher yield: however, also the dependence on burnup

is not so strong. For these reasons, no fuel safety criteria about the composition and burnup will be made.

Different authors report that Pd penetration in the SiC layer has an Arrenhius dependence on irradiation temperature, as shown in Figure 2.13. In this graph, palladium penetration rate results are reported as a function of the inverse of temperature. Then, all these data are fitted with an Arrenhius function, which is the red line in the graph. Furthermore, one of the main fuel performance models, called PARFUME, which is used to simulate the behaviour of TRISO particles, uses the combined fit of the data presented above.

For these reasons, it seems reasonable to set a fuel safety criterion on irradiation temperature to avoid the total penetration of the SiC layer making the particle fail:

Fuel safety criterion 4: Limit palladium attack - Temperature

During normal operation, the maximum irradiation temperature of the particle shall be limited to a value that ensures that the Palladium penetration rate during the irradiation lifetime of the reactor does not cause complete penetration of the SiC layer by the attack of Palladium, with a reasonable margin.

A precise value for this limit has not been found in the literature, and, indeed, it depends on the expected lifetime under irradiation of the reactor and the thickness of the SiC layer.

As far as the data by Tiegs are concerned, [Min+90] fairly points out that the data are scattered and it may be hard to conclude that the reaction rate is explained only by considering the irradiation temperature. For this reason, in their work, they calculated the total amount of Pd released from the kernel, with a complex function that takes into account burnup, diffusion coefficient, time and temperature.

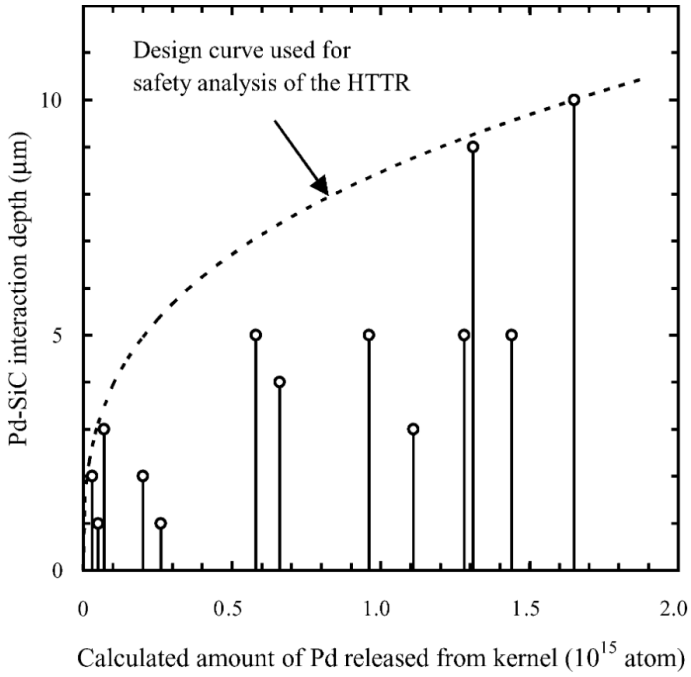

Figure 2.14: Pd-SiC interaction depth as a function of the calculated amount of pd release from the kernel. An open circle indicates the maximum reaction depth of a sample, while a vertical bar means that the reaction depths were distributed. Then, a cubic root function of the abscissa that envelopes all the results has been drawn, in order to be used for the HTTR safety analysis. From [Min+90].SE SERVE IMMAGINE SENZA FRECCIA, è depth amount.png

Then, they actually calculated the amount of Pd released from the kernel by the particle samples they were studying. After that, they plotted the observed reaction depth from their experiments, against the respective calculated amount of Pd released from the kernel, as can be seen in Figure 2.14. In this Figure, an open circle indicates the maximum reaction depth of a sample, while a vertical bar means that the depth values were distributed. A curve was drawn conservatively by authors to envelope the maximum reaction depths. They found that the envelope curve was expressed by a cubic function of the calculated Palladium amount released from the kernel, here called X, as

$$Y = aX^{\frac{1}{3}}$$

where a is a proportionality constant.

This formula has been used for the HTTR reactor safety analysis and for these reasons it is reasonable to settle a fuel safety criterion for the total amount of Palladium:

Fuel safety criterion 5: Limit palladium attack - Released palladium

The total amount of Palladium released from the kernel shall be limited to a value that ensures that the maximum expected Palladium penetration during the irradiation lifetime of the reactor does not cause complete penetration of the SiC layer by the attack of Palladium, with a reasonable margin.

Although other rare earth, metals and lanthanides are also produced (and some of them are less easily retained in the kernel than other elements), most of the literature focuses on Palladium, and it seems to agree that Palladium is the main concern. For this reason, the considerations made for Palladium could be considered conservative for the other elements. However, further experiments are needed to ensure that the considerations made for Palladium are also conservative for the other elements cited in precedent chapters. This is needed to gain a better understanding of their behaviour under irradiation conditions and the factors on which their behaviour depends.

The only exception is Silver, which is not retained by coatings, both pyrocarbon and SiC layers. The main concern is the isotope ^{110m}Ag, which has a half-life of 253 days and is produced by the neutron activation of ^{109}Ag, a fission product of low fission yield. For this reason, it is mainly a concern for radiological hazards for people working with primary circuit parts and unfueled graphite of the fuel element [NBO77].

The literature about Silver release has been analyzed by [RDR12], concluding that it is evident that more research is required because the mechanism underlying Silver transfer has not yet been identified. The hypothesis on causes are grain boundaries path, nano-cracks, some kind of SiC decomposition or Palladium attack, but no one of these explanations is completely convincing. Furthermore, limited work has been performed under neutron irradiation with the objective of identifying the Ag transport mechanism.

However, different authors in the literature agree with the fact that the diffusion of Silver in SiC is influenced by factors such as temperature and the microstructure of the SiC layer. While the causes concerning the microstructure need to be better investigated, to assess which production factors of the SiC layer influence the release of Silver, the irradiation temperature value can certainly be limited to avoid excessive silver release:

Fuel safety criterion 6: Limit silver release - Temperature

The irradiation temperature shall be limited, with a margin, to a value that ensures that the Silver release is within an acceptable value for SNR operations and maintenance.

The entity of the acceptable dose should be further investigated: as already said, the problem of Silver release is a concern mainly for its presence in the unfueled graphite matrix and for its presence in the primary circuit. In the current high-temperature reactor design, it is considered to be an occupational dose issue rather than a safety issue [Mor+04]. For these reasons, this problem could be approached by considering it in the context of a space reactor and the special characteristics this environment has. Just as an example, in a space reactor, the behaviour of the atmosphere is different, or human intervention should be kept to a minimum: the problem of radiological risk due to the primary circuit is indeed reduced. In addition, consideration could be given to shielding the reactor or the fuel element with a material that delays or blocks the release of Silver.

On the exact value of the limit further experiments are needed, and in literature only [NBO77] reports a temperature limit, saying that the temperature inside the particle should be kept below 1250 °C, from their available data in the seventies. Others, for example [Mor+04], report that silver is likely to be released only above 1100 °C.

2.5.3.2 Cesium attack

Although Cesium release is considered an important indicator of particle failure, the literature on the interactions of this element with the SiC layer is minimal. In fact, it seems that only experiments performed by Coen [CHQ72] in the 1970s demonstrate that Cesium vapour can attack the SiC layer: they found Cesium penetration in silicon carbide exposed to Cesium vapour at a temperature of 1500 °C and they report that this penetration depends on the microstructure of the SiC. So it seems that this process may depend on irradiation temperature and material properties of the SiC layer.

Unfortunately, no further experiments were made and, considering the minimal literature, it is difficult to extrapolate fuel safety criteria for this kind of process.

2.5.3.3 CO attack

About the attack of carbon monoxide, that oxidizes the SiC layer, in the literature there is no a clear dependence of this process on some parameter: the mechanism of corrosion seems to happen at reactor conditions when the CO gas comes into contact with the SiC layer because IPyC layer has failed, and its retention function is lost, as concluded in [Min+91]. A temperature dependence of this process can be possible, as CO pressure and production depend on temperature, and as lots of thermochemical reactions are involved in these processes.

Although it is difficult to extrapolate fuel safety criteria for the attack of carbon monoxide, one can consider reducing the failure probability by making conservative choices to reduce the production of CO, for example using a UCO kernel, and to reduce the failure probability of IPyC.

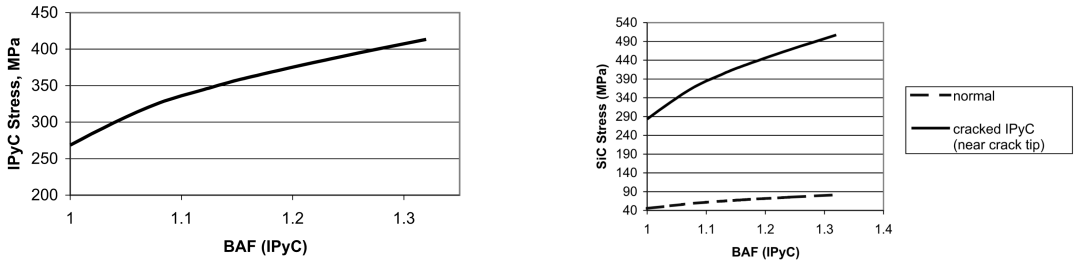

(a) Simulation of Maximum stress in the IPyC layer as a function of BAF.

(b) SiC stress as a function of BAF for an uncracked and a cracked particle (stress near the crack tip)

Figure 2.15: Both images are from [Mil+01]

2.5.4 Due to IPyC Cracking

As reported in paragraph 2.4.2, where this failure is explained, the shrinkage behaviour of the pyrocarbon layers is a beneficial characteristic, as they exert compressive forces on the SiC layer, counteracting gas pressure. However, this shrinkage produces tensile stress also in the pyrocarbon layer, which could crack and fail in some cases, if stresses are not relieved by creep.

The other big process that takes place in pyrocarbon layers that influence this failure mechanism is creep, which relieves stresses caused by shrinkage.

In general, shrinkage of the IPyC layer is a complex function of fast fluence, irradiation temperature, and coating material properties. In particular, in the article [Mil+01] particular attention is given to anisotropy of the IPyC layer and on temperature.

At first, they show that the magnitude of pyrocarbon strains increases as BAF increases, and so it does for increasing temperature too, as also reported in previous data on these strains. For these reasons, their simulation on an uncracked particle shows that the maximum stress in the IPyC layer increases as anisotropy (BAF) increases, as shown in Figure 2.15a. For the particle considered in their simulation, this also induces a higher failure probability of this layer as BAF increases, approaching 100% at a BAF of 1.33. These results pertain to particles with the IPyC layer that remains bonded to the SiC layer.

Then, they analyzed their simulation on a cracked particle. It shows that, at early stages of irradiation, the maximum stress in the SiC layer reaches a high tensile value in the vicinity of a crack tip, earlier than creep starts to relieve the stress in the pyrocarbon layer: before the internal pressure reaches its maximum amount, the stresses near the fracture tip have a peak and may lead the SiC layer to fail.

Furthermore, they showed that the SiC stress is sensible to BAF of the IPyC layer, both in the case of a cracked particle and an uncracked one, as shown in figure 2.15b, concluding that BAF is an important parameter that influences the stresses in both the layers, and consequently affecting the number of failures. The dependence on BAF is

also confirmed by experimental evidence, that suggests that this failure mechanism is not so important for isotropic pyrocarbon [Pet+03].

For this reason, a fuel safety criterion on the anisotropy factor of the pyrocarbon layer should be set.

Fuel safety criterion 7: Limit IPyC cracking - BAF

The BAF of pyrocarbon layers after the fabrication of TRISO particles shall be limited, in order to avoid an increase of particle failures due to cracks in the IPyC layer, with reasonable margin.

On the value of this limit, a hypothesis could be found in literature in [Ske+16]. In this article, using simulation with PARFUME fuel performance code, the authors identify critical limits above or below which an increase of fuel particle failure is expected to occur. For the IPyC BAF, the proposed range is below the value of 1.09. The calculation of this limit is however subject to uncertainties in material properties and was not added to the fuel safety criterion, but is however coherent with manufacturing values and other values found in literature: for example, [MS19] says that sufficiently isotropic layers that have a BAF value below 1.035 usually perform well under irradiation.

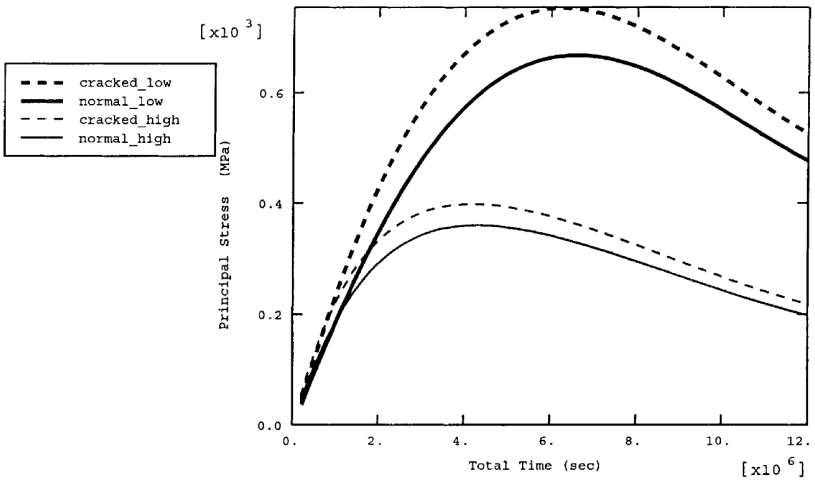

Figure 2.16: Stress history for normal and cracked particle, at 1200 °C (high) and 600 °C (low). Simulation from [Mil+01].

Swelling and creep depend also on irradiation temperature, which modifies in different ways various properties of both PyC and SiC layers. In particular, [Mil+01] shows that lower temperature induces higher stresses in both cracked and uncracked particles, as shown in Figure 2.16: in fact, although shrinkage is less at a lower temperature, creep

cannot relax the stresses caused by shrinkage. For example, the authors report that at 600 °C creep coefficient in pyrocarbon layers is about one-third of the coefficient at 1200 °C. The silicon carbide layer is also subject to the same phenomenon.

A value for the minimum irradiation temperature, to limit the IPyC cracking phenomenon has not been found in the literature, but a fuel safety criterion should be settled:

Fuel safety criterion 8: Limit IPyC cracking - Temperature

During normal operation, the irradiation temperature of the particle shall be greater, with a margin, than a value that ensures pyrocarbon layers in particles do not fail because of cracks.

Shrinkage and creep behaviour depend also on fluence. However, particle behaviour is dominated by dimensional changes in the early stage of irradiation and so, large tensile stresses in the IPyC that may lead to early failure. For this reason, and considering the fact that the reactor lifetime is required to be of the order of tens of years, seems reasonable to not limit fluence at too early stages, but to limit the other variables like BAF and irradiation temperature.

2.5.5 Due to debonding

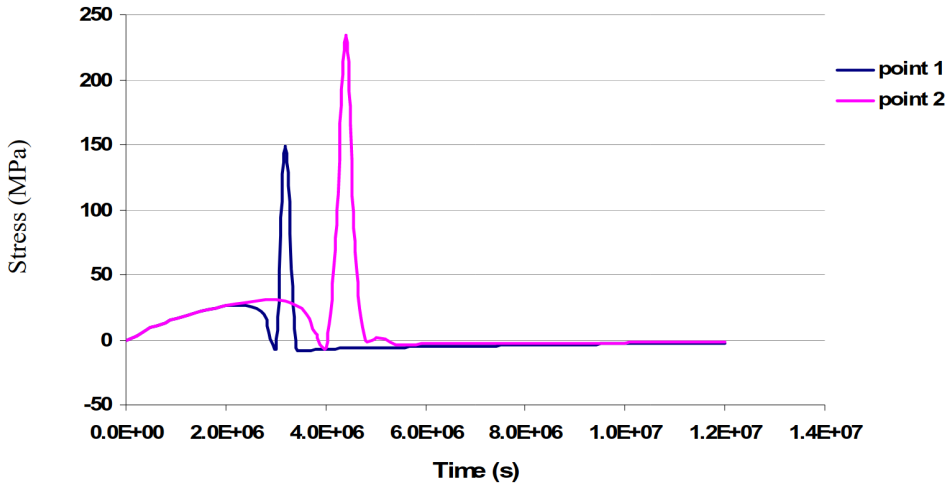

Figure 2.17: SiC layer stress histories of two points that experience debonding: the debonded region tip passes over point 1 before than point 2, so the peak is at a later time. Graph of simulation from [MPM04], in a coloured version from [Pet+04].

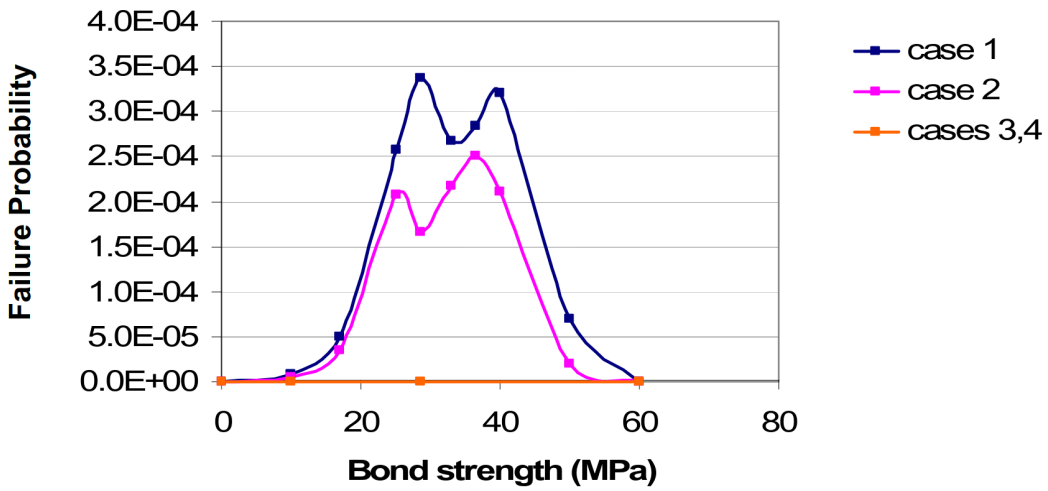

Figure 2.18: Failure probability due to debonding as a function of bond strength: cases one and two are at a lower temperature and differ for the BAF factor (lower for case 2); cases 3 and 4 are at higher irradiation temperature. Graph of simulation from [MPM04], in a colored version from [Pet+04].

As explained in paragraph 2.4.3, IPyC and SiC layers can de-bond from each other and it occurs when radial stress between the layers overcomes their bond strength, maybe in a weak interface point. Debonding can cause higher tensile stress in the SiC layer, especially at the tip of the debonded region, potentially leading to SiC failure. In fact, the passage of the debonded region tip causes a peak in the stresses of the SiC layer in that location, as shown in Figure 2.17 from simulation made in [MPM04].

The authors of this article have further investigated this failure mechanism using the PARFUME fuel performance code. With their simulations, they evaluated the failure probability caused by debonding failure alone as a function of bond strength between IPyC and SiC, and varying BAF and irradiation temperature for the different cases, as shown in Figure 2.18.

As far as it regards bond strength, results show that if the bond strength is low, the IPyC layer debonds readily, producing lower stress in SiC and resulting in a lower number of failures; on the other hand, a high bond strength prevents radial stress from overcoming this bond, still resulting in a low failure rate. Consequently, intermediate values of bond strength have higher failure rates. This trend can be seen both in case 1 and case 2, which have the same irradiation temperature (973 K), but different anisotropy (case 1 has a higher anisotropy - BAF=1.06 - than case 2 - BAF=1.03).

As mentioned above, the highest probability of failure is for intermediate values, so in principle one could choose values below intermediate values, which would cause readily debonded layers but consequently lower stress on SiC. However, a debonded particle might behave differently than expected in both mechanical and thermal aspects, e.g. in

the transmission of the heat produced: indeed, it seems reasonable and conservative to set the fuel safety criterion on bond strength imposing higher values than those that cause failure, avoiding debonded particle in this way.

For all these reasons, a fuel safety criteria should be set:

Fuel safety criterion 9: Limit debonding of IPyC - Bond strength

The bond strength between the IPyC and the SiC layers shall be greater, with a reasonable margin, than a minimum value, which will ensure that the debonding between those two layers is negligible, in order to avoid SiC failure.

A precise value for this criterion depends probably on the geometry of the particle under consideration, but it could be in principle found with simulation using fuel performance codes. This bond strength probably depends on the nature of the interface between the PyC and SiC layer: in fact, [Pet+03] says that a PyC layer deposited in a way that results in higher porosity produces a better-bonded interface between PyC and SiC, while a less porous surface of the IPyC layer may result in a less strong bond. However, there is little data about the actual bond strength between the IPyC and SiC layer, so further studies are probably needed.

As far as it regards temperature, a higher irradiation temperature induces higher shrinkage stress, that is however more than offset by the increase of pyrocarbon creep. As their simulations show [MPM04], authors conclude that a decrease in irradiation temperature increases the particle failures caused by debonding, as shown in Figure 2.18, where case 3 and 4, simulated at irradiation temperature of 1473 K, have no failure due to debonding. For this reason, a lower temperature limit during normal operation should be settled:

Fuel safety criterion 10: Limit debonding of IPyC - Temperature

During normal operation, the irradiation temperature of the particle shall be greater, with margin, than a value that ensures that pyrocarbon layers do not debond, in order to avoid SiC failure.

Finally, in [MPM04], authors report that anisotropy can have measurable effects on calculated failure probability. In fact, in Figure 2.18, case 2, which differs from case 1 because of a lower BAF, has a lower failure probability due to lower stresses. Although BAF dependency of debonding failure has not been investigated further in literature, for the sake of conservatism a fuel safety criteria on BAF should be set:

Fuel safety criterion 11: Limit debonding of IPyC - BAF

The BAF of pyrocarbon layers after the fabrication of TRISO particles shall be limited to a maximum value, considering also a reasonable margin, in order to avoid an increase of particle failures due to debonding of the IPyC layer from the SiC one.

No particular value for this criterion is found in literature, but it seems reasonable to assume that a lower value of BAF in general performs better than higher one, as far as it regards to failure.

2.5.6 Due to Kernel migration

In Section 2.4.5 it has been shown how and why the kernel migration takes place.

As already said, this failure is mainly temperature and temperature gradient dependent; in fact, the kernel migration distance $\vec{\delta}_{MIG}$ is defined as follows [Mak+07]:

$$\vec{\delta}_{MIG} = \int KMC \frac{\vec{\nabla} T}{T^2} d\tau$$

where $\vec{\nabla} T$ is the temperature gradient in the kernel, T the temperature, τ the time, and KMC the kernel migration coefficient.

This equation shows clearly the dependence of the migration distance on temperature and temperature gradient. KMC, however, is not a constant value and it depends itself on temperature: in fact, experimental results of KMC measurements are usually fitted with an Arrhenius function, as shown below:

$$KMC = KMC_0 e^{-\frac{Q}{RT}}$$

where KMC_0 and Q are two values that result from the fit and they depend on the kernel type and activation energy of the process (for example, UCO kernel has for sure a lower kernel migration coefficient with respect to UO_2 kernel).

An example of this kind of fit, used to obtain a kernel migration coefficient correlation for the PARFUME fuel performance model, is the red line shown in Figure 2.19. In this graph, which represents the kernel migration coefficient values versus the inverse of temperature, one can see that this coefficient is temperature dependent, with higher values when the temperature is higher.

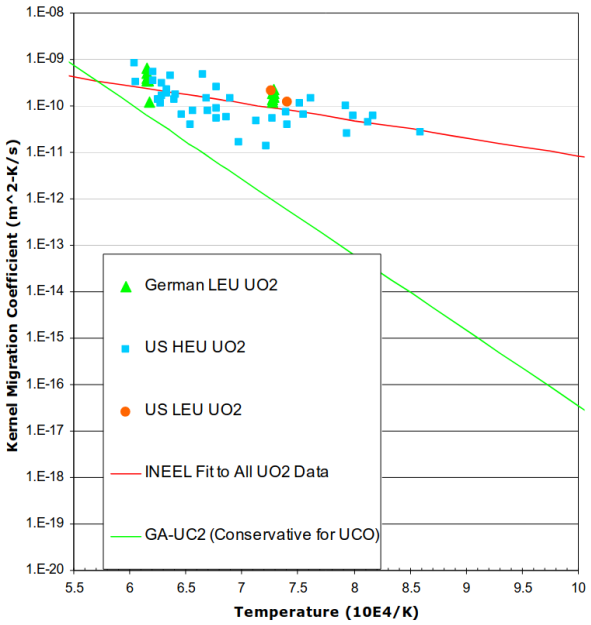

Figure 2.19: KMC from different experimental results as a function of the inverse of temperature, from [Pet+04]. In this graph, one can see the dependence of KMC on temperature. Blue and orange dots represent values from the US UO_2 experiment, while green dots from the German UO_2 experiment. References to those experiments can be found ibid. The red line is a fit to all UO_2 experiments with an Arrhenius function, while the green line is a fit to similar data for UC_2 fuel, which are however non shown because they are not public.

However, the temperature gradient term is dominant with respect to the temperature ones in the calculation of kernel migration distance [OFG21]; consequently, it seems reasonable to not settle a temperature safety criterion, and to consider as a conservative choice, the highest temperature in the fuel element in the calculation of kernel migration distance: in this way one should obtain the maximum kernel migration distance.

For all the reasons explained above, a fuel safety criterion regarding temperature gradient in the fuel compact should be established:

Fuel safety criterion 12: Limit kernel migration - Temperature gradient

During normal operation, the highest temperature gradient in the fuel compact shall be limited to a value that ensures that the migration distance during the expected lifetime of the reactor, is less than buffer plus IPyC layer thickness, with a reasonable margin.

Since the temperature gradient in the fuel compact is not uniform, it was chosen to consider the "highest gradient" in this criterion, so as to make a conservative choice that applies to the rest of the fuel compact.

According to the literature, this phenomenon seems to be not burnup dependent and so no safety fuel criteria have been developed. However, if the needed burnup for a space reactor lifetime is high, further experiments should be made in order to verify if the KMC has some kind of burnup dependence at high burnup.

In UCO kernels the production of CO is suppressed and no kernel migration is expected: in space reactors, this type of kernel could be considered as a viable alternative to minimize possible fuel failure mechanisms.

Chapter 3

Uranium Zirconium Hydride Fuel

3.1 History of this fuel

The history of Uranium zirconium hydride (UZrH) fuels dates back to the 1950s. UZrH was considered because of its ability to serve as both fuel and moderator, its thermal stability and its inherent safety characteristics.

In reactor technology, this fuel occupies a niche, with only some reactor programs having actual units used, or in function [Ola+09]. In particular, UZrH was used and developed in the SNAP (Systems for Nuclear Auxiliary Power) reactors program, where its compact size, reliability, and inherent safety characteristics made it suitable for space power applications.

Then, it gained popularity in the training and test reactor series of TRIGA reactors, which emphasized safety and ease of use. Other prototype reactors similar to TRIGA were built in China [Hui97].

On the other hand, among the proposed reactor designs without actual units produced, one may cite the hydride-moderated boiling-water superheat reactor [Gyl+62] and the MARVEL micro-reactor, actually under development [Eva+24].

Since almost all reactors that have used UZrH as fuel are part of the SNAP program or from the TRIGA series, a brief history of these two reactors will be presented below with particular attention given to the fuel [Ola+09].

3.1.1 History of SNAP program

The Space Nuclear Auxiliar Power (SNAP) program started in 1955 from a joint decision of the Air Force and the Atomic Energy Commission, that later became the Department of Energy. This program's objective was to develop compact, lightweight nuclear power sources for space, land, and sea applications, and it developed from the early studies made in the Pied Piper Program and the Weapons Systems 117-L program.

The SNAP program was terminated in 1973 because the emphasis shifted to radioisotope power sources, that were more aligned with the power needs of NASA's missions at that time [Vos84a].

The SNAP program developed different projects, with the even-numbered ones focusing on the development of reactor systems and odd-numbered ones developing radioisotope power sources. The SNAP program had different reactors tested, which will be presented below, and one that was tested and sent into orbit. Lastly, the SNAP 50 reactor was developed separately from the main program, it used different technologies that were never tested and will not be considered in this analysis [Vos84a].

3.1.1.1 SNAP reactors

SNAP Experimental Reactor (SER) was the first reactor built according to the program's specifications, achieving criticality in September 1959 and being operated until December 1961. The SER reactor was considered a success, leading the development of components and giving confidence in the development of the SNAP program;

Then, in 1961 the SNAP 2 Developmental Reactor (S2DR) was tested, with different studies made on the rate of reactivity changes caused by hydrogen loss and redistribution in the fuel and on transient response: all those testing increased the knowledge on reactor materials, and they were important to evaluate the performance of other SNAP reactors.

The next project, the SNAP8 project, was composed of two reactors: the SNAP 8 Experimental Reactor (S8ER), a proof-of-concept test reactor that was tested from May 1963 to April 1965, and the SNAP 8 Developmental Reactor (S8DR), which was a prototype flight system, but whose testing ended prematurely in December 1969 due to ruptured fuel cladding. The important conclusion that was drawn from these tests was the need to improve fuel rod design and the thermohydraulics of the system [Vos84a].

3.1.1.2 The SNAP 10A reactor

As already said, the only reactor that was flight-tested was the SNAP 10A, which was launched in April 1965 and operated only for 43 days because of a voltage failure in the electrical system. However, the overall mission was considered successful because the reactor itself worked as predicted from ground testing (which was completed successfully too) but also because it was correctly brought to the operating level and it confirmed that a space reactor could be safely launched into orbit [Vos84a]. Like almost all the reactors of the SNAP program, it ran with UZrH fuel and was designed for the production of about 500We.

The SNAP 10A reactor core consisted of 37 fuel elements, that will be presented later, arranged in a triangular array and held in place with grid plates, inside a vessel of stainless steel. Just to give an idea of the dimensions of the reactor vessel, it had a diameter of 22.5 cm and a length of 39.6 cm, as shown in Figure 3.1. The reactor had

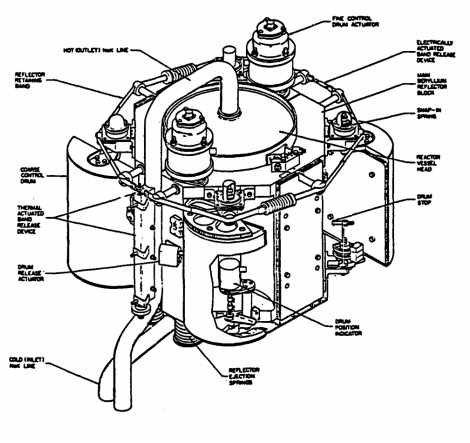

(a) a diagram of SNAP 10 exterior

(b) Snap 10 under testing

Figure 3.1: A diagram of the exterior part of the reactor and the reactor compared to a person. Respectively from [Vos84a] and Wikimedia Commons

a beryllium reflector layer and it had four semicylindrical control drums, regulating the neutron leakage from the reactor.

The reactor, relying on the fuel with its strong negative temperature coefficient, ran at a steady-state power without dynamic control. It could be shut down upon command with the ejection of the reflector parts [Vos84a].

The coolant was an alloy of Sodium and Potassium, that circulated through the core and the thermoelectric power conversion system. With the shield and the radiator, the overall system had a total weight of about 436 kg, with a height of 348 cm and a mounting base diameter of 127 cm [Vos84a].

This paragraph was a brief presentation of the history of the SNAP programme, with only the SNAP 10A reactor presented in more detail. The interested readers can deepen their knowledge in this reference [Vos84a]. Although the reactors in this programme had different characteristics, in terms of power conversion, power output, sizing, size and fuel characteristics, they all relied on UZrH as fuel (except for SNAP50).

3.1.2 History of TRIGA reactors

The TRIGA (Training, Research, Isotopes, General Atomics) reactor origin was a conference in Geneva on the Peaceful Uses of Atomic Energy, in 1955, when F. de Hoffmann, a nuclear physicist, was inspired by the conference to develop nuclear reactors for commercial use, leading to the creation of the General Atomic Division of General Dynamics Corporation.

In this new division, three groups were formed, one of which was assigned the chal-

lenge of designing a 'safe reactor'. This group, led by E. Teller and including the mathematician F. Dyson and the metallurgist M. Simnad, started to design this reactor that could be handled without risk, and that "could be given to a bunch of high school children to play with, without any fear that they would get hurt", as Teller said [Bar+16]. The group emphasized inherent safety in the reactor fuel, not only based on engineered safety, to ensure stability even if all control rods were removed.

The team quickly developed the TRIGA Mark I reactor, which became operational on May 3, 1958, at General Atomic's facilities in La Jolla, California, and was publicly announced on June 2, 1958 [Bar+16].

After the successful testing of this prototype, TRIGA reactors were commercialized with some design evolutions and, by the end of 1960, there were seven TRIGA reactors in operation, and by June 1967, 32 installations in 13 countries had been completed. One of the first TRIGA reactors was requested by The Italian National Committee for Nuclear Research, which began operations in 1960.

3.1.3 TRIGA reactors

General Atomics has developed six reactor designs under the trademark TRIGA: all of them have in common the principle of inherent safety and the use of UZrH fuels, evolving from the original 1958 concept to accommodate more complex irradiation experiments [Bar+16].

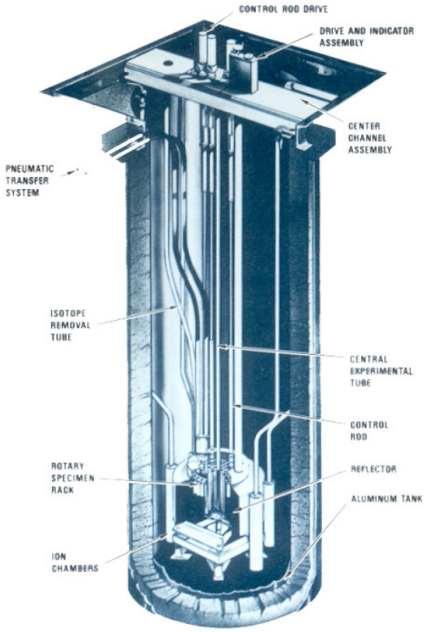

Figure 3.2: Cutaway view of the Mark I core, from [Bar+16].

(a) TRIGA Mark II in Rome

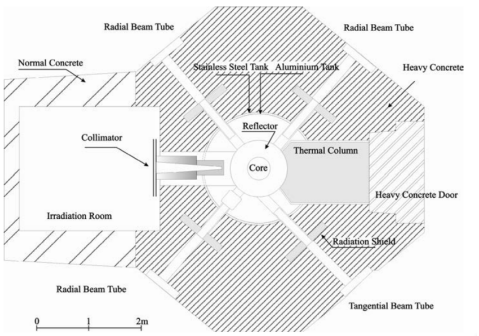

(b) Diagram of a mark 2 from above

Figure 3.3: A picture of a Mark II reactor and a diagram of Mark II reactor layout showing experiment column and neutron beam ports. From from [Bar+16].

The basic design of a TRIGA reactor is an open pool light water reactor, moderated both with water and the fuel element itself.

As one can see in figure 3.2, the initial TRIGA Mark I design was a below-ground reactor with a graphite reflector, cooled by natural convection and positioned in an aluminium tank. The Mark I was upgraded from its original 10 kW to 250 kW steady state and pulse power levels up to 1000 MW.

The Mark II reactor design is similar to the Mark I, with a fixed core and graphite reflector, but it is above-ground and contained in a concrete shell, as shown in Figure 3.3. It included beam ports for experiments: in fact, the ability to perform irradiation experiments had become an important feature of TRIGA reactors, and GA wanted to enhance this capability. The power of this reactor design goes from 100 KW to 2 MW in the steady state.

The Mark III design combines features of the Mark II and Mark F, a prototype reactor with a movable core which is suspended from the reactor bridge, as shown in Figure 3.4. Indeed, it has an open pool configuration, it is water reflected and cooled by natural convection. The movable core, the multiple beam columns and the dry exposure room inside the pool maximize experimental capabilities.

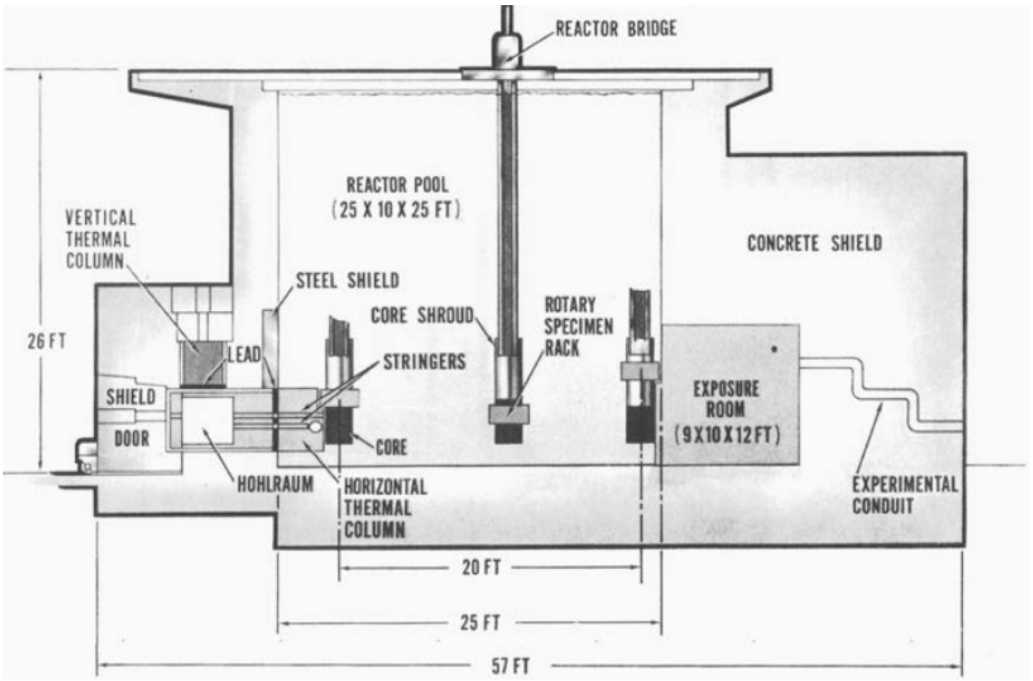

Figure 3.4: Cutaway view of the Mark III core with its movable core, from [Bar+16]

The Annular Core Pulsing Reactor (ACPR) design uses a modified fuel rod design to generate even higher power in pulsing. The main function of the ACPR is the study of materials under intense radiation for short time durations.

The Multi-Purpose Reactor (MPR) design is the highest power TRIGA reactor concept, with a more compact core configuration to produce steady-state power levels from 5 MW to 20 MW. [Bar+16].

TRIGA reactors have been used for educational and teaching purposes (e.g.: reactor physics and radiation measurement courses) and academic research. The research may cover almost all the fields of natural sciences and technology, especially medicine, biology, chemistry, geology and metallurgy.

Just as examples: the study of materials with neutron radiography, the study of aluminium corrosion for spacecraft, the behaviour of moisture in building materials, and the study of the performance of lithium batteries.

In medicine, it is of particular interest the study of Boron neutron Capture therapy, which is a technique for treating cancer, that needs a neutron flux because it is based on the nuclear capture and decay reactions that occur in Boron-10 when irradiated with neutron of appropriate energy. The academic research has also important implications for industrial uses [Bar+16].

3.2 Fuel structure

The fuel for SNAP and TRIGA reactors had different geometries and has been modified over time. TRIGA fuel rods, for example, have varied in terms of uranium content (from 8.5 to 45%), uranium enrichment (<20 to 93%), cladding type (aluminium, stainless steel etc...) and geometries. So here the fuel element of the SANP 10A reactor and a standard TRIGA fuel rod will be presented for the reader's knowledge.

3.2.1 SNAP 10A Fuel

The SANP-10 reactor fuel elements measured 32.6 cm in length and had a diameter of 3.17 cm. The cladding was made of a nickel-based alloy called Hastelloy N and had a wall thickness of almost 0.04 cm. The end of the fuel element was made of the same material welded to the cladding tube. The fuel material inside the cladding was 31.11 cm long with a diameter of 3.07 cm, and the gap of 0.0076 cm between the fuel and the cladding was filled with hydrogen to enhance heat transfer. To prevent hydrogen leakage, cladding tubes were coated with a special ceramic layer called Solarmic, which also included a burnable poison to decrease initial reactivity. For almost all the SNAP fuel, the Uranium was highly enriched [Vos84b].

3.2.2 TRIGA fuel

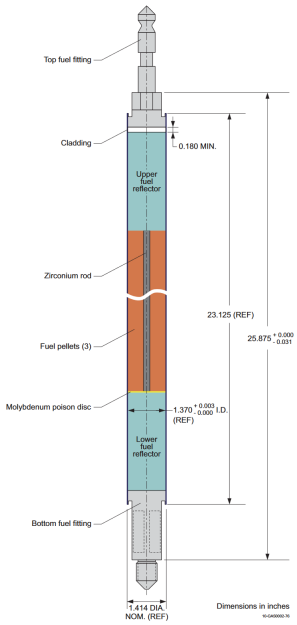

Figure 3.5: Cutaway of a standard TRIGA fuel rod, from [Bes+13]

The TRIGA fuel elements evolved over time, with rods made with different cladding, having different enrichment, uranium content, size, and presence of burnable poisons. For example, at first, the clad material used was aluminium, but, with increasing reactor power, it was later replaced by stainless steel and Incoloy-800.

Different fuel variations were created for specific core functions, including instrumented rods with thermocouples for temperature monitoring and fuel follower control rods (FFCRs, which are control rods with extensions that increase the reactivity when the control rod is withdrawn: usually, these regions are made of solid or hollow aluminium, or even with UZrH fuel). [Bar+16]

The standard TRIGA fuel element is a cylindrical rod whose length is approximately 71 cm, with a diameter of 3.8 cm. It is shown in Figure 3.5. The stainless steel cladding tube acts as a barrier to fission product release and contains the fuel material, which is a homogeneous mixture of Uranium and zirconium hydride. It is divided into cylindrical elements whose total length is 38 cm, with a hole of 6 mm diameter that runs through the centre of the fuel material, filled by a zirconium rod.

At the top and the bottom of the fuel material, there are graphite slugs that act as axial reflectors [Bar+16]. Between the fuel and the bottom graphite reflector, a 0.8 mm thick molybdenum disc is placed to prevent damage to the lower reflector and maintain the proper position of the fuel material. The early fuels also had samarium poison discs between the fuel rod and the graphite. Then there are end fixtures that help fuel positioning, handling and the correct flow of the coolant.

The fuel is a homogeneous mixture of uranium and zirconium hydride; however, H/Zr ratio and weight percentage of Uranium changed over the years. Early fuels previous to 1960 used a H/Zr ratio of 1.0, while now the H/Zr ratio is nominally 1.6. Regarding the weight percentage of uranium, at first TRIGA fuel elements contained 8.5–12 wt% uranium, enriched to 20%. Also, highly enriched versions incorporating erbium were made (70% to 93%), as reactors with higher power were developed. [Bar+16]

However, in the late 1970s, General Atomics developed fuels with a higher percentage of Uranium (up to 45%), but lowered the enrichment to LEU, to address proliferation issues. Fuel tests under irradiation and post-irradiation examination showed that the irradiation and structural behaviour of this high-density fuel are similar to those of the already proven 8.5 wt% and 12 wt% fuels.

The fuel development continued until 1996 at General Atomics' facility in La Jolla, California, when it was moved to France under TRIGA International [Bar+16].

3.3 Fuel characteristics and behaviour

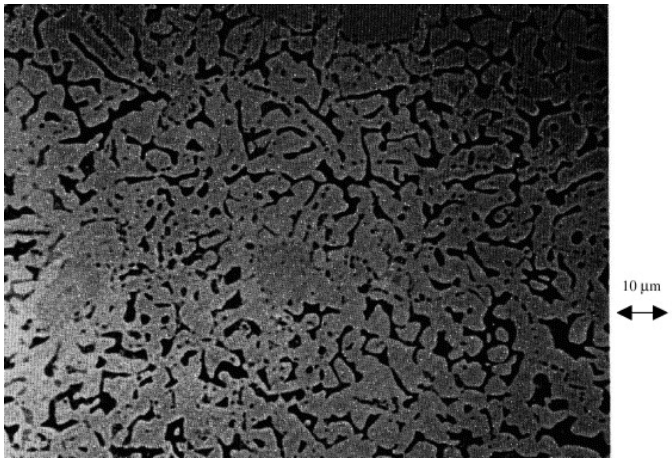

Figure 3.6: Microstructure of unirradiated UZrH fuel. Black areas are uranium metal; $ZrH_{1.6}$ is grey. From [ON05].

For a good understanding of the fuel performance, the knowledge of the fuel and moderator phase space is needed.

The fuel meat is created by hydriding an alloy of Uranium and Zirconium. During this process, Zirconium is hydrided and the uranium is usually believed to be rejected from the mixture, giving rise to a microstructure of finely dispersed uranium metal embedded in a zirconium hydride matrix, as shown in Figure 3.6, where black parts are uranium and grey parts are zirconium hydride. This microstructure is believed to be maintained all over the fuel cycle [Eva+24].

However, even if the fuel meat contains 30 wt% of uranium, the latter occupies only 11% of the total volume. Furthermore, the microstructural behaviour of the fuel is considered independent of uranium content up to 45 wt% uranium. Indeed, to better understand the fuel behaviour is useful to understand the zirconium hydride matrix thermophysical behaviour.

3.3.1 The phase diagram

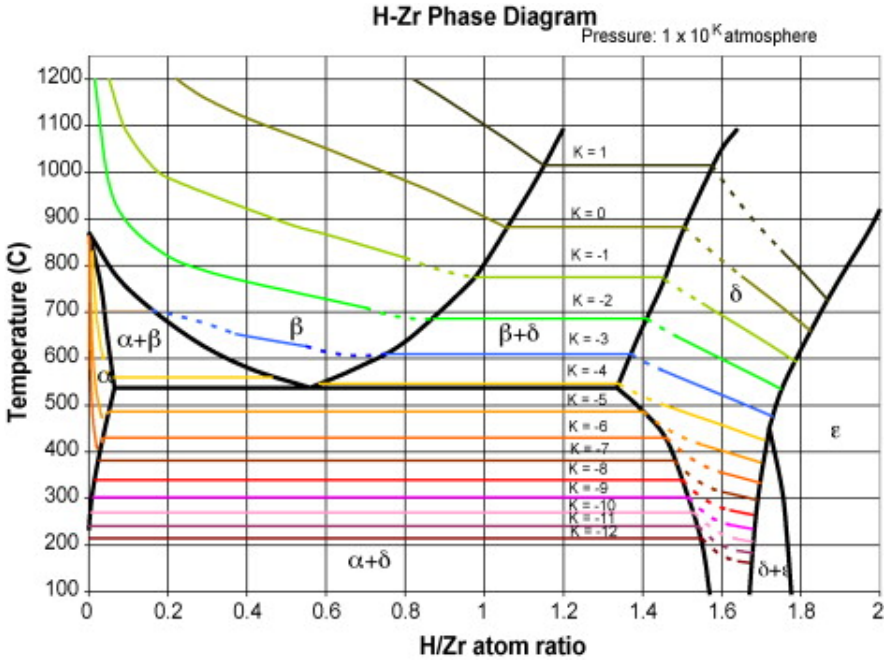

Figure 3.7: H-Zr phase diagram with isobars of equilibrium H_2 pressure superimposed. From [Ola+09]

ZrH is a simple eutectoid system, with at least four separate hydride phases. Figure 3.7 shows the phase diagram, the different phase regions and the equilibrium hydrogen pressure superimposed, which will be discussed later. The diagram is reported as a function of temperature and H/Zr ratio.

The hydride equilibrium phases are:

- an α phase, which is a solid solution of hydrogen in the hexagonal close-packed (alpha) zirconium lattice, it is present at a lower temperature.
- β phase, a solid solution where the hydrogen is dissolved in a body-centered cubic (bcc) zirconium phase, which is present at higher temperature
- δ phase, which is a face-centred cubic (fcc) hydride phase
- ϵ phase, which is a face-centred tetragonal (fct) hydride phase, that extends from the δ phase to ZrH_2; however, it is not a true equilibrium phase, being derived from the delta by a martensitic reaction

Then, there exist regions of the phase diagram where two or more of those phases coexist; for example, at room temperature, there is a δ plus ϵ region between $ZrH_{1.64}$ and

$ZrH_{1.74}$, whose width diminishes as temperature increases, closing at 455 °C at $ZrH_{1.70}$. Above this temperature, the two phases are divided by a single boundary.

In all these phases, tetrahedral interstitial sites are occupied at random by hydrogen [Zuz+90].

As already said, during the fabrication process, the uranium seems to be partially rejected by the solution and it is present as a fine and uniform dispersion. The addition of Uranium causes, in the phase diagram of the ZrH system, a slight shift of all the phase boundaries to lower temperatures. At higher uranium contents (25-50 wt.%), the phase boundaries are relatively unaffected in the region of high hydrogen content, while the β and α result markedly shifted (in particular, the range of the α phase is increased): in those cases, in fact, hydrogen is like a breakdown of the UZr alloy, reacting with zirconium and giving rise to a region of Uranium, zirconium and zirconium hydride phases [SFW76].

However, with the addition of uranium, no new phases were detected or uranium hydride either [SFW76].

Just to have an idea of the H/Zr ratio actually used, TRIGA reactor fuel has a nominal hydrogen-to-zirconium ratio of 1.6, which places it in the $\delta - phase$, while SNAP designs used an H/Zr ratio between 1.68 and 1.83 (ranging from δ to $\epsilon - phase$) [Ola+09]. The choice of 1.6, in particular for TRIGA fuels, ensures that the fuel remains in the $\delta - phase$ for a wide range of temperatures, eliminating density changes problem due to phase changes [SFW76].

3.3.2 Dissociation pressure

Another important thermodynamic property of the Zr-H system is the equilibrium H_2 pressure.

Indeed, metal hydrides become less stable with increasing temperature. In a sealed vessel, some hydrogen dissociates from the hydride to fill the internal free space and increase the pressure, while some other hydrogen already present in the gas phase recombines with the solid, lowering the pressure inside the vessel.

The hydrogen concentration in the metal hydride at the metal-solid surface, the hydrogen concentration in the gas phase (so, the hydrogen partial pressure), and the temperature at which the rates of hydrogen transfer from gas-to-solid and solid-to-gas are equal determine the equilibrium dissociation conditions.

For the $\delta - phase$, the equilibrium dissociation condition is usually expressed in literature with different (but equivalent) formulas, that link the logarithm of the equilibrium pressure $ln(p)$ with the inverse of temperature and the H/Zr ratio [Eva+24].

Equilibrium pressure is usually shown as isobars in the H-Zr phase diagram, as a function of temperature and H/Zr ratio. These isobars can be seen in figure 3.7.

3.3.3 Temperature distribution

The thermal conductivity of this metallic fuel is higher than those of oxide fuels, almost 5-6 times larger [ON05]. Thermal conductivity is almost independent or varies slightly with the H/Zr ratio. UZrH fuel with an H/Zr ratio of 1.6 (which is the ratio of general interest), even if it is difficult to calculate [Sim81], results to be independent of temperature and uranium weight fraction.

For all these reasons, the thermal conductivity can be considered constant: for a constant conductivity, the temperature distribution inside the fuel cylinder as a function of the radius is parabolic:

$$\frac{T(r) - T_s}{T_0 - T_s} = 1 - (\frac{r}{R})^2$$

where r is the radial position in the pellet, R is the fuel radius, T_s is the fuel surface temperature and T_0 is the fuel centerline temperature.

This is one way of modelling the temperature distribution; however, other ways to calculate the temperature distribution are available according to the design under consideration (for example, that considers the central zirconium rod in MARVEL fuel) [Eva+24].

3.3.4 Hydrogen redistribution

A peculiar characteristic of hydride fuel is the behaviour of hydrogen inside the fuel. In fact, hydrogen redistributes according to concentration gradient and to thermal gradient: hydrogen tends to move to colder regions and regions with a lower concentration of hydrogen.

So, considering an initial uniform hydrogen distribution and the temperature distribution presented above, the hydrogen tends to move to the colder periphery, resulting in a higher concentration in this region, but also to diffuse back due to the difference in concentration.

Although the difference in temperature between the centreline and the periphery is lower compared to oxide fuels, the heat of transport of H in the hydride is high: this ensures that a steady state hydrogen distribution is quickly reached. If the steady state is reached, it means that the flux is constant. Furthermore, considering negligible the loss of hydrogen from the fuel pellet, the radial flux J_r of hydrogen in the hydride is zero and equal to:

$$J_r = -D_S \left(\frac{\mathrm{d}C_S}{\mathrm{d}r} + \frac{T_Q}{T} \frac{C_S}{T} \frac{\mathrm{d}T}{\mathrm{d}r} \right) = -D_S \frac{\rho_{Zr}}{M_{Zr}} \left(\frac{\mathrm{d}C}{\mathrm{d}r} + \frac{T_Q}{T} \frac{C}{T} \frac{\mathrm{d}T}{\mathrm{d}r} \right) = 0$$

where D_S is the diffusion coefficient of hydrogen in the hydride, C_S is the concentration of hydrogen in the solid, T_Q is the heat of transport divided by the gas constant, T the

temperature, ρ_{Zr} the density of zirconium in ZrH_x, M_{Zr} the atomic weight of Zirconium and C the H/Zr ratio.

In the parentheses, one can see the terms deriving from the ordinary and the thermal diffusion.

From the above equation, one can get.

$$\left(\frac{\mathrm{d}C}{\mathrm{d}r} + \frac{T_Q}{T}\frac{C}{T}\frac{\mathrm{d}T}{\mathrm{d}r}\right) = 0$$

The solution of this equation in C is in the form of

$$C = Ae^{\frac{T_Q}{T(r)}}$$

where the constant A is obtained from a condition on the average H/Zr ratio (i.e. the average ratio should be obtained by integrating the ratio over the fuel meat radius, using the thermal distribution under consideration).

So, the H/Zr ratio, in a steady state equilibrium, has an exponential behaviour that depends on temperature, whose distribution depends on radius, as discussed above.

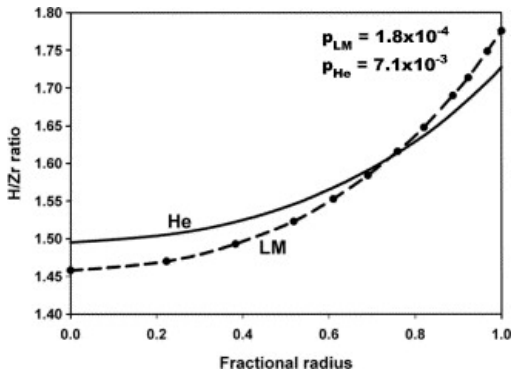

Figure 3.8: H/Zr ratio as a function of the fractional radius, for a LWR fuel pellet with helium or a liquid metal in the gap. From [ON05]

Indeed, Figure 3.8 shows how hydrogen redistribution affects the H/Zr ratio: in fact, it shows the H/Zr ratio as a function of the fractional radius of the pellet, for an LWR fuel pellet with helium or a liquid metal in the fuel-cladding gap. As one can see, hydrogen accumulates at the periphery (on the surface), with a depleted area near the centreline.

This fuel redistribution can cause different kinds of problems that will be further analysed:

- if the hydrogen, which is indeed the moderator, remains in the fuel there are no neutronic consequences of redistribution; however, if the H/Zr ratio increases at the surface of the fuel pellet, it increases the loss of hydrogen from the fuel meat;

- redistribution of hydrogen causes stresses in the fuel, in addition to the stresses due to thermal expansion, due to the change of density in the hydride; the density, in fact, decreases with increasing hydrogen content and the material expands;
- the loss of hydrogen from fuel to the gap and the plenum may induce an increase in pressure.

3.3.5 Fission products and fission gas release

During irradiation, hydride fuels produce fission products due to fission. At first during irradiation fission products like rare earth, Ba and Sr tend to form oxide with the oxygen impurity present in the fuel in the form of ZrO_2. This reaction frees some Zr reducing indeed the stochiometric H/Zr ratio. This depletion must be evaluated and therefore considered for an accurate analysis of the behaviour of the fuel under irradiation. However, being the oxygen considered as an impurity of 1000 wt ppm, this side reaction will not be further analysed.

Then, after the conversion of ZrO_2 in oxides, the rare-earth, Ba and Sr react with the zirconium hydride matrix and tend to form hydride compounds. The hydrogen is indeed extracted from the matrix and this results in a gradual decrease in the H/Zr ratio [Eva+24]. However, this process may not be as detrimental as it appears: the hydrogen removed from the zirconium hydride matrix remains in the fuel as fission product hydrides. Furthermore, these compounds are more stable thermodynamically than ZrH [Ola+09].

Then, also fission gases are produced. Data on fission gas release is not always robust or well documented, as for oxide fuels, and no clear or unique model can describe fission gas release from hydride fuel [Ola+09].

Literature, based on the available data, agrees on some key characteristics, such as the really low fractional release at lower temperatures (under 600-700°C) [Ola+09].Furthermore, it agrees with the fact that the fission gas release is controlled by two different mechanisms. All the gas release up to 400°C is solely or mainly by the recoil of fission fragments, while at higher temperatures another diffusion-like mechanism becomes more and more predominant. The fission gases then accumulate in the gap between the fuel meat and the clad, and at higher temperatures may increase the pressure inside the rod.

3.3.6 Fuel Swelling

The swelling behaviour of uranium-zirconium hydride fuels is different from oxide ones, which shrink and densify at the beginning of irradiation due to the destruction of porosity by fission fragment. The peculiarity of hydride fuels is that early in life they swell and, at higher temperatures, they do it consistently when compared to later swelling. This unusual swell is called *offset* swelling and consists of this rapid increase in volume if the

temperature is above approximately 650-700°C [Ola+09]. After this initial high swelling phase, the fuel continues to swell linearly with burnup, but at a lower rate, due to the accommodation of fission gases in the matrix.

So, to avoid the mechanical interaction between the fuel and the cladding, fuel safety criteria should be set on swelling of the fuel.

3.3.7 Negative temperature coefficient

The important inherent safety characteristic of uranium zirconium hydride fuel is the prompt negative temperature coefficient. It comes from the fact that the actual fuel and the moderator are mixed in the same fuel element. When the fuel is heated, the temperature increase of the hydride raises the probability that thermal neutrons, necessary for fission, will receive energy from exited oscillating hydrogen atoms in the lattice: gaining energy, the neutrons spectrum hardens in the fuel and results in a loss of reactivity. The coefficient is prompt because the actual fuel, uranium, is mixed with the solid moderator and their temperature raises simultaneously [Ato67]. This means that if the temperature in the fuel increases (for example because of a reactivity insertion), the reactivity reduces bringing the reactor to an equilibrium.

3.4 Identified failure

From the survey of the fuel behaviour, two main failure mechanisms have been identified. The first is the pellet cladding mechanical interaction, which can happen when the fuel, swelling at a higher rate than the cladding, comes in touch with the cladding exerting stresses on it.

The second one is the failure due to overpressure, from fission gases and hydrogen dissociation pressure.

Then, the effect of hydrogen redistribution and outgassing will be analysed. This issue regards the fundamental safety function of reactivity control primarily, but it will be analysed because a reactivity control loss may lead to a containment failure.

The fuel melting should be also considered as a failure and will be analysed.

Finally, the stresses inside the fuel meat will be analysed since can be deemed safety significant, meaning they do not directly influence the confinement function, as the fuel meat and the cladding are separate, but can contribute to failure.

3.4.1 FCMI due to fuel swelling

As already said, the swelling behaviour of hydride fuel is characterized by a peculiar and rapid increase of fuel swelling at the early stages of irradiation. This 'offset swelling' is attributed to the formation of voids, that were found with microscopic examination,

near Uranium particles. These voids are not fission-gas bubbles, but rather true voids formed by the condensation of irradiation-produced vacancies, with a process similar to the production of voids in stainless steel in breeder reactors. However, the possibility that those cavities contained fission gas was not investigated, and this mechanism is not supported by other experiments on unfueled hydride: for these reasons, the physical reason of the early offset swelling mechanism remains, indeed, unknown [ON05].

From experiments, offset swelling results to be highly temperature sensitive, increasing with the temperature at temperatures above 700 °C. However, this offset behaviour is negligible at temperatures lower than 650 °C. It is also dependent on the fission rate, with a higher burnup rate associated with lower offset swelling [Ola+09].

Offset swelling saturates at a certain burnup level. Saturation seems to be reached at approximately around 10^{-3} FIMA burnup. This saturation may be explained by some theories on the saturation of void growth in metals: [Ola+09] cite two of them. The first one consider a stationary state where all voids are connected by curved dislocations, without free dislocations left to climb, counteracting the preference of interstitials for dislocation lines, which is the root cause of void swelling in metal. The second model examines the effect of dislocation loops near voids which makes the void behave like a dislocation and consequently, point defects from irradiation are either annihilated by recombination or equally distributed between voids and dislocations, leading to the cessation of void growth.

However, these theories are based on the creation of voids due to fast neutron irradiation, while in hydride fuel the principal atom displacement agents are fission fragments. Furthermore, it is not excluded that other models could explain this process [Ola+09]: the origin of saturation remain still unknown.

Then, after the cessation of offset swelling, the swell continues due to the accommodation of fission products. This process is almost independent from temperature.

The studying and analysis of the swelling behaviour are important to avoid the closure of the gap between the fuel and the clad and to avoid indeed the interaction between them, also called Fuel cladding mechanical interaction (FCMI) [Ola+09].

3.4.2 Pressure increase

3.4.2.1 Due to fission gases

As said earlier, literature agrees that fission gas release from hydride fuel seems to be really low. However, data and experiments on fission gas release are not always robust or well-documented.

All the literature reviewed agrees on the fact that fission gas release from hydride fuel is the result of two mechanisms. The first one, which predominates at lower temperatures, is the fission fragment recoil into the gap between the fuel and the cladding; this mechanism is independent from temperature and depends only on the surface-to-volume

of the fuel element design [SFW76]. Then, at higher temperatures, the predominant fission gas release mechanism seems to be some kind of diffusion process, which is not well modelled and understood as in the case of oxide fuels [Ola+09]. The exact temperature at which one mechanism becomes predominant on the other one is not clearly defined and it is in the range between 400°C [SFW76] and 700°C [Ola+09], according to different authors. The second process depends on temperature, surface-to-volume ratio, time of irradiation and isotope half-time [SFW76]. However, fixed the design (and so the surface-to-volume ratio), and considering that some experiment indicates that the effect of long-term irradiation on fission product release is small [SFW76], the main dependence remains the temperature. However, even at higher temperatures, around 800°C, the fission gas release fraction is much lower than oxide fuel at their maximum temperature of 1500°C [Ola+09]. Fission gas production from high-burned fuel seems to not differ from fresh fuel [SCW88].

3.4.2.2 Due to hydrogen pressure increase

Another factor that may increase the pressure inside the cladding is the dissociation of hydrogen from the zirconium hydride. The pressure caused by hydrogen is the equilibrium pressure cited above, which represents the pressure that is reached inside a volume when the process of hydrogen dissociation reaches equilibrium. As already said, for the $\delta - phase$, this pressure can be calculated with different formulas, that usually link the pressure natural logarithm $ln(p)$ with a function of the H/Zr ratio and the inverse of temperature, which can be found for example in [SFW76] and [ON05].

Whatever the cause, the stresses caused by the pressure must not exceed the ultimate tensile strength or the ductility limit of the cladding to avoid the rupture of the latter.

3.4.3 Hydrogen loss from fuel meat

The equilibrium pressure of hydrogen could in principle be high enough to reduce the H/Zr ratio in the fuel with a consequent loss of hydrogen in the gap and plenum of the fuel rod. This behaviour may be deleterious because the loss of hydrogen from the fuel meat could reduce its inherent safety characteristic, the prompt negative temperature coefficient.

This problem certainly falls into what may affect the fundamental safety function of reactivity control, however, a temperature rise due to the loss of negative temperature coefficient could lead to various subsequent problems, that could affect the confinement of radioactive material and the integrity of barriers too. For this reason, this problem will be analyzed.

As already said, the equilibrium pressure of hydrogen depends on the H/Zr ratio and temperature. So the loss of hydrogen from the fuel meat should depend on these two

variables too. For sure, the quantity of hydrogen loss depends on the space available around the fuel meat and consequently on the design of the fuel rod.

However, the kinetics of the process behind the release of hydrogen from the surface is still not well understood [Ola+09] and other dependencies may be present.

Finally, in the specific case of a zircaloy cladding, to further prevent the hydrogen absorption or permeation of hydrogen into the cladding, [Ola+09] proposes some remedies, like the use of stainless steel, or providing an hydrogen impervious coating layer inside the cladding, or the use of a liquid metal in the fuel cladding gap.

3.4.4 Fuel melting

Another failure that can influence both the radioactive material confinement and the reactivity control is the fuel melting. The fuel should remain in the shape foreseen by design and safety considerations. This failure is, indeed, temperature-dependent. However, this temperature dependence may be influenced by the design factor, such as the cladding material, because zirconium hydride can form eutectics with some cladding material if they are in contact [Eva+24].

3.5 Stresses inside the fuel meat

The stresses in the fuel meat do not directly affect the fundamental safety function of confinement of radioactive material, as they do in the TRISO. A crack in one layer of TRISO can induce higher failure probability or even the loss of particle confinement if the layer is the SiC one. In fuel with separate fuel meat and cladding, stresses or cracks in the fuel meat are less important and may be detrimental to fundamental safety functions only in very unlikely conditions. For these reasons, stresses in the fuel meat will be presented for the reader's knowledge, but no fuel safety criteria will be set.

The main causes of stresses in UZrH fuel are the thermal stress and the so-called "hydrogen stress". The first one is due to thermal dilatation, while the latter is due to hydrogen redistribution, which causes dimensional changes in the fuel. Indeed, zirconium hydride density decreases with hydrogen content, and so the material expands.

The stresses in cylindrical fuel meat are usually analysed starting from the three general principles presented in the section about mechanical modelization in the TRISO fuel: the stress and strain relation, the equilibrium condition and the compatibility relation.

The stress and strain relation presented in a general way with tensor, in the case of cylindrical coordinates, and in the case of UZrH reduces to [ON05]:

$$\varepsilon_r = \frac{1}{E}[\sigma_r - \nu(\sigma_\theta + \sigma_z)] + \alpha\Delta T, \tag{3.1}$$

$$\varepsilon_\theta = \frac{1}{E}[\sigma_\theta - \nu(\sigma_r + \sigma_z)] + \alpha\Delta T, \tag{3.2}$$

$$\varepsilon_z = \frac{1}{E}[\sigma_z - \nu(\sigma_r + \sigma_\theta)] + \alpha\Delta T, \tag{3.3}$$

where ε_i are the radial, azimuthal and axial strains, σ_i are the radial, azimuthal and axial stresses, ν the Poisson ratio, E the Young modulus and α the linear thermal expansion coefficient.

The strain compatibility equation in cylindrical coordinates, when plane strain is assumed (ϵ_z is constant), is

$$\frac{d\varepsilon_\theta}{dr} + \frac{\varepsilon_\theta - \varepsilon_r}{r} = 0,$$

while the equilibrium condition is

$$\frac{d}{dr}(r\sigma_r) - \sigma_\theta = 0.$$

With these three sets of equations, one can calculate the three components of thermal stresses. The hydrogen stress in [ON05] is described mathematically with a relationship very similar to that of thermal expansion, with the substitution of $\alpha\Delta T$ with $\beta\Delta C$ and T with C, where C is the H/Zr ratio and β is the linear coefficient of hydrogen expansion. This coefficient is obtained in [ON05] taking $\frac{1}{3}$ of the fractional volume change.

[ON05] made a stress analysis, on the design under consideration (a LWR rod fuelled with UZrH pellets) and considering a parabolic temperature distribution in the pellet. According to this analysis, the thermal stresses in general increase with radius, starting as compressive near the centreline and becoming more tensile with radius. On the other hand, the hydrogen stress tends to decrease at the pellet periphery and become more and more compressive.

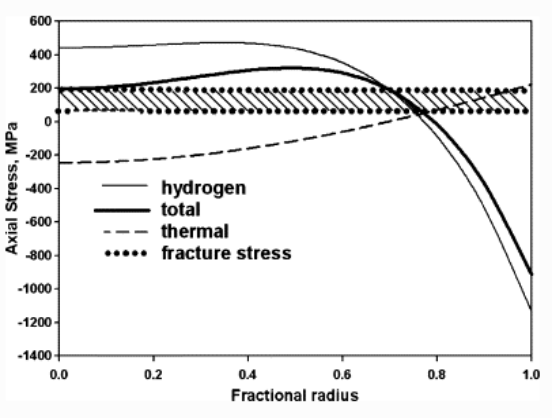

Figure 3.9: Axial stresses in an LM-bonded hydride fuel rod, from [Ola+09]

[Ola+09] summarize the consideration made in [ON05] showing the Figure 3.9. It represents the hydrogen, thermal and total stress for an LM-bonded fuel rod, which seems to be the more stressful condition. In particular, it shows the axial components, because these components are larger than azimuthal and radial ones. The total stress is calculated as the sum of hydrogen and thermal stress

$$\sigma_i^{tot} = \sigma_i^{thermal} + \sigma_i^{hydrogen}$$

where i means radial, azimuthal or axial stress. Figure 3.9 also shows the region of the fracture stress of ZrH. It is shown as a region because, as far as it regards the tensile fracture stress, [Ola+09] reports different values: 200 MPa and 55 MPa for tensile stress, and 100 MPa, for compressive one. Furthermore, the value of 200 MPa was found for ZrH_1 at room temperature, but the dependence on temperature and H/Zr ratio is unknown. More studies are indeed needed to understand which value is more accurate and to understand if it is dependent on some variable.

As one can see in the Figure 3.9, the thermal stress alone could crack the fuel meat at the surface, but its action is counteracted by the hydrogen stress which is highly compressive at higher radii. Even if the fracture stress is exceeded in the interior of the pellet, [ON05] says that is unlikely that cracking will occur because these region are surrounded by compressive regions.

However, some considerations should be made. The two kinds of stresses have different time responses, being the thermal stress developed as soon as the temperature distribution is reached, while the hydrogen stresses are developed according to the diffusion of hydrogen, which usually takes more time than the thermal equilibrium. So the interpretation of this paragraph and possible safety analysis should take these time differences into account.

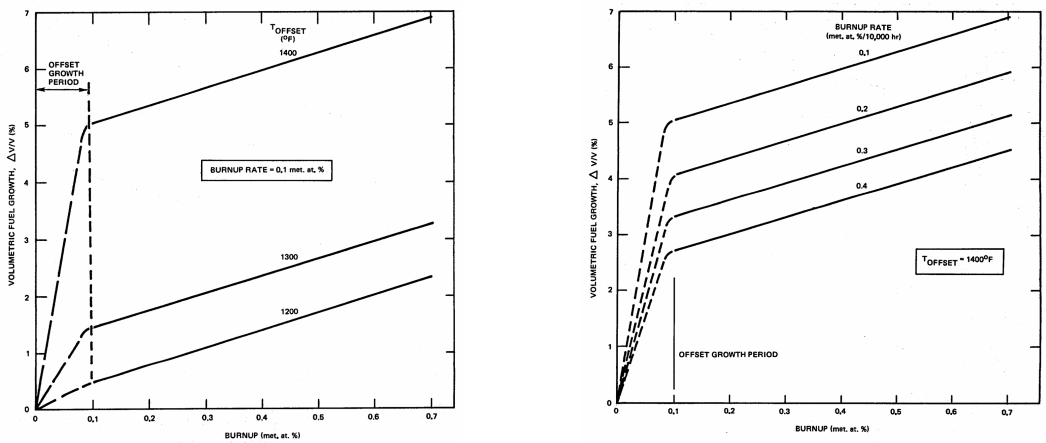

(a) Effect of offset temperature

(b) Effect of Burnup rate

Figure 3.10: Effect of offset temperature on fuel growth for a constant burnup rate, and the effect of burnup rate on fuel growth at constant offset temperature. From [Lil+73]

3.6 Fuel safety criteria for UZrH

3.6.1 FCMI failure due to fuel swelling

As presented above, the swelling behaviour of hydride fuel shows a rapid increase at the early stages of irradiation, known as "offset swelling," due to the formation of voids near uranium particles. After offset swelling ceases, swelling continues due to the accommodation of fission products.

To understand the fuel swell behaviour, let's take a closer look at the plots that show the dependence of swelling on various variables in Figure 3.10.

The information and details about the experiments that lie under the swelling plots have not been found [ON05]. For example, the H/Zr ratio of the fuel from which data are obtained is not known.

The swelling behaviour correlation was developed with a semi-empirical model that was used to fit irradiation test data. In general, it is in the form:

$$\frac{\Delta V}{V} = A_g + B$$

where $\frac{\Delta V}{V}$ is the fuel growth (%), A_g is a function that represents offset growth, while B is a function that represents the linear growth associated with solid fission product [Lil+73].

For example, the function that correlates better with the dataset containing selected

data of irradiation of the SNAP S8DR reactor is this one:

$$\left(\frac{\Delta V}{V} - 3b\right) = 5.5 \exp\left(-\left\{2.3\dot{b} \exp\left[\frac{21.5}{2}\left(\frac{1860}{T} - 1\right)\right] + 21.5\left(\frac{1860}{T} - 1\right)\right\}\right)$$

where $\dot{b}$ is the burnup rate, expressed as burnup/10,000 hr of operation, T the temperature expressed in Rankine degree of fuel at the time of completed offset swelling, b the burnup expressed as 100 FIMA [SFW76]. As one can see, on the left there is a term that depends on burnup and represents swelling after the offset one, while on the right there is a term that represents the offset swelling. Figure 3.10 illustrates the temperature, burnup and burnup rate dependencies expressed by this correlation [Lil+73].

The swelling behaviour of UZrH can be described with other similar relations, that link together the same variables [Eva+24].

Figure 3.10a shows that offset swelling is indeed large and is temperature dependent, with higher offset swelling with increasing temperature. For temperature, [SFW76] specifies that it is intended the average temperature that the fuel reaches after the offset swelling has been completed. As one can see, fixed the burnup rate of 0.1 FIMA/10,000 hr and at the end of offset swelling, at 760 °C the $\frac{\Delta V}{V}$ is almost 5%, while it is negligible at a temperature of 650 °C. Then Figure 3.10b shows the dependence of offset swelling on burnup rate, with increasing swelling with lower value of burnup rate. As one can see, the effect on offset swelling of decreasing the burnup rate, at higher temperatures, is lower than the effect of increasing temperature at the lower burnup rate.

So it seems reasonable to set a fuel safety criteria on temperature at the lower foreseen burnup rate, to limit excessive swelling:

Fuel safety criterion 1: Limit FCMI - Temperature

The average temperature of the fuel at the end of offset swelling shall be limited, with a reasonable margin, to a value that ensures that fuel swelling does not cause interaction between the fuel and the cladding which could lead to failure of the latter.

As far as it regards TRIGA fuel, this value is sometimes set to the value of 750 °C for the centreline temperature of the fuel [Ola+09]. For some other authors, this limit may be aggressive and they suggest a value of 650 °C [Ola+09]. This limit refers to the normal and steady state condition of the reactor, as this limit is increased to higher values as far as it regards pulse heating of the reactor.

Then, following the relation presented above, is reasonable to set a fuel safety criteria on burn up rate:

Fuel safety criterion 2: Limit FCMI - Burnup rate

The burnup rate shall be greater, with a margin, than a value that ensures that fuel swelling does not cause interaction between the fuel and the cladding which could lead to failure of the latter.

No value for this limit has been found in the literature, probably because the effect of temperature seems more demanding than burnup rate one.

Finally, to ensure that swelling after the offset one does not cause FCMI, a fuel safety criteria on burnup can be set:

Fuel safety criterion 3: Limit FCMI - Burnup

The burnup shall be limited, with a reasonable margin, to a value that ensures that fuel swelling does not cause the interaction between the fuel and the cladding which could lead to failure of the latter.

Even for this limit, no value has been found in the literature.

While the first two limits (on temperature and burnup rate) are set mainly to reduce the effects of offset swelling, the limit on burnup regards mainly the swelling after the end of offset swelling. But the principle of avoiding contact between fuel and cladding throughout the entire life of the fuel should be always considered while setting those limits.

However other research and data are needed to better understand the swelling behaviour of hydride fuel. For example, [Ola+09] points out that it is improbable that experiments considered by [Lil+73] accurately measured the burnup of saturation of offset swelling and that it seems unlikely that saturation of offset swelling occurred at 10^{-3} for all the temperatures and burnup rate.

3.6.2 Due to overpressure

The basic principle to maintain the intactness of the barrier is that stresses due to the pressure inside the cladding should not overcome the ultimate tensile strength of the clad material. So, the following analysis will focus on the factors influencing the increase in particle pressure, which are fission gas release and hydrogen equilibrium pressure.

3.6.2.1 Due to hydrogen equilibrium pressure

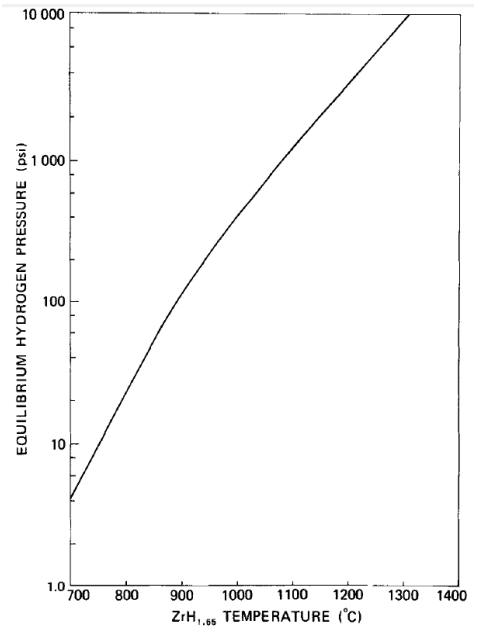

Figure 3.11: Equilibrium hydrogen pressure versus temperature for $ZrH_{1.65}$

As explained above, the equilibrium pressure of dissociation of hydrogen from the hydride depends on temperature and H/Zr ratio. Fixed the temperature, the equilibrium pressure is higher for a higher H/Zr ratio. Fixed the H/Zr ratio, pressure increases with increasing temperature [SFW76]. Temperature is an important dependence of hydrogen equilibrium pressure. Just to give an idea, Figure 3.11 shows how the pressure increases as temperature increases: it is lower than 0.6 atm (10 psi) at 700 °C, 1 atm at 760 °C and above 680 atm at a temperature around 1300 °C. However, the temperature is not constant all over the fuel but decreases at increasing radius. So hydrogen pressure will be lower than those calculated for the maximum temperature [SFW76].

So it seems reasonable to set a fuel safety criteria for temperature:

Fuel safety criterion 4: Limit overpressure failure - Temperature

The maximum temperature of the fuel during normal operation shall be limited, with a reasonable margin, to a value that ensures that the stresses due to the pressure from the outgassing of hydrogen do not cause cladding failure.

About the value of this limit, some consideration could be made. For example, the

limit of steady state temperature of the fuel is usually at 750 °C, but this value is chosen for a lot of reasons, in particular, due to fuel dimensional changes.

For the pulsed use, the maximum temperature admitted is higher. However, due to the higher temperature, also the strength of the cladding decreases. So the outgassing of the fuel and the dependence of cladding strength on temperature can set the value of this limit. For example, [SFW76] makes an approximate evaluation for this temperature limit for the Anular Core Pulsing Reactor (ACPR) fuel, which is optimized for pulsing. The author says that the cladding temperature does not overcome 138 °C, due to a gap between the fuel and the stainless steel clad. At this temperature, the yield strength of the 304L Stainless steel is 38000 psi, while the ultimate strength is 68000 psi. To produce such a stress S on the clad, the internal pressure needed can be calculated with this formula:

$$P_h = S\frac{t_c}{r_c}$$

where P_h is the pressure of hydrogen, t_c is the clad thickness, r_c is the radius. From this formula, the pressure needed to cause the yield stress is 1025 psi (about 69 atm) and 1840 (125 atm) to reach the ultimate strength. Those hydrogen pressure are obtained respectively at temperatures of 1080 and 1140 °C, under equilibrium conditions. However, as already said, the temperature is not the same over the fuel meat, and consequently the hydrogen pressure will be lower than those calculated for the highest temperature. The limit for pulsed use of the reactor, indeed, is 1150 °C if the clad temperature does not overcome 500 °C, and 950 °C if the clad temperature can reach those of the fuel [SFW76]. These last two limits are for the pulsing behaviour of the reactor, and a space reactor is not expected to work in these conditions. These values can be however considered as a starting point for consideration on limit values for transients.

Then, as already said, the equilibrium pressure depends on the H/Zr ratio, so a fuel safety criteria for this ratio could be set:

Fuel safety criterion 5: Limit overpressure failure - H/Zr ratio

The maximum H/Zr on the surface of the fuel shall be limited, with a reasonable margin, to a value that ensures that the stresses due to the pressure from the outgassing of hydrogen do not cause cladding failure.

Figure 3.7 shows dissociation equilibrium pressure as a function of temperature and H/Zr ratio. As one can see, even if at the periphery of the fuel meat the H/Zr ratio reaches 1.8 due to hydrogen redistribution, the pressure of 10 atm is reached at almost 800 °C. In this case, the temperature is higher than the temperature limit for the TRIGA reactor's normal operation (without considering that the surface temperature is even lower) and the pressure is almost 7 times lower than the one needed to produce the yield stress on

the ACPR fuel cladding. So the exact evaluation of the limit on the H/zr ratio should consider the design, materials and conditions of the considered space reactor fuel.

3.6.2.2 Due to fission gases

As already said, the low release of fission products from hydride fuel seems to be caused by two different processes. The first one, the recoil of fission product into the gap, is predominant at temperatures below 400 °C and it is temperature independent. The other one is some kind of diffusion process that is temperature-dependent.

According to [SFW76] the fractional release ϕ of fission product gases into the gap for a standard TRIGA fuel element is given by this formula:

$$\phi = 1.5 \cdot 10^{-5} + 3600 e^{\frac{-1.34 \cdot 10^4}{T_K}}$$

where T is the fuel temperature (K). The first term represents the initial low-temperature behaviour, due to recoil, which is independent from temperature. Then, the second term represents the mechanism of diffusion and is dependent on temperature.

The curve represented by the formula applies to a fuel element irradiated for a time long enough to ensure that fission product activity is at equilibrium [SFW76] and it applies to both the high and the 8.5% uranium loaded fuel, for which it was derived [BFG80].

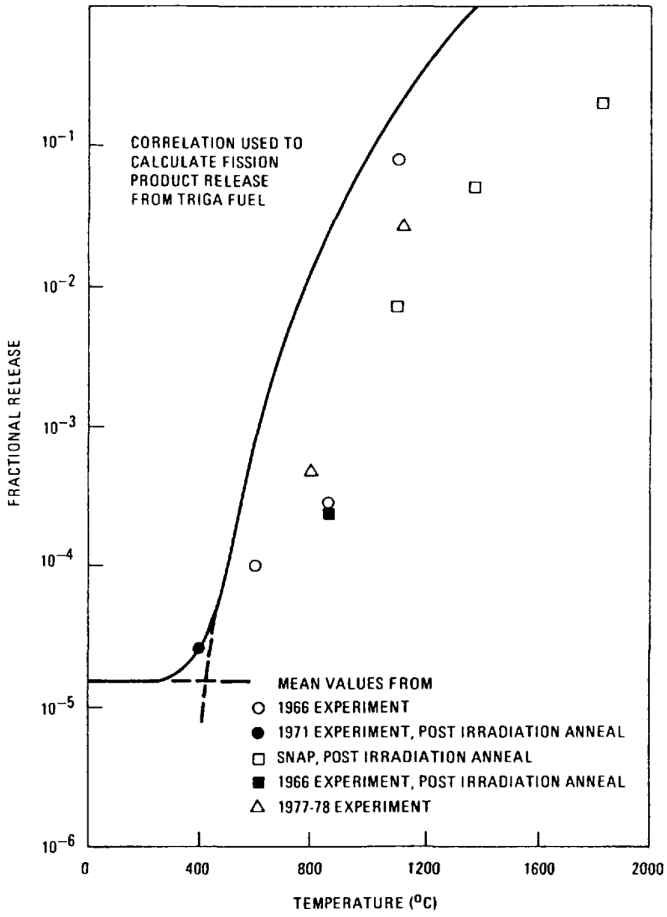

Figure 3.12: Fractional release of gaseous fission products from U-ZrH fuel

As one can see in figure 3.12, this correlation predicts higher fission product releases than experiments, therefore giving conservative values for safety consideration.

So temperature results to be the main dependence of the release of fission product into the gap between the fuel and the clad and a fuel safety criteria can be set:

Fuel safety criterion 6: Limit overpressure failure - Temperature

The maximum temperature of the fuel during normal operation shall be limited, with a reasonable margin, to a value that ensures that the stresses due to the pressure from fission gases do not cause cladding failure

An explicit value for a temperature limit to avoid overpressure due to fission gas has not been found in the literature, with only a maximum temperature value set to

prevent unusual swelling. For sure, this value will depend on the geometry of the fuel meat, because of both the surface-to-volume ratio of the fuel and the volume able to accommodate fission gases.

Finally, [Ola+09] reports some data limitations: for example, no data have been obtained from in-reactor rods, numerous reports on fission products are not the source of data, and in general a lack of details on Zr/U and H/Zr ratios, or irradiation temperatures, or annealing times in annealing experiments. For these reasons, more detailed studies may be needed.

3.6.3 Due to hydrogen loss from fuel meat

As already said, the loss of hydrogen in the void space depends on the equilibrium pressure of hydrogen. Release from the fuel should occur when the equilibrium pressure of hydrogen is higher than the one in the gap and the plenum. For this reason, two fuel safety criteria can be set, on temperature and H/Zr ratio.

Fuel safety criterion 7: Limit loss of hydrogen from fuel meat - Temperature

The maximum temperature of the fuel during normal operation shall be limited, with a reasonable margin, to a value that ensures that the loss of hydrogen from the fuel meat does not impair the intrinsic reactivity feedback characteristics of the fuel to a point which is detrimental for reactivity control

Fuel safety criterion 8: Limit loss of hydrogen from fuel meat - H/Zr ratio

The maximum H/Zr on the surface of the fuel shall be limited, with a reasonable margin, to a value that ensures that the loss of hydrogen from the fuel meat does not impair the intrinsic reactivity feedback characteristics of the fuel to a point which is detrimental to reactivity control

No explicit values for these limits have been found in the literature and are bound to be somewhat design dependent. However, some authors tried to evaluate the quantity of hydrogen that can escape from the fuel meat, according to the geometry under consideration.

For example, [ON05] calculated at first the equilibrium pressure of hydrogen using the surface temperature and the H/Zr ratio. Then, they calculated the available combined volume of the gap and the plenum, raising the value of the latter due to thermal expansion

consideration. For their fuel rod design, an LWR rod fuelled with UZrH pellets, the gas volume would contain $\sim 10^{-5}$ moles of H, calculated from the ideal gas law. Considering the volume of solid hydride, they conclude that it would contain ~ 25 moles of hydrogen. So they conclude that the loss of hydrogen into the gas phase is negligible, in the normal condition of use they consider for their fuel design. Indeed, in a consideration that seems to regard hydride fuel in general, [Ola+09] tells that the loss of hydrogen from $ZrH_{1.6}$ to the gas phase is not significant during normal operation, because of the low pressure at fuel temperature. So, the loss of hydrogen from the fuel meat seems to regard, in particular, accident conditions and further experiments under these conditions may be needed.

3.6.4 Due to fuel melting

As explained above, fuel melting failure depends on the temperature. A fuel approaching its melting temperature can lose its original shape and induce issues regarding radioactive material confinement, reactivity control, and coolability.

So, a fuel criteria on temperature should be set:

Fuel safety criterion 9: Limit fuel melting - Temperature

The maximum fuel temperature shall be limited, with a reasonable margin, to a value that ensures that fuel melting is avoided.

The melting temperature of $\delta - phase$ Uranium Zirconium hydride is greater than the Uranium melting point and alloys of Uranium and Zirconium (U-10Zr). This can be explained by the fact that Uranium is assumed to be a micro inclusion in a hydride matrix, rather than a heterogeneus solid solution alloy. So, even if uranium inclusion is liquid above its melting temperature (about 1130 °C), the matrix will remain solid. Furthermore, with increasing temperature, hydrogen dissociates from the matrix and the melting temperature of the hydride approaches that of zirconium. Indeed, the melting temperature of $\delta - phase$ Uranium Zirconium hydride is above 1800 °C but a more precise value has not been found [Eva+24].

However, while searching for a value for this limit, one should also consider eutectic fuel/cladding melting. Uranium forms eutectics with iron, nickel, and chromium which are some of the principal constituents of cladding material used with UZrH. Localized fuel melting has been observed due to the formation of low melting eutectics when uranium is in contact with those materials.

In all cases, the extent of eutectic melting would be limited by the relatively small volume fraction of uranium in the fuels. Furthermore, the cladding failure due to hydrogen overpressure is expected to happen before eutectic fuel/cladding or fuel melting and

does not constitute a more severe limit than overpressure [Eva+24].

Chapter 4

Conclusions

Because the reactor design has yet to be defined, this thesis focused on identifying safety criteria under normal operation that will ensure the fuel's barriers remain intact, thus ensuring the fundamental safety function of radioactive material confinement.

The first chapter reviewed briefly the history of space reactors, developed by both the United States and the Soviet Union. However, these reactors were used for relatively low-power applications and relied on highly enriched uranium: actual requirements are different and have been presented briefly.

Then, a brief overview of the key components of a space reactor has been presented, such as the coolant, the conversion and the dissipation systems. A focus section on the fuel technologies available highlights their pros and cons, especially in the context of space reactors.

Among them, TRISO and UZrH fuel are chosen for a deeper analysis, due to their maturity level and suitable characteristics for space reactors. TRISO is a particle fuel with an oxide or oxy-carbide kernel covered with different layers of ceramic material. This fuel is innovative and has passive safety features related to thermal resistance and confinement capability. UZrH fuel is considered because it has already been used in different reactors on Earth and space and it has the ability to serve as both fuel and moderator (enhancing compactness), good thermal stability and the inherent safety characteristic of a prompt negative temperature coefficient.

Then, safety concepts about reactors have been presented. In particular, the concept of defence in depth, barrier, Fundamental Safety Function, Fuel Safety criteria and margin have been explained. The thesis focuses, indeed, on the integrity of the fuel and cladding barriers, searching for limits during normal operation to ensure these barriers remain intact and the safety function of radioactive material confinement is correctly performed.

The second chapter focused on the TRISO fuel. After a presentation of the fuel behaviour, the known fuel failures have been analysed. Among them, those for which fuel safety criteria have been identified are:

- Pressure vessel failure
- IPyC crack-induced failure
- IPyC debonding induced failure
- SiC thermal decomposition
- Kernel migration
- Fission product interaction or attack and CO attack

From the analysis of this fuel, twelve fuel safety criteria have been identified: six of them regard temperature, two BAF, and one burnup, released Palladium, the bond strength between the IPyC and the SiC layer and one on the temperature gradient. They are summarized in Tables 4.1 and 4.2.

Among them, an explicit value for the limit has been found only for SiC thermal decomposition: the irradiation temperature should not exceed 1600 °C. This failure is independent from design and so a precise value has been assigned.

As far as the BAF factor is concerned, a hypothesis of value is 1.09 [Ske+16]. However, this value refers to a TRISO particle with the standard dimension for the Advanced Gas Reactor of the US Department of Energy and may vary according to the design considered.

The values for other limits have not been found in the literature and are somehow dependent on the particle design values (like the thickness of the SiC layer, or the thermal gradient foreseen by the reactor design).

As far as it regards temperature, as one can see in Tables 4.1 and 4.2, different fuel criteria are set to limit its maximum value, while two of them set a lower limit. From this analysis, it seems reasonable to think that an intermediate range of values could be ideal for the irradiation temperature, to ensure the lowest possible failure probability. The intermediate value of the temperature and the value for other limits can be found using fuel performance model codes, finding the values for which the failure probability is lower than an acceptable value. Using fuel performance code will allow also to take into consideration different time dependences of the failures.

The third chapter focused on the UZrH fuel. After a presentation of the fuel behaviour, the known fuel failures have been analysed. Among them, those for which fuel safety criteria have been identified are:

- FCMI due to swelling
- Overpressure
- Hydrogen loss

TRISO			
Failure	**Variable**	**Limit**	**Fuel Safety Criteria**
SiC thermal decomposition	Temperature	Upper <1600 °C	The temperature of the SiC layer in the particles of the fuel shall not exceed 1600 °C during normal operation and at any anticipated operational occurrence, to avoid failures due to the thermal decomposition of the SiC layer.
Overpressure	Temperature	Upper	The irradiation temperature of the particle during normal operation shall be limited, with a margin, in order to avoid tensile stress on the SiC layer, due to the total amount of pressure inside the particle, is above the ultimate tensile strength of the SiC layer during the lifetime of the reactor
	Burnup	Upper	The burnup of the particle kernel shall be limited, with a margin, in order to avoid that tensile stress on the SiC layer, due to the total amount of pressure inside the particle, is above the ultimate tensile strength of the SiC layer during the lifetime of the reactor
Palladium attack	Temperature	Upper	During normal operation, the maximum irradiation temperature of the particle shall be limited to a value that ensures that the Palladium penetration rate during the irradiation lifetime of the reactor does not cause complete penetration of the SiC layer by the attack of Palladium, with a reasonable margin.
	Released palladium	Upper	The total amount of Palladium released from the kernel shall be limited to a value that ensures that the maximum expected Palladium penetration during the irradiation lifetime of the reactor does not cause complete penetration of the SiC layer by the attack of Palladium, with a reasonable margin.

Figure 4.1: Summary of fuel safety criteria for TRISO. This table continues in the next page

Silver release	Temperature	Upper	The irradiation temperature shall be limited, with a margin, to a value that ensures that the Silver release is within an acceptable value for SNR operations and maintenance.
IPyC layer cracking	BAF	Upper	The BAF of pyrocarbon layers after the fabrication of TRISO particles shall be limited, in order to avoid an increase of particle failures due to cracks in the IPyC layer, with reasonable margin.
	Temperature	Lower	During normal operation, the irradiation temperature of the particle shall be greater, with a margin, than a value that ensures pyrocarbon layers in particles do not fail because of cracks.
IPyC layer debonding	Bond Strength	Lower	The bond strength between the IPyC and the SiC layers shall be greater, with a reasonable margin, than a minimum value, which will ensure that the debonding between those two layers is negligible, in order to avoid SiC failure.
	BAF	Upper	The BAF of pyrocarbon layers after the fabrication of TRISO particles shall be limited to a maximum value, considering also a reasonable margin, in order to avoid an increase of particle failures due to debonding of the IPyC layer from the SiC one.
	Temperature	Lower	During normal operation, the irradiation temperature of the particle shall be greater, with margin, than a value that ensures that pyrocarbon layers do not debond, in order to avoid SiC failure.
Kernel migration	Temperature Gradient	Upper	During normal operation, the highest temperature gradient in the fuel compact shall be limited to a value that ensures that the migration distance during the expected lifetime of the reactor, is less than buffer plus IPyC layer thickness, with a reasonable margin.

Figure 4.2: continued: Summary of fuel safety criteria for TRISO

UZrH			
Failure	**Variable**	**Limit**	**Fuel Safety Criteria**
FCMI due to swelling	Temperature	Upper	The average temperature of the fuel at the end of offset swelling shall be limited, with a reasonable margin, to a value that ensures that fuel swelling does not cause interaction between the fuel and the cladding which could lead to failure of the latter.
	Burnup Rate	Lower	The burnup rate shall be greater, with a margin, than a value that ensures that fuel swelling does not cause interaction between the fuel and the cladding which could lead to failure of the latter.
	Burnup	Upper	The burnup shall be limited, with a reasonable margin, to a value that ensures that fuel swelling does not cause the interaction between the fuel and the cladding which could lead to failure of the latter.
Overpressure	Temperature (hydrogen outgassing)	Upper	The maximum temperature of the fuel during normal operation shall be limited, with a reasonable margin, to a value that ensures that the stresses due to the pressure from the outgassing of hydrogen do not cause cladding failure.
	H/Zr ratio	Upper	The maximum H/Zr on the surface of the fuel shall be limited, with a reasonable margin, to a value that ensures that the stresses due to the pressure from the outgassing of hydrogen do not cause cladding failure.
	Temperature (fission gas)	Upper	The maximum temperature of the fuel during normal operation shall be limited, with a reasonable margin, to a value that ensures that the stresses due to the pressure from fission gases do not cause cladding failure

Figure 4.3: Summary of fuel safety criteria for UZrH. This table continues in the next page

Hydrogen loss	Temperature	Upper	The maximum temperature of the fuel during normal operation shall be limited, with a reasonable margin, to a value that ensures that the loss of hydrogen from the fuel meat does not impair the intrinsic reactivity feedback characteristics of the fuel to a point which is detrimental for reactivity control
	H/Zr ratio	Upper	The maximum H/Zr on the surface of the fuel shall be limited, with a reasonable margin, to a value that ensures that the loss of hydrogen from the fuel meat does not impair the intrinsic reactivity feedback characteristics of the fuel to a point which is detrimental to reactivity control
Fuel melting	Temperature	Upper	The maximum fuel temperature shall be limited, with a reasonable margin, to a value that ensures that fuel melting is avoided.

Figure 4.4: Continued: Summary of fuel safety criteria for UZrH

- Fuel melting

From the analysis of this fuel, nine fuel safety criteria have been identified: five of them regard temperature, two the H/Zr ratio and one on the burnup and burnup rate They are summarized in Tables 4.3 and 4.4.

Consistently with literature, the basic limit on this fuel is temperature [SFW76]. For TRIGA standard fuel, for example, a limit on maximum temperature is set to 750 °C under steady-state conditions. This limit allows insignificant calculated fuel growth for temperature-dependent irradiation effects. However, this limit can be increased under pulsing conditions to 1150 °C, in this case, to avoid overpressure due to the outgassing of hydrogen from the fuel meat.

As far as it regards to H/Zr ratio, no explicit limit values for this variable at the surface of the fuel meat have been found. The choice of a nominal value of 1.6 is a trade-off between incorporating the largest hydrogen concentration for moderation purposes, without generating too much overpressure [Ola+09]. For this reason, while setting the limit value, these considerations must be taken into account.

For both fuels, the fuel safety criteria presented in this work may not be an exhaustive list of fuel safety criteria, also because the reactor has not been identified. However, these fuel safety criteria can be used to guide fuel designers to develop an appropriate fuel for a space reactor, highlighting what dependencies are the most important and guide specifications for fabrication purposes.

New experiments are needed to deepen the knowledge of these fuels, their behaviour under irradiation and their material properties. Further experiments can indeed deepen the knowledge which is in some cases not completely robust and not further analysed [Ola+09]. New knowledge added to the existent datasets will improve performance code modelling capabilities, which will enable better safety analysis for a space (and terrestrial) reactor. Even for terrestrial applications, in fact, both fuels are the subject of renewed interest: the TRISO as a fuel for some prototype of generation IV reactor, while UZrH as a fuel for the MARVEL experimental microreactor.

Bibliography

[Gyl+62] JD Gylfe et al. *Evaluation of Zirconium Hydride as Moderator in Integral, Boiling Water-Superheat Reactors*. Tech. rep. Atomics International. Div. of North American Aviation, Inc., Canoga Park ..., 1962.

[Ato67] General Atomic. *Kinetic Behavior of TRIGA Reactors*. Tech. rep. General Atomic, 1967.

[CHQ72] V Coen, H Hausner and D Quataert. "Cesium migration in silicon carbide". In: *Journal of Nuclear Materials* 45.2 (1972), pp. 96–104.

[Lil+73] AF Lillie et al. *Zirconium hydride fuel element performance characteristics*. Tech. rep. Atomics International Div., 1973.

[SFW76] Massoud T Simnad, Fabian C Foushee and Gordon B West. "Fuel elements for pulsed TRIGA® research reactors". In: *Nuclear Technology* 28.1 (1976), pp. 31–56.

[NBO77] Heinz Nabielek, Peter E Brown and Peter Offermann. "Silver release from coated particle fuel". In: *Nuclear Technology* 35.2 (1977), pp. 483–493.

[BFG80] NL Baldwin, FC Foushee and JS Greenwood. *Fission-product release from TRIGA-LEU reactor fuels*. Tech. rep. General Atomics, San Diego, CA (United States), 1980.

[Sim81] MT Simnad. "The U-ZrHx alloy: Its properties and use in TRIGA fuel". In: *Nuclear Engineering and Design* 64.3 (1981), pp. 403–422.

[Vos84a] Susan S Voss. "Snap (space nuclear auxiliary power) reactor overview". In: *Final Report* (1984).

[Vos84b] Susan S. Voss. *Snap (space nuclear auxiliary power) reactor overview*. AIR FORCE WEAPONS LAB KIRTLAND AFB NM, 1984.

[SCW88] MT Simnad, GL Copeland and GB West. *Final results from TRIGA LEU fuel post-irradiation examination and evaluation following long term irradiation testing in the ORR*. Tech. rep. 1988.

[Nab+89] Heinz Nabielek et al. "The performance of high-temperature reactor fuel particles at extreme temperatures". In: *Nuclear Technology* 84.1 (1989), pp. 62–81.

[Min+90] Kazuo Minato et al. "Fission product palladium-silicon carbide interaction in HTGR fuel particles". In: *Journal of Nuclear Materials* 172.2 (1990), pp. 184–196.

[Zuz+90] E Zuzek et al. "The H-Zr (hydrogen-zirconium) system". In: *Bulletin of alloy phase diagrams* 11.4 (1990), pp. 385–395.

[Min+91] Kazuo Minato et al. "Carbon monoxide-silicon carbide interaction in HTGR fuel particles". In: *Journal of materials science* 26 (1991), pp. 2379–2388.

[STS94] Shinzo Saito, Toshiyuki Tanaka and Yukio Sudo. *Design of high temperature engineering test reactor (HTTR)*. Tech. rep. Japan Atomic Energy Research Inst., 1994.

[Hui97] Zuo Huizhong. "The uranium-zirconium hydride pulsed reactor and its use in science and technology". In: *Nuclear engineering and design* 168.1-3 (1997), pp. 305–311.

[INS97] IAEA INSAG. *10, Defence in Depth in Nuclear Safety*. 1997.

[Mil+01] Gregory K Miller et al. "Consideration of the effects on fuel particle behavior from shrinkage cracks in the inner pyrocarbon layer". In: *Journal of Nuclear Materials* 295.2-3 (2001), pp. 205–212.

[03] *Fuel Safety Criteria in NEA Member Counties*. Tech. rep. Nuclear Energy Agency NEA, 2003.

[Pet+03] David Andrew Petti et al. "Key differences in the fabrication, irradiation and high temperature accident testing of US and German TRISO-coated particle fuel, and their implications on fuel performance". In: *Nuclear Engineering and Design* 222.2-3 (2003), pp. 281–297.

[MPM04] Gregory K Miller, David A Petti and John T Maki. "Consideration of the effects of partial debonding of the IPyC and particle asphericity on TRISO-coated fuel behavior". In: *Journal of Nuclear Materials* 334.2-3 (2004), pp. 79–89.

[Mor+04] R. N. Morris et al. "TRISO-Coated Particle Fuel Phenomenon Identification and Ranking Tables (PIRTs) for Fission Product Transport Due to Manufacturing, Operations, and Accidents". In: *TRISO-Coated Particle Fuel Phenomenon Identification and Ranking Tables (PIRTs) for Fission Product Transport Due to Manufacturing, Operations, and Accidents*. Washington, DC: U.S. Nuclear Regulatory Commission, 2004. Chap. 2. URL: https://www.nrc.gov/docs/ML0406/ML040650051.pdf.

[Pet+04] David Petti et al. *Development of Improved Models and Designs for Coated-Particle Gas Reactor Fuels–Final Report under the International Nuclear Energy Research Initiative (I-NERI)*. Tech. rep. Idaho National Lab.(INL), Idaho Falls, ID (United States); Centre d'Etude ..., 2004.

[SU04] Kazuhiro Sawa and Shohei Ueta. "Research and development on HTGR fuel in the HTTR project". In: *Nuclear Engineering and Design* 233.1-3 (2004), pp. 163–172.

[Wan04] Jing Wang. "An integrated performance model for high temperature gas cooled reactor coated particle fuel". PhD thesis. Massachusetts Institute of Technology, 2004.

[IAE05] IAEA. *ASSESSMENT OF DEFENCE IN DEPTH FOR NUCLEAR POWER PLANTS*. IAEA, 2005.

[ON05] Donald R Olander and Marowen Ng. "Hydride fuel behavior in LWRs". In: *Journal of nuclear materials* 346.2-3 (2005), pp. 98–108.

[Sta05] A Stanculescu. *The role of nuclear power and nuclear propulsion in the peaceful exploration of space*. Vol. 1197. IAEA, 2005.

[Hre+07] Miroslav Hrehor et al. *Task group on safety margins action plan (smap). safety margins action plan-final report*. Tech. rep. Organisation for Economic Co-Operation and Development, 2007.

[Mak+07] John T Maki et al. "The challenges associated with high burnup, high temperature and accelerated irradiation for TRISO-coated particle fuel". In: *Journal of Nuclear Materials* 371.1-3 (2007), pp. 270–280.

[Bea+09] M Beauvy et al. "Nuclear fuels". In: (2009).

[Cam+09] Michael D Campbell et al. "The role of nuclear power in space exploration and the associated environmental issues: an overview". In: *A Report by the Uranium Committee of the Energy Minerals Division to the Astrogeology Committee of the AAPG* (2009), pp. 2010–2011.

[El-09] Mohamed S El-Genk. "Deployment history and design considerations for space reactor power systems". In: *Acta Astronautica* 64.9-10 (2009), pp. 833–849.

[Ola+09] D Olander et al. "Uranium–zirconium hydride fuel properties". In: *Nuclear Engineering and Design* 239.8 (2009), pp. 1406–1424.

[PCC09] D Petti, D Crawford and N Chauvin. "Fuels for advanced nuclear energy systems". In: *MRS bulletin* 34.1 (2009), pp. 40–45.

[Age10] International Atomic Energy Agency. *High temperature gas cooled reactor fuels and materials*. IAEA, 2010.

[PW10] Jeffrey J Powers and Brian D Wirth. "A review of TRISO fuel performance models". In: *Journal of Nuclear Materials* 405.1 (2010), pp. 74–82.

[ZT11] XW Zhou and CH Tang. "Current status and future development of coated fuel particles for high temperature gas-cooled reactors". In: *Progress in Nuclear Energy* 53.2 (2011), pp. 182–188.

[Bec+12] Winfried Beck et al. "Nuclear Fuel Safety Criteria Technical Review". In: (2012).

[RDR12] IJ van Rooyen, ML Dunzik-Gougar and PM van Rooyen. "Silver (Ag) transport mechanisms in TRISO coated particles". In: *A Critical Review, Paper HTR2012-3-040, Proceedings of the HTR* (2012).

[Bes+13] John D Bess et al. *Fresh-Core reload of the Neutron radiography (NRAD) reactor with Uranium (20)-Erbium-Zirconium-Hydride fuel*. Tech. rep. Idaho National Lab.(INL), Idaho Falls, ID (United States), 2013.

[Pos+14] David I Poston et al. "Experimental demonstration of a heat pipe–stirling engine nuclear reactor". In: *Nuclear Technology* 188.3 (2014), pp. 229–237.

[Bar+16] KM Bartholomew et al. *History, Development and Future of TRIGA Research Reactors*. International Atomic Energy Agency (IAEA), 2016.

[Ske+16] William F Skerjanc et al. "Evaluation of design parameters for TRISO-coated fuel particles to establish manufacturing critical limits using PARFUME". In: *Journal of Nuclear Materials* 469 (2016), pp. 99–105.

[AG18] Elvis Falcão de Araújo and Lamartine Nogueira Frutuoso Guimarães. "American space nuclear electric systems". In: *Journal of Aerospace Technology and Management* 10 (2018), e4418.

[PHM18] Aiden Peakman, Zara Hodgson and Bruno Merk. "Advanced micro-reactor concepts". In: *Progress in Nuclear Energy* 107 (2018), pp. 61–70.

[SD18] William F Skerjanc and Paul A Demkowicz. *PARFUME theory and model basis report*. Tech. rep. Idaho National Lab.(INL), Idaho Falls, ID (United States), 2018.

[DLH19] Paul A Demkowicz, Bing Liu and John D Hunn. "Coated particle fuel: Historical perspectives and current progress". In: *Journal of Nuclear Materials* 515 (2019), pp. 434–450.

[Lai+19] Marc Lainet et al. "GERMINAL, a fuel performance code of the PLEIADES platform to simulate the in-pile behaviour of mixed oxide fuel pins for sodium-cooled fast reactors". In: *Journal of Nuclear Materials* 516 (2019), pp. 30–53.

[MS19] C Marciulescu and A Sowder. "Uranium Oxycarbide (UCO) Tristructural Isotropic (TRISO) Coated Particle Fuel Performance". In: *Electric Power Research Institute* (2019).

[Li+20] Zeguang Li et al. "Design of a hundred-kilowatt level integrated gas-cooled space nuclear reactor for deep space application". In: *Nuclear Engineering and Design* 361 (2020), p. 110569.

[Pos+20] David I Poston et al. "KRUSTY reactor design". In: *Nuclear Technology* 206.sup1 (2020), S13–S30.

[Ass+21] World Nuclear Association et al. "Nuclear reactors and radioisotopes for space". In: *June 2018* (2021).

[OFG21] Shoichiro Okita, Yuji Fukaya and Minoru Goto. "Derivation of ideal power distribution to minimize the maximum Kernel migration rate for nuclear design of pin-in-block type HTGR". In: *Journal of Nuclear Science and Technology* 58.1 (2021), pp. 9–16.

[RKJ21] Morgan Rogers, Dinyar Ramin Kadkhodaian and Logan Jeffery. "Fuel Mass Optimization for a TRISO-Based Lunar Nuclear Reactor". PhD thesis. 2021.

[WPG21] BE Wells, NR Phillips and KJ Geelhood. "TRISO fuel: properties and failure modes". In: *PNNL-31427, PNNL* (2021).

[Got22] H Goto. "High-temperature Gas-cooled Reactors and Industrial Heat Applications". In: *Nuclear Technology Development and Economics, Nuclear Energy Agency* (2022), pp. 2022–06.

[IAE22] IAEA. *IAEA nuclear safety and security glossary / International Atomic Energy Agency*. IAEA, 2022.

[Kan+22] Joshua J Kane et al. "3D analysis of TRISO fuel compacts via X-ray computed tomography". In: *Journal of Nuclear Materials* 565 (2022), p. 153745.

[Ole+22] Steven Oleson et al. *A Deployable 40 kWe Lunar Fission Surface Power Concept*. Tech. rep. 2022.

[And+23] David A Andersson et al. "The past, present, and future of nuclear fuel". In: *MRS Bulletin* 48.11 (2023), pp. 1154–1162.

[PL23] Aiden Peakman and Ben Lindley. "A review of nuclear electric fission space reactor technologies for achieving high-power output and operating with HALEU fuel". In: *Progress in Nuclear Energy* 163 (2023), p. 104815.

[Woo+23] Nicolas Woolstenhulme et al. "TREAT testing of additively manufactured SiC canisters loaded with high density TRISO fuel for the Transformational Challenge Reactor project". In: *Journal of Nuclear Materials* 575 (2023), p. 154204.

[Eva+24] Jordan A Evans et al. "Uranium-zirconium hydride nuclear fuel performance in the NaK-cooled MARVEL microreactor". In: *Journal of Nuclear Materials* 598 (2024), p. 155145.

[Ske24] William F Skerjanc. *Fuel Performance Modeling Plan to Support the Advance Gas Reactor Program*. Tech. rep. Idaho National Laboratory (INL), Idaho Falls, ID (United States), 2024.

[ESA] ESA. *Why go to Mars?* https://www.esa.int/Science_Exploration/Human_and_Robotic_Exploration/Exploration/Why_go_to_Mars. Accessed: 2025-01-10.

[TVO] TVO. *Reactor safety*. https://www.tvo.fi/en/index/production/plantunits/safeoperation/reactorsafety.html. Accessed: 2025-01-10.